Cent. Eur. J. Geosci. • 5(1) • 2013 • 112-173
DOI: 10.2478/s13533-012-0121-z

VERSITA

Central European Journal of **Geosciences**

Consistent patterns of rare earth element distribution in accessory minerals from rocks of mafic-ultramafic complexes

Review Article

Felix Petrovich Lesnov*

Institute Geology and Mineralogy Novjsibirsk, Russian Federation

Received 29 November 2012; accepted 13 February 2013

Abstract: This paper summarizes analytical data accumulated in the world literature and other materials about the regularities of the REE distribution in minerals contained in ultramafic and mafic rocks as accessory phases. These minerals are tentatively divided into two groups. The first includes garnets, zircons, apatites and perovskites, which can accumulate increased amounts of REE in their structure. The second consists of minerals whose structure can accumulate only limited contents of these trace elements. These are chrome-spinels, ilmenites, and micas. These minerals, in respect of REE geochemistry, are studied to a varying degree because of the different levels of accumulations of these elements, different degrees of occurrence in rocks, tiny sizes of their grains and other reasons. The analytical database formed on their basis includes about 600 original analyses. The overwhelming majority of presently available data on REE geochemistry in accessory minerals from ultramafic and mafic rocks have been published only in the recent 15 years. The studies became possible due to the development and introduction of new highly sensible microprobe analyses allowing detection of REE and many other trace elements in minerals grains directly in thin sections. The greatest numbers of these analyses were performed for garnets and zircons, fewer for apatites, and the fewest for chrome-spinels, ilmenites, micas, and perovskites. In general, the regularities of REE distribution in these minerals from ultramafic and mafic rocks are less studied compared to the rock-forming minerals from ultramafic and mafic rocks. Among the analytical methods, which were used to study the REE composition of accessory minerals, the most efficient was the mass-spectrometry with inductively coupled plasma (ICP-MS).

Keywords: REE distribution • ultramafic and mafic rocks • accessory minerals

1. Introduction

This paper summarizes analytical data accumulated in the world literature and other materials about the regularities of the Rare Earth Element (REE) distribution in minerals contained in ultramafic and mafic rocks as accessory phases. These minerals are tentatively divided into two groups. The first includes garnets, zircons, apatites and perovskites, which can accumulate high concentrations of REE in their structure. The second consists of minerals whose structure can accumulate only limited contents of these trace elements. These are chrome-spinels, ilmenites, and micas. These minerals, with respect to REE geochemistry, are studied to a varying degree because of the differ-

*E-mail: felix@igm.nsc.ru

ent levels of accumulations of these elements, different degrees of occurrence in rocks, tiny sizes of their grains and other reasons. The analytical database presented here includes about 600 original analyses. The overwhelming majority of available data on REE geochemistry in accessory minerals from ultramafic and mafic rocks have been published only in the last 15 years. The studies have become possible due to the development and introduction of new highly sensitive microprobe analyses allowing detection of REE and many other trace elements in minerals grains directly in thin section. The greatest numbers of these analyses were performed for garnets and zircons, fewer for apatites, and the fewest for chrome-spinels, ilmenites, micas, and perovskites. In general, the regularities of REE distribution in these minerals from ultramafic and mafic rocks are less studied compared to the rock-forming minerals from ultramafic and mafic rocks. Among the analytical methods, which were used to study the REE composition of accessory minerals, widely used was the mass-spectrometry with inductively coupled plasma with laser ablation (LA ICP-MS). This compilation of data on the geochemistry of REE in these minerals will help clarify their taxonomy and identification of possible conditions for their formation.

2. Garnets

Garnets occur in more than 30 mineral parageneses forming rocks of magmatic, metamorphoric and metasomatic origin, which suggests their crystallization over a wide range of physicochemical conditions [1]. Usually garnet is present in rocks as an accessory phase, but in some rocks, such as eclogites and skarns, it is a rock-forming mineral. According to the data available, the crystalline structure of garnets can accumulate considerable amounts of different trace elements, including Rare Earth Elements (REE). The latter are, in most cases, intensely fractionated, which results in significant predominance of heavy elements. In geochemical analyses of garnets from ultramafic and mafic deep xenoliths in kimberlites and alkali basalts and for the interpretation of their results, researchers often use the numerical modeling techniques with regard to data on REE.

The first findings of REE in garnets were performed when studying single garnet samples from eclogites of Japan and New Zealand [2]. Soon data were obtained which showed that the values of REE distribution coefficients in the garnet-bearing rock and garnet-clinopyroxene systems increase from light to heavy. Based on these data, an assumption was made that garnets accumulate mainly heavy elements [3]. The keen interest to the problems of geochemistry of REE in garnets, especially those from deep xenoliths, contributed to the accumulation of numerous new analytical data on the REE composition of this mineral. In recent years, local (microprobe) methods of their analyses are used more frequently than others. The published analyses were dominated by those of garnets from peridotite and eclogite deep xenoliths as well as from microinclusions in diamonds. Far fewer data are available on garnets from eclogite rocks, occurring in metamorphic complexes, and from some gabbroid rocks, effusive rocks and skarns. The most abundant data are available on Ce, Nd, Sm, Eu, Dy, Er, Yb, scarcer are for La, Gd, Ho, Tm and Lu, and still scarcer are for Pr. The analyses show that garnets are characterized by considerable variations in the total contents of REE and differ in the ratios of light, medium, and heavy elements.

The calculations performed using the database (about 300 analyses) show that for the light (except Ce) and medium REE the differences between the maximum and minimum contents amount to two-three orders of magnitude, whereas for Yb, Lu and Ce they may increase to four orders of magnitude. The average content of elements for these samples in all types of garnets increases in the following series (ppm): 0.8 - Eu; 1.1 - La; 1.5 - Pr; 2.6 - Tb; 2.8 - Nd; 3.3 - Tm; 3.6 - Ce; 4.1 - Er; 6.5 - Lu; 8.3 - Gd; 55 - Sm; 315 - Dy; 387 - Ho; 554 - Yb. The total REE content decreases from the varieties of garnets enriched in Ca and Fe occurring in gabbroids, metamorphic rocks and metasomatic rocks to low-Ca and high-Mg pyropes from ultramafic rocks contained in xenoliths from kimberlites and alkali basalts. The chondrite-normalized concentrations of light REE in the garnets of all types vary in the range of 0.1–1.0, and those of HREE, in the range of 10–800. The preferred accumulation of HREE in the garnet structure is responsible for the observed steep positive slope of their REE pattern and low values of the $(La/Yb)n$ parameter.

In publications dealing with the REE distribution in garnets the most frequently discussed problems are: 1) comparative evaluation of the levels of REE accumulation in the samples of different chemical compositions and different paragenetic types; 2) systematization of garnets on the basis of distribution parameters of chondrite-normalized contents of REE; 3) physicochemical processes causing various anomalies in the distribution of REE in a mineral; 4) estimation of the distribution coefficients of REE between garnets and coexisting phases, including melts of different compositions (in natural and experimental systems); 5) calculation of the REE composition of model parental melts, using the distribution coefficients of REE; 6) crystallochemical properties of garnets and the related problems of REE isomorphism.

Table 1. REE compositions of garnets from harzburgites, lherzolites and peridotites from xenoliths in kimberlites of some provinces and pipes (ppm).

	Roberts Victor pipe, Ghana [154], SIMS										
Element	RV168	RV162	RV167	RV174	RV175	RV177	RV179	BD1174	BD1195	RV160	RV161
	Harzburgites										*Lherzolite*
La	0,190	0,210	0,080	1,920	0,330	0,810	0,400	0,080	0,240	0,070	0,050
Ce	1,500	0,760	0,800	7,930	3,060	5,360	3,950	0,840	2,070	0,960	0,780
Pr	0,390	0,100	0,270	1,210	0,490	0,910	0,600	0,320	0,430	0,230	0,360
Nd	2,270	0,310	2,190	4,930	2,060	4,320	1,870	3,490	1,460	0,970	1,920
Sm	0,510	0,020	0,660	0,750	0,260	0,770	0,120	2,890	0,060	0,110	0,390
Eu	0,130	0,010	0,220	0,200	0,050	0,170	0,030	1,060	0,010	0,020	0,090
Gd	0,490	0,010	0,710	0,670	0,090	0,480	0,200	3,120	0,040	0,040	0,510
Tb	0,120	N.d.	0,140	0,090	0,010	0,070	0,010	0,320	0,010	N.d.	0,100
Dy	0,820	0,010	0,940	0,350	0,050	0,280	0,050	1,490	0,020	0,010	0,740
Ho	0,230	N.d.	0,190	0,070	0,010	0,070	0,010	0,150	N.d.	N.d.	0,200
Er	0,730	»	0,720	0,200	0,040	0,220	0,040	0,310	0,020	0,010	0,710
Tm	N.d.	»	N.d.	N.d.	N.d.	N.d.	N.d.	N.d.	N.d.	N.d.	N.d.
Yb	1,060	0,010	0,910	0,210	0,090	0,340	0,040	0,310	0,130	0,050	1,130
Lu	0,170	0,010	0,170	0,040	0,030	0,080	0,020	0,060	0,040	0,030	0,210
Total	8,61	1,45	8,00	18,57	6,57	13,9	7,34	14,4	4,53	2,50	7,19
$(La/Yb)_n$	0,12	14,2	0,06	6,17	2,47	1,61	6,75	0,17	1,25	0,94	0,03

	Roberts Victor pipe, Ghana [154], SIMS						Bultfontein pipe, South Africa [143], IDMS		Jagersfontein pipe, South Africa [45], IPMA		Endekuil pipe, South Africa
Element	RV166	RV169	RV170	RV176	BD1173	BD1196	BUL6	JJG352	JAG9006A	JAG84595	EDKI
	Lherzolites										*Peridotite*
La	0,060	0,010	0,130	1,200	N.d.	0,020	N.d.	N.d.	0,062	0,017	N.d.
Ce	0,670	0,090	0,700	5,530	0,050	0,150	0,957	0,763	0,460	0,286	0,282
Pr	0,240	0,040	0,180	0,390	0,020	0,060	N.d.	N.d.	N.d.	N.d.	N.d.
Nd	2,140	0,330	1,350	2,080	0,200	0,760	3,000	3,960	1,493	2,480	1,005
Sm	0,750	0,360	0,570	0,470	0,090	0,710	1,570	1,870	1,252	2,780	0,869
Eu	0,210	0,110	0,220	0,120	0,030	0,350	0,842	0,679	0,500	1,350	0,380
Gd	1,130	0,420	0,860	0,450	0,070	1,500	2,520	2,050	N.d.	N.d.	N.d.
Tb	0,160	0,120	0,130	0,040	0,020	0,250	N.d.	N.d.	»	»	»
Dy	1,160	0,860	1,150	0,290	0,080	1,810	1,690	1,470	2,583	3,420	3,439
Ho	0,260	0,210	0,270	0,040	0,020	0,350	N.d.	N.d.	N.d.	N.d.	N.d.
Er	0,820	0,760	1,020	0,110	0,070	1,010	0,604	0,688	2,050	1,890	2,373
Tm	N.d.	N.d.	N.d.	N.d.	N.d.	N.d.	N.d.	N.d.	N.d.	N.d.	N.d.
Yb	0,760	1,060	1,190	0,110	0,120	0,860	0,572	0,757	2,132	2,670	2,405
Lu	0,160	0,130	0,180	0,020	0,020	0,180	N.d.	N.d.	N.d.	N.d.	N.d.
Total	8,52	4,50	7,95	10,9	0,79	8,01	11,8	12,2	10,5	14,9	10,8
$(La/Yb)_n$	0,05	0,01	0,07	7,36	N.d.	0,02	N.d.	N.d.	0,02	N.d.	N.d.

	Kimberley province, South Africa		Lesotho province, South Africa		Lourensia prov., South Africa		Premier pipe, South Africa	Rietfontein pipe, South Africa		Sanddreift province
	[45], IPMA									
Element	AJE25	AJE1181	PHN1611	PHN2302	L24	L14	PREM9006	RVD408	RIET5	RIET2	SDD591
	Peridotites										
La	0,047	0,072	N.d.	N.d.	0,045	N.d.	0,054	0,059	N.d.	N.d.	0,040
Ce	0,451	0,715	0,983	3,850	0,211	0,989	0,535	0,615	0,211	0,527	0,864
Pr	N.d.	N.d.	N.d.	N.d.	N.d.	N.d.	N.d.	N.d.	N.d.	N.d.	N.d.
Nd	2,190	4,872	1,770	3,590	0,476	3,390	2,237	2,130	1,300	2,580	3,160
Sm	2,020	4,025	1,220	1,940	0,594	3,380	2,351	1,250	2,040	3,190	2,138
Eu	0,949	1,165	0,570	0,831	0,374	1,380	0,998	0,341	1,140	1,180	0,823
Gd	N.d.	N.d..	N.d.	N.d.	N.d.	N.d.	N.d.	N.d.	N.d.	N.d.	N.d.
Tb	»	»	»	»	»	»	»	»	»	»	»
Dy	5,840	0,709	3,040	1,420	4,170	3,930	5,921	0,652	5,950	1,730	3,414
Ho	N.d.	N.d.	N.d.	N.d.	N.d.	N.d.	N.d.	N.d.	N.d.	N.d.	N.d.
Er	4,590	0,562	1,970	0,356	3,550	1,850	3,752	0,404	3,500	0,752	2,037
Tm	N.d.	N.d.	N.d.	N.d.	N.d.	N.d.	N.d.	N.d.	N.d.	N.d.	N.d.
Yb	6,330	0,632	1,880	0,355	3,770	2,070	4,890	0,469	4,180	1,200	1,545
Lu	N.d.	N.d.	N.d.	N.d.	N.d.	N.d.	N.d.	N.d.	N.d.	N.d.	N.d.
Total	22,4	12,8	11,4	12,3	13,2	17,0	20,7	5,92	18,3	11,2	14,0
$(La/Yb)_n$	0,01	0,08	N.d.	N.d.	0,01	N.d.	0,01	0,08	N.d.	N.d.	0,02

	Lighobong province	Thaba Putsoa province		Mothae pipe	Udachnaya pipe, Yakutia, Russia						
					[143], IDMS						
	PHN2302	PHN1566	PHN1611	PHN1925	379/86	667/86	394/86	404	404k	465/86	450/89
Element	*Lherzolites*				*Peridotites*						
La	N.d.	N.d.	N.d.	N.d.	6,940	1,260	0,340	0,400	0,450	0,650	1,840
Ce	3,850	1,540	0,983	»	18,890	8,440	3,410	2,400	2,710	5,660	7,310
Pr	N.d.	N.d.	N.d.	»	N.d.	N.d.	N.d.	N.d.	N.d.	N.d.	N.d.
Nd	3,590	3,100	1,770	1,330	4,920	7,400	2,920	2,610	2,530	2,850	5,240
Sm	1,940	2,140	1,220	0,912	0,990	2,990	0,740	0,760	0,760	0,140	1,220
Eu	0,831	1,040	0,570	0,483	0,130	0,650	0,150	0,270	0,240	0,080	0,250
Gd	2,440	3,820	2,280	2,110	N.d.	N.d.	N.d.	N.d.	N.d.	N.d.	N.d.
Tb	N.d.	N.d.	N.d.	N.d.	»	»	»	»	»	»	»
Dy	1,420	5,040	3,040	3,360	0,360	0,510	0,090	0,390	0,440	0,140	0,560
Ho	N.d.	N.d.	N.d.	N.d.	N.d.	N.d.	N.d.	N.d.	N.d.	N.d.	N.d.
Er	0,356	3,290	1,970	2,360	0,400	0,310	0,120	0,230	0,210	0,190	0,230
Tm	N.d.	N.d.	N.d.	N.d.	N.d.	N.d.	N.d.	N.d.	N.d.	N.d.	N.d.
Yb	0,355	2,960	1,880	2,450	0,500	0,410	0,180	0,260	0,240	0,770	0,400
Lu	N.d.	N.d.	N.d.	N.d.	N.d.	N.d.	N.d.	N.d.	N.d.	N.d.	N.d.
Total	14,8	22,9	13,7	13,0	33,1	22,0	7,95	7,32	7,58	10,5	17,1
$(La/Yb)_n$	N.d.	N.d.	N.d.	N.d.	9,37	2,07	1,27	1,04	1,27	0,57	3,10

	Udachnaya pipe, Yakutia, Russia									
	[119], IPMA					[148], IPMA				
Element	251/86	251/86k	514/86	177/89	441/86	52/76	80/92	239/89	51/92	74/89c	74/89r
	Peridotites									
La	1,090	0,630	0,040	0,300	0,010	0,184	0,190	0,239	0,083	0,091	0,055
Ce	2,620	1,700	0,120	2,440	1,370	1,785	1,450	2,050	0,739	0,606	0,662
Pr	N.d.	N.d.	N.d.	N.d.	N.d.	N.d.	N.d.	N.d.	N.d.	N.d.	N.d.
Nd	0,600	0,410	0,500	2,010	4,170	5,030	3,110	4,410	2,300	1,410	1,590
Sm	0,150	0,170	1,000	0,560	8,690	2,930	2,460	2,920	1,250	0,591	1,170
Eu	0,020	0,070	0,600	0,060	9,910	1,220	0,986	1,060	0,529	0,323	0,564
Gd	N.d.	N.d.	N.d.	N.d.	N.d.	N.d.	N.d.	N.d.	N.d.	N.d.	N.d.
Tb	»	»	»	»	»	»	»	»	»	»	»
Dy	0,050	0,050	3,950	0,250	6,310	2,620	4,480	1,650	3,220	1,660	2,520
Ho	N.d.	N.d.	N.d.	N.d.	N.d.	N.d.	N.d.	N.d.	N.d.	N.d.	N.d.
Er	0,090	0,080	2,680	0,390	3,990	1,110	2,090	0,777	1,880	0,923	1,140
Tm	N.d.	N.d.	N.d.	N.d.	N.d.	N.d.	N.d.	N.d.	N.d.	N.d.	N.d.
Yb	0,420	0,280	2,550	1,050	4,420	1,140	2,150	0,961	2,120	0,980	1,440
Lu	N.d.	N.d.	N.d.	N.d.	N.d.	N.d.	N.d.	N.d.	N.d.	N.d.	N.d.
Total	5,04	3,39	11,4	7,06	38,9	16,0	16,9	14,1	12,1	6,58	9,14
$(La/Yb)_n$	1,75	1,52	0,01	0,19	N.d.	0,11	0,06	0,17	0,03	0,06	0,03

	Yubileynaya pipe, Yakutia, Russia					Lakkerfontein province, South Africa			Monastery pipe, South Africa	
	[2], LA ICP-MS					[56], RNAA				
Element	Asch-1	Asch-2	Asch-3	Asch-4	Asch-5	RAJ L26	2631A	2631B	2631C	2631D
	Peridotites					*Megacrystals in kimberlites*				
La	0,150	0,050	0,030	0,020	0,160	0,040	N.d.	N.d.	N.d.	N.d.
Ce	0,610	0,140	0,100	0,110	0,290	0,260	0,510	0,450	0,410	0,380
Pr	0,130	0,030	0,020	0,020	0,080	N.d.	N.d.	N.d.	N.d.	N.d.
Nd	1,000	0,410	0,230	0,270	0,470	0,990	1,960	1,660	1,660	1,540
Sm	0,370	0,270	0,200	0,160	0,510	0,890	1,750	1,420	1,500	1,400
Eu	0,100	0,100	0,070	0,070	0,270	0,480	0,910	0,740	0,780	0,740
Gd	0,250	0,440	0,300	0,210	1,140	1,850	3,680	3,400	3,680	3,400
Tb	0,010	0,070	0,050	0,040	0,200	N.d.	N.d.	N.d.	N.d.	N.d.
Dy	0,080	0,420	0,310	0,150	1,120	»	7,060	6,710	7,100	5,900
Ho	0,010	0,100	0,060	0,020	0,180	»	N.d.	N.d.	N.d.	N.d.
Er	0,040	0,290	0,150	0,050	0,350	2,930	5,850	4,530	5,160	4,720
Tm	0,010	0,050	0,020	N.d.	0,040	N.d.	N.d.	N.d.	N.d.	N.d.
Yb	0,070	0,250	0,170	0,060	0,260	2,830	5,410	4,540	4,890	4,680
Lu	0,010	0,050	0,030	0,020	0,040	N.d.	N.d.	N.d.	N.d.	N.d.
Total	2,84	2,67	1,74	1,20	5,11	10,27	27,13	23,45	25,18	22,76
$(La/Yb)_n$	1,45	0,13	0,12	0,22	0,42	N.d.	N.d.	N.d.	N.d.	N.d.

	Monastery pipe, South Africa		Premier pipe, South Africa		Frank Smith pipe, South Africa	Saskatchewan province, Canada				Harterbest-fontein pipe
	[56], RNAA	[50]	[56], RNAA			[28], LA ICP-MS				[45], IPMA
Element	2631E	M-1	RA P10	RA P11	FS-1	KM1P	KM2P	KM3P	KM4P	HBF27
	Megacrysts in kimberlites					*Heavy fraction of kimberlites*				*Peridotite*
La	N.d.	0,049	0,070	0,330	0,300	0,030	0,030	0,550	0,020	0,037
Ce	0,420	N.d.	0,410	1,050	0,800	0,370	0,350	8,300	0,150	0,353
Pr	N.d.	»	N.d.	N.d.	0,190	0,180	0,160	2,800	0,070	N.d.
Nd	1,630	»	1,240	2,030	1,900	2,000	2,600	18,000	0,700	0,924
Sm	1,470	1,670	0,970	1,540	1,600	0,900	1,360	3,400	0,640	0,781
Eu	0,770	0,800	0,490	0,800	0,800	0,220	0,450	0,560	0,270	0,228
Gd	3,680	5,100	2,170	3,450	3,800	0,700	1,000	0,840	0,800	N.d.
Tb	N.d.	0,800	N.d.	N.d.	0,750	0,110	0,100	0,050	0,140	»
Dy	6,600	N.d.	4,010	4,570	6,200	0,800	0,510	0,170	1,040	0,983
Ho	N.d.	1,470	N.d.	N.d.	0,140	0,230	0,150	0,020	0,220	N.d.
Er	4,900	N.d.	2,800	6,570	4,400	0,800	0,750	0,050	0,740	0,883
Tm	N.d.	»	N.d.	N.d.	0,630	0,150	0,140	0,010	0,110	N.d.
Yb	4,940	5,000	2,900	4,950	4,300	1,190	1,200	0,130	0,900	1,099
Lu	N.d.	0,840	0,470	0,780	0,630	0,200	0,250	0,030	0,130	N.d.
Total	24,41	15,73	15,53	26,07	26,44	7,88	9,05	34,91	5,93	5,29
$(La/Yb)_n$	N.d.	0,01	0,02	0,04	0,05	0,02	0,02	2,86	0,01	0,02

Note. Here and further: N.d. – no data. After the references are listed the analytical methods for determination of REE.

Table 2. REE compositions of garnets from lherzolites and pyroxenites from xenoliths in alkaline basalts of Vitim province (Russia) (ppm).

	[49]									[82], SIMS		
Element	313-1	313-3	313-37	313-4	313-5	313-54	313-6	313-8	313-113G	V-231	V-102	V-437
	Lherzolites									*Pyroxenites*		
La	N.d.	N.d.	N.d.	N.d.	N.d.	N.d.	N.d.	N.d.	N.d.	0,010	0,020	0,020
Ce	»	»	»	»	»	»	»	»	»	0,090	0,060	0,140
Pr	»	»	»	»	»	»	»	»	»	N.d.	N.d.	N.d.
Nd	»	»	»	»	»	»	»	»	»	0,630	0,590	0,700
Sm	0,560	0,550	0,475	0,720	0,580	0,590	0,550	0,630	0,660	0,650	0,790	0,570
Eu	0,375	0,416	0,470	N.d.	0,420	0,395	Н.д.	0,440	0,463	0,340	0,460	0,310
Gd	N.d.	N.d.	N.d.	»	N.d.	N.d.	»	N.d.	2,950	N.d.	N.d.	N.d.
Tb	0,710	0,550	0,700	0,750	0,540	0,530	0,620	0,560	0,720	»	»	»
Dy	N.d.	N.d.	N.d.	N.d.	N.d.	N.d.	N.d.	N.d.	N.d.	4,280	9,580	2,910
Ho	1,37	1,19	1,64	1,64	1,70	1,16	1,01	1,45	1,80	N.d.	N.d.	N.d.
Er	N.d.	N.d.	N.d.	N.d.	N.d.	N.d.	N.d.	N.d.	N.d.	3,42	10,61	2,08
Tm	»	»	»	»	»	»	»	»	»	N.d.	N.d.	N.d.
Yb	4,78	3,79	7,45	5,45	4,73	3,49	2,99	5,65	8,75	4,27	15,42	2,38
Lu	0,710	0,650	1,09	0,830	0,770	0,510	0,462	0,990	1,42	N.d.	N.d.	N.d.
Total	N.d.	N.d.	N.d.	N.d.	N.d.	N.d	N.d.	N.d.	N.d.	13,7	37,5	9,11
$(La/Yb)_n$	»	»	»	»	»	»	»	»	»	0,002	0,001	0,006

Features of geochemistry of REE in garnets are considered depending on those petrographic types of rocks they participate in. The most common types of garnet-bearing rocks are the following: 1) high-pressure peridotites, mainly harzburgites and lherzolites from xenoliths in kimberlites, and 2) lherzolites and pyroxenites from xenoliths in alkaline basalts, and 3) inclusions in diamonds, and 4) eclogites from xenoliths in kimberlites and alkaline basalts, and 5) eclogites from high-pressure metamorphic complexes, and 6) some types of gabbros, and 7), some varieties of effusive rocks, and 8) skarns, and 9) gneisses, schist and other metamorphic mesobaric rocks.

High-pressure garnet peridotites, mainly harzburgites and lherzolites, from massifs and xenoliths. Garnets from these ultramafic rocks are studied in detail particularly regarding the REE distribution in samples from diamondiferous and non-diamondiferous deep-seated xenoliths presented in kimberlites (Table 1, Fig. 1). By chemical composition they are predominantly high-chromium (> 5% Cr_2O_3) and calcium-poor pyropes. The observations indicate significant heterogeneity of the REE distribution in them, in-

cluding their total compositions and the levels of accumulation of certain elements, the degree of fractionation of REE and configuration of the patterns. Based on the total sample of analysis of garnets from these rocks, compiled from our database, we found that the total REE content in these garnets is from a few grams per ton to 35 ppm.

In the garnets from harzburgite xenoliths presented in the Roberts Victor kimberlite pipe, the total REE concentrations vary in the range of 1.5–18.6 ppm, while for garnets from lherzolite xenoliths – 0.8–10.9 ppm. Garnets from harzburgites show wider fluctuations in concentrations of medium and heavy REE, while those from lherzolites show wider fluctuations for light elements. Some samples of garnets from harzburgites show depletion in heavy elements, starting with Sm and ending with Yb, which gives their REE patterns a sinusoidal appearance (Fig. 1-1). These garnets show smooth peaks around Pr, as well as smooth minima in the range between Gd and Er. Almost all analyzed garnets from lherzolite xenoliths of Roberts Victor pipe are depleted in light REE (LREE), and in the medium and heavy elements area their patterns have a flattened shape (Fig. 1-2). Evidence of heterogeneity of REE distribution in garnets from xenoliths of this pipe is wide variations in (La/Yb)n values from 0.01 to 14.2. REE compositions of garnets from diamondiferous peridotite xenoliths of Roberts Victor pipe correspond to the composition of REE in garnet from the primitive mantle. It is assumed that garnets from lherzolite parageneses characterize the event of its enrichment in LREE, whereas the samples of garnets from harzburgite parageneses have not been subjected to such enrichment [4, 5]. Having examined the representative collection of samples of garnets from peridotite xenoliths of Udachnaya kimberlite pipe (Yakutia), Pokhilenko et al. [6] and Shimizu et al. [7] determined that the total REE content in these garnets varies over a wide range (0.7–39.8 ppm). A significant portion of the studied garnets had sinusoidal REE pattern (Fig. 1-13, 15). Such patterns are commonly seen in garnets from peridotite xenoliths of Yubileynaya pipe (Fig. 1-16). Apart from the garnets with sinusoidal patterns in the xenoliths from Udachnaya pipe, there were also some garnets that were significantly depleted in LREE and at the same time enriched in heavy REE (HREE). These garnets are characterized by more simple, positively inclined patterns, flattened in the HREE (Fig. 1-14). An overwhelming majority of the garnets from xenoliths of Udachnaya pipe is characterized by very low values of (La/Yb)n = 0.01–0.20. Rarer are samples with (La/Yb)n = 2.1–9.4. By configuration of garnet patterns of Udachnaya pipe are comparable with some samples from peridotite xenoliths of South African kimberlite from Jagersfontein, Kimberley, Lourensia, Premier (Fig. 1-4, 5, 7, 8) and some other occurrences (Fig. 1–9, 10, 11, 12). Relatively simple, positively inclined REE distribution patterns were observed in garnets of megacrystals in kimberlites of Monastery (Fig. 1-18, 19) and Premier pipes (Fig. 1-20). All of these garnets are characterized by a fairly intense fractionation of REE, the level of accumulation of LREE in them is 0.2–2.0 times chondrite (hereafter: t.ch.) and of HREE is 20–40 t.ch. According to Pokhilenko et al. [6] calcium-poor chromian pyropes from peridotite xenoliths from Udachnaya pipe have undergone mantle metasomatism under the influence of fluids that allegedly had the geochemical characteristics of carbonatite melt. Probably, as a result of this process, pyrope garnets were enriched to varying degrees in LREE and simultaneously depleted in Ti. Features of the REE compositions of garnets composition from lherzolites and pyroxenites from xenoliths in alkali basalts are considered using the example of individual samples from xenoliths of Vitim province (Russia). In some samples of lherzolite only a partial range of REE was determined (Table 2). In the garnets from pyroxenites the fractionation of REE is more intense, they are significantly depleted in LREE (La $\approx$ 0.1 t.ch.) and are enriched with HREE (Lu $\approx$ 100 t.ch.). The parameter (La / Yb)n in these garnets is extremely low (~0.001–0.006).

Inclusions in diamonds. The adoption of microprobe methods of analysis of REE, including the method of LA ICP-MS, into geochemical studies of minerals allowed us to obtain much more reliable data on the concentrations of REE in garnets present in diamond crystals in the form of monomineralic or polymineralic microinclusions. The prevailing elements of these microinclusions are calcium-poor and high-chrome pyropes, which in association with clinopyroxene, orthopyroxene and olivine form a peridotite parageneses. Garnets of other compositions are usually found in association only with clinopyroxene (eclogite parageneses), characterized by low content of Cr and Mg and high contents of Ca and Al.

Let us consider the peculiarities of REE distribution in garnets from diamond microinclusions on the example of samples from Udachnaya, Mir and Aykhal kimberlite pipes (Yakutia province) [7], as well as pipes with placer occurrences confined to them, that are present in several provinces of South Africa and Canada (Table 3, Fig. 2). In general, the garnets that are present in diamond microinclusions from peridotite xenoliths are usually divided into two paragenetic types that to a certain extent differ in Ca content: harzburgite and lherzolite. In harzburgite parageneses samples the content of CaO varies in the range of ~0–6 wt %, which is considerably less than in the garnets from the microinclusions of lherzolite parageneses (5–8.6 wt %) [8]. Nevertheless, both types of garnets are almost identical by a total level of REE accumula-

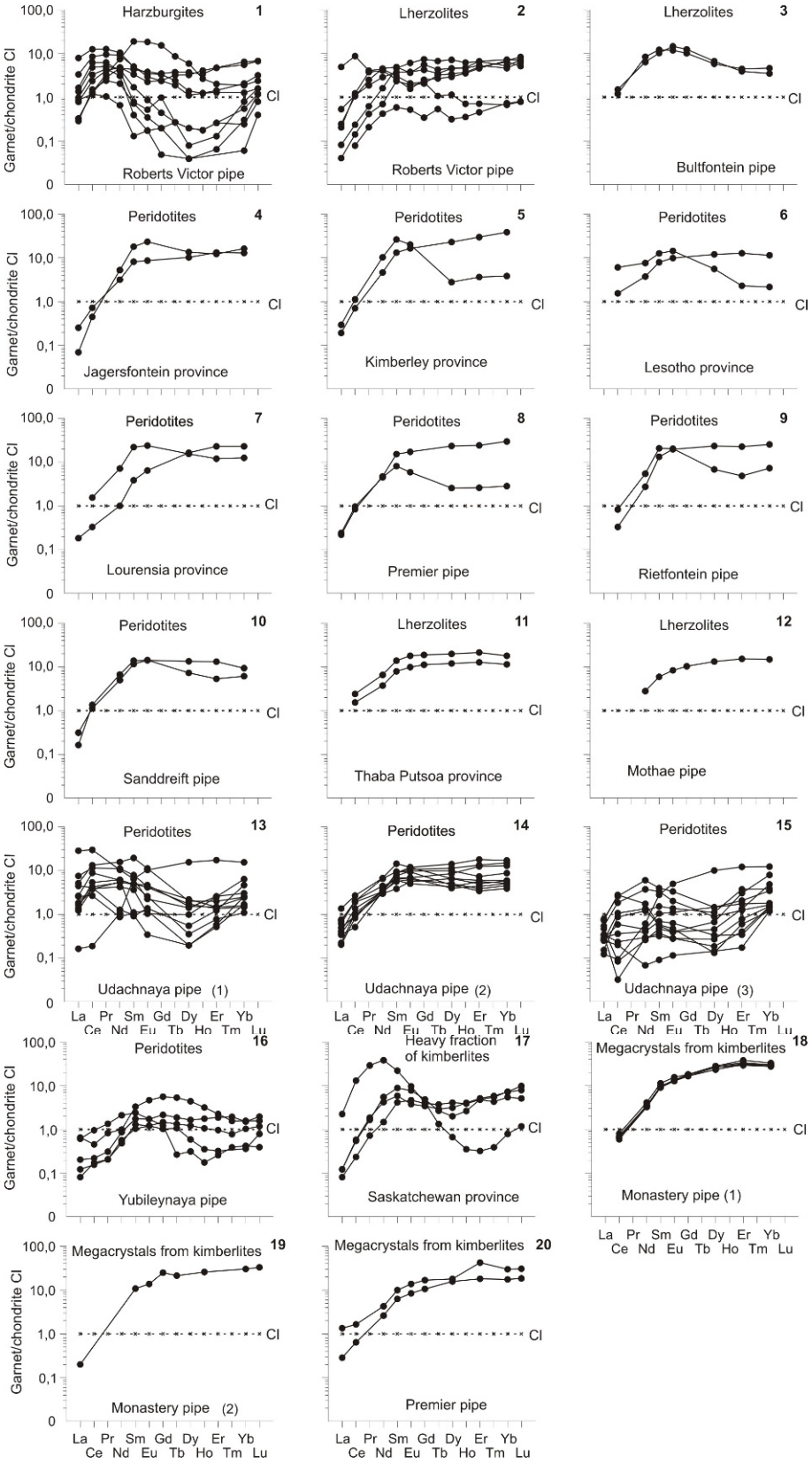

Figure 1. Chondrite-normalized REE patterns for garnets from peridotites from xenoliths from kimberlites, as well as megacrystals from kimberlites. Here and below, the normalization carried out on the chondrite C1 according (data [26]) (beginning).

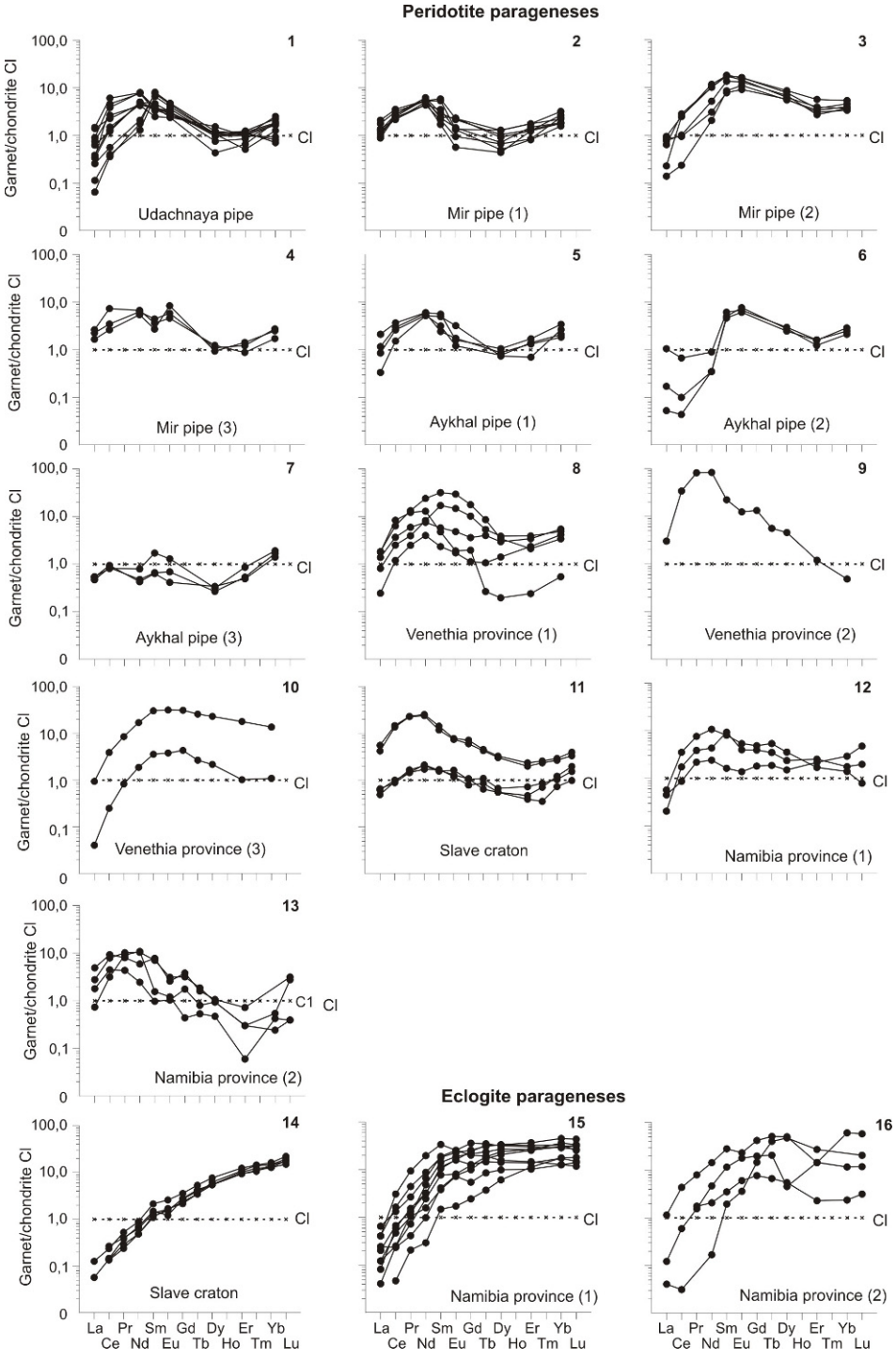

Figure 2. Chondrite-normalized REE patterns for garnets from microinclusions in diamonds (peridotite and eclogite parageneses) from xenoliths from kimberlites, as well as products of their disintegration.

Table 3. REE compositions of garnets from microinclusions in diamonds from kimberlites of some provinces, pipes and placers (peridotitic and eclogitic parageneses) (ppm).

Udachnaya pipe, Yakutia, Russia

[149], IPMA

Element	133/9-1	133/9-3	133/9-7	56K	136/9	118/29-1	118/29-6	135/9-21	135/9-22	135/9-23	135/9-3
					Peridotitic parageneses						
La	0,028	0,016	0,063	0,185	0,362	0,086	0,221	0,154	0,343	0,094	0,082
Ce	0,254	0,230	0,358	1,700	3,890	2,470	2,930	0,784	1,450	0,957	0,848
Pr	N.d.	N.d.	N.d.	N.d.	N.d.	N.d.	N.d.	N.d.	N.d.	N.d.	N.d.
Nd	0,617	0,841	0,992	2,01	3,72	3,78	3,63	2,40	2,150	2,10	2,35
Sm	1,02	1,24	1,17	0,386	0,590	0,605	0,511	0,553	0,531	0,610	0,716
Eu	0,234	0,275	0,260	0,138	0,183	0,162	0,209	0,176	0,156	0,140	0,182
Gd	N.d.	N.d.	N.d.	N.d.	N.d.	N.d.	N.d.	N.d.	N.d.	N.d.	N.d.
Tb	»	»	»	»	»	»	»	»	»	»	»
Dy	0,270	0,311	0,273	0,110	0,192	0,275	0,249	0,292	0,290	0,390	0,246
Ho	N.d.	N.d.	N.d.	N.d.	N.d.	N.d.	N.d.	N.d.	N.d.	N.d.	N.d.
Er	0,085	0,181	0,170	0,109	0,141	0,207	0,165	0,181	0,196	0,162	0,196
Tm	N.d.	N.d.	N.d.	N.d.	N.d.	N.d.	N.d.	N.d.	N.d.	N.d.	N.d.
Yb	0,210	0,134	0,273	0,318	0,292	0,368	0,416	0,290	0,117	0,155	0,303
Lu	N.d.	N.d.	N.d.	N.d.	N.d.	N.d.	N.d.	N.d.	N.d.	N.d.	N.d.
Total	2,72	3,23	3,56	4,96	9,37	7,95	8,33	4,83	5,23	4,61	4,92
$(La/Yb)_n$	0,09	0,08	0,16	0,39	0,84	0,16	0,36	0,36	1,98	0,41	0,18

Mir pipe, Yakutia, Russia

[149], IPMA

Element	717-1	717-5	51-10	51-11	51-12	92/9-26	92/9-27	92/9-28	92/9-29	92/9-30	92/9-31
						Peridotitic parageneses					
La	0,337	0,643	0,269	0,335	0,302	0,156	0,233	0,056	0,034	0,187	0,208
Ce	3,72	4,67	1,53	1,41	1,38	1,80	1,58	1,59	0,151	0,644	0,603
Pr	N.d.	N.d.	N.d.	N.d.	N.d.	N.d.	N.d.	N.d.	N.d.	N.d.	N.d.
Nd	2,60	3,18	2,06	2,08	2,36	4,79	5,55	4,86	0,972	2,45	1,46
Sm	0,793	0,560	0,538	0,327	0,262	2,68	2,74	2,80	1,32	2,10	1,20
Eu	0,167	0,266	0,077	0,055	0,033	0,846	0,948	0,931	0,644	0,769	0,529
Gd	N.d.	N.d.	N.d.	N.d.	N.d.	N.d.	N.d.	N.d.	N.d.	N.d.	N.d.
Tb	»	»	»	»	»	»	»	»	»	»	»
Dy	0,410	0,314	0,128	0,169	0,112	1,59	1,98	2,19	1,40	1,74	1,46
Ho	N.d.	N.d.	N.d.	N.d.	N.d.	N.d.	N.d.	N.d.	N.d.	N.d.	N.d.
Er	0,219	0,146	0,135	0,140	0,208	0,649	0,607	0,937	0,557	0,451	0,507
Tm	N.d.	N.d.	N.d.	N.d.	N.d.	N.d.	N.d.	N.d.	N.d.	N.d.	N.d.
Yb	0,278	0,284	0,260	0,397	0,295	0,601	0,756	0,887	0,652	0,609	0,554
Lu	N.d.	N.d.	N.d.	N.d.	N.d.	N.d.	N.d.	N.d.	N.d.	N.d.	N.d.
Total	8,52	10,1	5,00	4,91	4,95	13,1	14,39	14,25	5,73	8,95	6,52
$(La/Yb)_n$	0,82	1,53	0,70	0,57	0,69	0,18	0,21	0,04	0,04	0,21	0,25

Aykhal pipe, Yakutia, Russia

[149], IPMA

Element	49-17-1	49-17-3	49-17-5	267-2	267-8	267-10	217-1	217-2	217-5	189
					Peridotitic parageneses					
La	0,284	0,518	0,209	0,131	0,133	0,115	0,258	0,013	0,042	0,082
Ce	1,88	2,34	1,66	0,598	0,517	0,539	0,429	0,028	0,064	0,969
Pr	N.d.	N.d.	N.d.	N.d.	N.d.	N.d.	N.d.	N.d.	N.d.	N.d..
Nd	2,77	2,85	2,52	0,203	0,375	0,226	0,424	0,166	0,165	2,46
Sm	0,371	0,862	0,486	0,098	0,265	0,102	0,945	0,711	0,761	0,761
Eu	0,101	0,093	0,070	0,024	0,075	0,040	0,392	0,353	0,445	0,186
Gd	N.d.	N.d.	N.d.	N.d.	N.d.	N.d.	N.d.	N.d.	N.d.	N.d.
Tb	»	»	»	»	»	»	»	»	»	»
Dy	0,222	0,268	0,195	0,087	0,080	0,068	0,750	0,627	0,704	0,187
Ho	N.d.	N.d.	N.d.	N.d.	N.d.	N.d.	N.d.	N.d.	N.d.	N.d.
Er	0,220	0,283	0,233	0,082	0,143	0,089	0,268	0,263	0,205	0,116
Tm	N.d.	N.d.	N.d.	N.d.	N.d.	N.d.	N.d.	N.d.	N.d.	N.d.
Yb	0,304	0,566	0,345	0,232	0,316	0,277	0,406	0,476	0,349	0,439
Lu	N.d.	N.d.	N.d.	N.d.	N.d.	N.d.	N.d.	N.d.	N.d.	N.d.
Total	6,15	7,78	5,72	1,46	1,90	1,46	3,87	2,64	2,74	5,20
$(La/Yb)_n$	0,63	0,62	0,41	0,38	0,28	0,28	0,43	0,02	0,08	0,13

	Venetia province, South Africa								Slave craton, Canada	
	[155], SIMS								[122]	
Element	V-64a	V-87b	V-95	V-112a	V-167b	V-169a	V-195a	V-197ab	3-3/00-1	3-3/00-2
	Peridotitic parageneses									
La	0,440	0,450	0,010	0,740	0,340	0,200	0,230	0,060	0,150	0,160
Ce	5,33	4,05	0,160	21,6	2,34	1,60	2,48	0,760	0,640	0,560
Pr	1,17	1,28	0,080	7,88	0,570	0,380	0,820	0,240	0,140	0,140
Nd	6,12	11,3	0,890	39,5	3,570	3,87	8,01	1,89	0,810	1,01
Sm	0,730	4,89	0,550	3,42	0,890	2,61	4,66	0,360	0,260	0,250
Eu	0,110	1,71	0,220	0,720	0,280	0,850	1,83	0,100	0,069	0,075
Gd	0,400	3,60	0,880	2,71	0,740	2,07	6,35	0,230	0,160	0,220
Tb	0,010	0,320	0,100	0,210	0,150	0,200	0,960	0,040	0,032	0,024
Dy	0,050	0,870	0,550	1,16	0,750	0,980	5,83	0,360	0,140	0,140
Ho	0,010	0,150	0,080	0,120	0,170	0,150	1,13	0,090	0,019	0,034
Er	0,040	0,350	0,170	0,200	0,570	0,650	2,96	0,390	0,065	0,078
Tm	N.d.	N.d.	N.d.	N.d.	N.d.	N.d.	N.d.	N.d.	0,009	0,018
Yb	0,090	0,560	0,180	0,080	0,900	0,800	2,24	0,680	0,120	0,200
Lu	0,040	0,090	0,060	0,010	0,130	0,150	0,280	0,150	0,025	0,050
Total	14,5	29,6	3,93	78,4	11,4	14,5	37,8	5,35	1,91	2,96
$(La/Yb)_n$	3,30	0,54	0,04	6,24	0,25	0,17	0,07	0,06	0,84	0,54

	Slave craton, Canada							Namibia province	
	[122]							[38], SIMS	
Element	3-3/00-3	31-3/00-35	31-3/00-36	5-6/00-112	5-6/00-113	6/00-114	5-6/00-115	5-6/00-116	Nam-24	Nam-46
	Peridotitic parageneses			*Eclogitic parageneses*					*Peridotitic parageneses*	
La	0,120	1,03	1,36	0,031	N.d.	0,014	N.d.	N.d.	0,110	0,140
Ce	0,590	8,66	9,36	0,150	0,170	0,089	0,093	0,086	0,550	2,24
Pr	0,160	2,20	2,22	0,051	0,039	0,028	0,037	0,023	0,210	0,730
Nd	0,970	11,3	12,0	0,420	0,300	0,230	0,330	0,230	1,14	5,06
Sm	0,240	1,81	2,19	0,330	0,210	0,180	0,230	0,170	0,250	1,23
Eu	0,095	0,430	0,450	0,150	0,095	0,089	0,070	0,098	0,080	0,310
Gd	0,210	1,22	1,46	0,730	0,480	0,570	0,550	0,440	0,370	0,990
Tb	0,041	0,160	0,170	0,200	0,130	0,160	0,150	0,130	0,070	0,200
Dy	0,170	0,770	0,830	1,95	1,58	1,40	1,38	1,38	0,380	0,900
Ho	0,026	0,150	0,130	0,530	0,410	0,440	0,360	0,380	0,100	0,140
Er	0,120	0,330	0,390	2,05	1,79	1,69	1,56	1,55	0,360	0,280
Tm	0,022	0,060	0,066	0,370	0,360	0,310	0,270	0,280	N.d.	N.d.
Yb	0,170	0,440	0,480	2,67	2,39	2,13	2,43	2,11	0,480	0,230
Lu	0,039	0,084	0,100	0,560	0,440	0,450	0,490	0,380	0,120	0,020
Total	2,97	28,6	31,2	10,2	N.d.	7,78	N.d.	N.d.	4,22	12,5
$(La/Yb)_n$	0,48	1,58	1,91	0,01	»	N.d.	»	»	0,15	0,41

	Namibia province									
	[38], SIMS					[155], SIMS				
Element	Nam-110	Nam-71	Nam-118	Nam-33	Nam-92	Nam-13	Nam-35	Nam-38	Nam-47	Nam-5
	Peridotitic parageneses					*Eclogitic parageneses*				
La	0,180	0,680	0,130	0,080	0,070	0,020	0,100	0,060	N.d.	0,100
Ce	2,01	5,03	2,41	0,580	0,480	0,380	1,050	0,150	0,030	1,98
Pr	0,880	0,980	0,940	0,150	0,090	0,150	0,430	0,040	0,020	0,910
Nd	5,12	4,91	5,88	0,990	1,10	1,55	4,17	0,470	0,140	9,30
Sm	0,240	1,08	1,98	1,29	0,790	1,62	2,80	0,640	0,230	5,22
Eu	0,070	0,180	0,580	0,530	0,070	0,94	1,33	0,440	0,100	1,48
Gd	0,090	0,650	1,59	1,75	0,460	4,92	5,25	2,04	0,500	7,32
Tb	0,020	0,070	0,150	0,080	0,030	1,22	1,16	0,640	0,140	1,31
Dy	0,120	0,240	0,370	0,310	0,220	8,49	8,50	5,27	1,56	8,10
Ho	0,010	0,030	0,030	0,050	0,050	1,93	1,90	1,28	0,450	1,67
Er	0,010	0,050	0,090	0,040	0,120	5,40	6,14	4,20	1,89	5,01
Tm	N.d.	N.d.	N.d.	N.d.	N.d.	N.d.	N.d.	N.d.	N.d.	N.d.
Yb	0,070	0,040	0,160	0,100	0,080	5,39	7,44	5,11	2,91	4,75
Lu	0,010	0,010	0,020	0,030	0,030	0,650	1,11	0,820	0,460	0,680
Total	8,83	14,0	14,3	5,98	3,59	32,7	41,4	21,2	N.d.	47,8
$(La/Yb)_n$	1,74	11,47	0,55	0,54	0,59	0,003	0,009	0,008	»	0,014

tion, as well as by the configuration of REE pattern, and both show a generally sinusoidal shape in REE pattern. Compared with the garnets from the microinclusions in diamonds that belong to the peridotite parageneses, the samples of microinclusions of eclogite parageneses have rare earth pattern of a simpler form. Most often it is a slightly convex upward line with an overall steep positive slope.

Within the available sample analyses of garnets from microinclusions in diamond, the total REE concentrations vary in the range of 1.2–78 ppm. The value of the (La/Yb)*n* parameter varies from 0.008 to 11.5, with an average of ~9.6 ppm. For particular samples of analysis of garnets from diamond microinclusions, the total REE concentrations vary within the following ranges by different pipes: 1) xenoliths of megacrystalline peridotites of Udachnaya pipe – 3–39 ppm; 2) xenoliths of peridotites of Aykhal pipe – 1.5–1.9 ppm; 3) xenoliths of peridotites of Mir pipe – ~5 ppm; 4) xenoliths of peridotites in Yubileynaya pipe – 1.2–5.1 ppm.

Heterogeneity of the REE composition of garnets from diamond inclusions, represented in each of kimberlite pipes, manifests in variations of not only the total content of elements, but also of the configuration of the pattern. For example, in the garnets from Udachnaya and Mir pipes the peak of the patterns is in the Sm area, while in other cases the peak is in the Nd area (Fig. 2-1, 2, 3, 4). Such differences in the pattern were observed also for the garnets from xenoliths from Aykhal pipe (Yakutia province, Russia), Venetia, and Namibia provinces (South Africa), as well as Slave craton (Canada) (Fig. 2-5, 6-13). All of these garnets in one way or another differ in the (La/Sm)*n* parameter values, by using these values we divided the garnets from diamond microinclusions of Udachnaya pipe into two groups: for the first, (La/Sm)n = 0.01–0.1 and for the second – 0.22–0.41. The garnets from microinclusions in the diamonds of Mir pipe are divided into three groups with different (La/Sm)*n* values: 0.01–0.11, 0.27–0.73 and 1.35–1.44, respectively. Similar differences in REE composition were observed in garnets from some other kimberlite occurrences and provinces. As emphasized above, the garnets from the microinclusions in diamonds of eclogite parageneses differ significantly in the REE composition from those that are present in peridotite parageneses. Within the whole range of analysis of these garnets, the total REE compositions vary in the range of 6.4–56 ppm with an average of 22.6 ppm, while (La/Yb)*n* values vary from 0.003 to 0.050 with an average value of 0.015. The REE patterns generally have a steep positive slope, which is most clearly observed in samples from the Slave craton (Canada) and Namibia province. However, it should be noted that in contrast to the pattern of garnets from the Slave craton, which have a nearly linear shape (Fig. 2-14), the patterns of the samples from Namibia province are characterized by a subhorizontal portion in the area of heavy REE (Fig. 2-15), and more rarely they have a negative slope due to the relative depletion in heavy elements (Fig. 2-16).

Eclogites from xenoliths. The REE composition of garnets from eclogite xenoliths is characterized by the example of samples from Roberts Victor, Bobbejaan and Koidu pipes (Table 4). Garnets of this type contain a relatively low pyrope fraction and a high content of grossular. The total REE contents in garnets from eclogites of Roberts Victor pipe vary in the range of 3–13 ppm. The exception is specimen HRV-175, for which the total REE is as high as 35 ppm, which is mainly due to the anomalous enrichment with medium elements. In the garnets from Bobbejaan and Koidu pipes the total REE contents are comparable to those for samples from Roberts Victor pipe (3.3–18.1 ppm). The only exception is sp. KEC 86-19 for which the total REE is 52 ppm due to enrichment with medium and heavy elements. Chondrite-normalized HREE contents in all garnets from eclogite parageneses are much higher than that of light elements, the values of (La/Yb)*n* range from 0.001 to 0.47. This pattern is most clearly expressed in samples from xenoliths of Roberts Victor and Koidu pipes. By their configuration of REE pattern the garnets from Roberts Victor pipe are divided into two types: 1) garnets that are moderately depleted in LREE and, accordingly, have a flattened form of the patterns in the area of medium and heavy elements, and 2) garnets intensively depleted in LREE, particularly cerium. In one of the samples the garnet is anomalously enriched with Eu. Moreover, some garnets from eclogites, provided in the xenoliths from kimberlites of Udachnaya pipe, are characterized by a zonal distribution of REE, which becomes apparent in a gradual increase of the content of light elements moving from the central zone of garnet grains to the marginal, as well as in the depletion by HREE in the same direction. *Eclogites of high-pressure metamorphic complexes.* Eclogites of this type are spread in tectonically exhumed high-pressure metamorphic formations among the ancient folded structures. Some features of the REE distribution in garnets of these areas are considered by the example of the samples from Norway, Switzerland, Kazakhstan and Kyrgyzstan metamorphic complexes. Garnets from eclogites presented in Norwegian metamorphic complexes are notable for a much lower total REE content (6.5–18.2 ppm) compared with the samples from Soazza complex (Switzerland) (34–148 ppm). Garnets from eclogites represented in Kazakhstan (22–44 ppm) and Kyrgyzstan (16.4–31.6 ppm) metamorphic complexes occupy an intermediate position on this basis. The samples of Soazza complex demonstrate the most intense fractionation of REE, which is due to its depletion by LREE and enrichment with heavy elements, as it is shown on the configuration of REE pattern. Due to the relative enrichment with LREE, patterns of garnets from Kazakhstan complexes (Kumdy-Kol', Sulu Tube, Chiglinka, Kulet), as well as from Atbashi complex in South Tien Shan (Kyrgyzstan) [9], have a more gentle positive slope. In some patterns we can observe neg-

Table 4. REE compositions of garnets from eclogites from xenoliths in kimberlites of some provinces and pipes (ppm).

	Roberts Victor pipe, South Africa								
	[40], SIMS								
Element	IIRV-145	IIRV-247	IIRV-173	IIRV-110	IIRV-30-7	IIRV-243	IIRV-30-1	IIRV-30-6	IIRV-244
	Eclogites								
La	0,030	0,060	0,040	0,010	0,140	0,030	0,270	0,040	0,010
Ce	0,230	0,570	0,250	0,080	0,450	0,250	0,660	0,210	0,010
Pr	N.d.	N.d.	N.d.	N.d.	N.d.	N.d.	N.d.	N.d.	N.d.
Nd	1,79	1,96	0,870	0,280	1,25	0,790	1,18	0,890	0,140
Sm	0,840	1,22	0,450	0,330	1,00	0,420	0,800	0,810	0,280
Eu	0,390	0,580	0,230	0,220	0,480	0,240	0,390	0,390	0,220
Gd	N.d.	N.d.	N.d.	N.d.	N.d.	N.d.	N.d.	N.d.	N.d.
Tb	0,200	0,340	0,420	0,140	0,440	0,220	0,360	0,330	0,290
Dy	1,44	2,33	3,820	1,170	3,10	2,010	2,63	2,39	2,29
Ho	0,260	0,480	0,980	0,300	0,710	0,560	0,610	0,600	0,540
Er	0,830	1,22	3,10	1,01	2,35	1,93	1,86	1,78	1,79
Tm	N.d.	N.d.	N.d.	N.d.	N.d.	N.d.	N.d.	N.d.	N.d.
Yb	»	»	»	»	»	»	»	»	»
Lu	0,110	0,130	0,440	0,300	0,350	0,450	0,290	0,290	0,330
Total	6,12	8,89	10,6	3,84	10,3	6,90	9,05	7,73	5,90
$(La/Yb)_n$	0,03	0,06	0,04	0,01	0,14	0,03	0,27	0,04	0,01

	Roberts Victor pipe, South Africa				Bobbejaan pipe , South Africa				
	[40], SIMS				[15], INAA				
Element	HRV-67	HRV-175	HRV-277	HRV-98	SBB-2H	SBB-3H	SBB-7P	SBB-25	SBB-34
	Eclogites								
La	0,010	0,020	0,230	0,020	0,224	0,107	0,576	0,563	0,320
Ce	0,020	0,020	1,40	0,260	0,644	0,381	2,050	1,26	0,895
Pr	N.d.	N.d.	N.d.	N.d.	N.d.	N.d.	N.d.	N.d.	N.d.
Nd	0,080	0,240	4,04	0,660	0,397	0,642	4,85	0,653	0,395
Sm	0,200	0,960	2,62	0,510	0,179	0,215	1,88	0,580	0,461
Eu	0,170	0,700	1,43	0,200	0,148	0,206	0,843	0,266	0,269
Gd	N.d.	N.d.	N.d.	N.d.	N.d.	N.d.	N.d.	N.d.	N.d.
Tb	0,190	1,42	0,340	0,090	0,090	0,291	0,418	0,233	0,299
Dy	1,87	13,0	1,49	0,570	1,01	0,136	0,906	1,56	1,95
Ho	0,460	3,50	0,290	0,100	N.d.	N.d.	N.d.	N.d.	N.d.
Er	1,60	13,1	0,800	0,360	»	»	»	»	»
Tm	N.d.	N.d.	N.d.	N.d.	»	»	»	»	»
Yb	»	»	»	»	0,552	2,710	0,824	1,80	4,88
Lu	0,330	2,53	0,110	0,080	0,071	0,429	0,128	0,272	0,804
Total	4,93	35,4	12,8	2,85	N.d.	N.d.	N.d.	N.d.	N.d.
$(La/Yb)_n$	0,01	0,02	0,23	0,02	0,27	0,03	0,47	0,21	0,04

	Bobbejaan pipe, South Africa			Koidu province, Sierra Leone						
	[15], INAA			[5], LA ICP-MS						
Element	SBB-37	SBB-39	SBB-61	KEC 80-B1	KEC 81-2	KEC 86-15	KEC 86-19	KEC 86-58	KEC 86-73B	KEC 86-107
				Eclogites						
La	0,398	0,082	0,995	0,030	0,015	0,030	0,030	0,100	0,200	0,031
Ce	0,827	0,360	1,85	0,037	0,120	0,034	0,160	0,080	0,090	0,200
Pr	N.d.	N.d.	N.d.	0,050	N.d.	0,020	N.d.	N.d.	N.d.	0,060
Nd	0,905	0,301	1,81	0,300	0,500	0,230	0,830	0,350	0,520	0,640
Sm	0,854	0,409	1,42	0,610	0,720	0,360	0,970	0,490	0,700	0,600
Eu	0,456	0,190	0,708	0,390	0,400	0,280	0,530	0,220	0,330	0,340
Gd	N.d.	N.d.	N.d.	2,20	2,070	1,47	3,000	1,430	1,600	1,70
Tb	0,521	0,275	0,461	0,550	N.d.	0,370	N.d.	N.d.	N.d.	0,450
Dy	3,73	0,266	2,24	4,75	3,69	3,140	11,3	3,75	3,91	3,60
Ho	N.d.	N.d.	N.d.	1,11	0,870	0,760	N.d.	N.d.	N.d.	0,850
Er	»	»	»	3,56	2,78	2,35	14,0	3,40	2,96	3,83
Tm	»	»	»	0,510	N.d.	0,340	N.d.	N.d.	N.d.	0,390
Yb	6,55	3,07	1,66	3,47	2,73	2,11	17,9	3,78	3,19	2,70
Lu	1,02	0,493	0,239	0,580	0,450	0,330	2,93	0,630	0,470	0,430
Total	N.d.	N.d.	N.d.	18,2	N.d.	11,8	N.d.	N.d.	N.d.	15,8
$(La/Yb)_n$	0,04	0,02	0,40	0,006	0,004	0,010	0,001	0,018	0,042	0,008

ative Eu anomalies (Sulu Tube complex), or Nd and Sm anomalies (Norwegian complexes). Eclogites from Atbashi metamorphic complex are denuded in a series of small tectonic blocks in the valley of Kembel' river, draining the western spurs of Atbashi ridge. Their first structural-geological description was given by [10], and then a detailed petrographic, petrochemical, mineralogical and geochemical study of eclogites was carried out from this, as well as from some other eclogite-bearing complexes of Tien Shan [7, 11, 12].

Gabbros. Garnets are uncommon in gabroic rocks. Garnets from the Ivrea-Verbano granulite-facies mafic-ultramafic complex have range from 47-52% almandine and 16-19% grossular, with low Cr concentrations (20-300 ppm) [85]. These garnets occur both as primary igneous phenocrysts and as reaction rims between plagioclase and olivine/clinopyroxene. The phenocrysts have slight negative Eu anomalies and total REE from 40-80 ppm, whereas the reaction rims often have large positive Eu anomalies (presumably inherited from the plagioclase) and lower total REE (10-50 ppm).

Effusive rocks. The REE composition of garnets from volcanic rocks is characterized by the example of a small collection of samples with different chemical compositions, which are presented in the form of relatively large phenocrysts or megacrystals in alkali olivine basalts (pyrope), hawaiites (almandine), nepheline basanites (pyrope), andesites (almandine), dacites (almandine), rhyodacites (almandine) and rhyolites (almandine). Most of them are characterized by high total REE content (167-653 ppm); the highest values are in the mineral from rhyolites. A partial exception is the garnet from basanite with a total REE content ~17 ppm. The REE patterns of garnets from effusive rocks of mafic composition have the form of almost straight lines with a steep positive slope: $(La/Yb)n \approx 0.002$-0.015. The REE patterns of garnets from dacites, rhyodacites and rhyolites are complicated by intense negative Eu anomalies, which is probably due to the preferential occurrence of Eu in plagioclase that is prevailing in these effusions.

Skarns. The REE composition of garnets from skarns was studied in samples of Broken Hill lead-zinc-silver deposit (Australia), as well as from Ocna de Fier province (Romania) [14]. In the ore bodies of Broken Hill deposit as a part of fine-medium-grained skarns the garnets make up 80-95% of their volume, excelling with very low MgO content (0.14-2.8 wt %). Given the distribution of MnO, the spessartine (18.3-28.4 wt %) and the almandine (2.4 wt %) are singled out among them. Within the individual grains of these garnets, the REE distribution is uneven: in the inner areas the total content varies in the range of 12.4-48.3 ppm, and in the peripheral areas it is slightly higher (12.5-54.5 ppm) which is associated with a significant accumulation of heavy REE. On this basis the garnets from skarns differ from garnets from eclogites and other rocks of metamorphic complexes, in which the peripheral zones of grains are depleted in HREE. Garnets from skarns are characterized by intense fractionation of REE: $(La/Yb)n = 0.002$-0.033. REE compositions of garnets from skarns of Broken Hill deposit were inherited from the composition of protolith which was enriched with REE well in advance of the appearance of metamorphic garnet, i.e. it is not associated with later hydrothermal processes [15].

Garnets from skarns of Once de Fier province (Romania) are andradite (sample NM33b) and grossular-andradite (sample NM34). The total REE content in them is much lower (6.8-7.5 ppm) than in samples from Broken Hill deposit. Because of the anomalous enrichment of these garnets with LREE, their patterns have a negative slope: $(La/Yb)n = 11$-16. Garnets from skarns of Crown Jewel gold deposit (Washington State, USA) [16] were studied in more detail. They are represented by varieties of grossular-andradite series with fairly wide variations in the contents of grossular and andradite. Among them there are both anisotropic and isotropic versions. All of these garnets are depleted in large-ion lithophile elements, as well as Ta, Hf and Th. The total REE contents in them vary over a wide range, in certain samples some of the elements are contained within the limit of detection.

Our analyses included in the compiled database yielded estimates of the average content of REE in garnets from rocks of various composition and genesis. The average REE contents vary from very low, typical of garnets from peridotite xenoliths of Aykhal pipe (2.36 ppm), to very high (314 ppm), ascertained in the samples of dacites volcanogenic complex (Japan). The vast majority of these values are in some way superior to the content of REE in Cl chondrite. In the garnets from peridotite xenoliths of Aykhal pipe, from pyroxenite xenoliths in basalts of Vitim plateau, from eclogites in xenoliths of Roberts Victor pipe, from Soazza metamorphic complex, as well as from skarns of Brocken Hill deposit, the average content of light REE is smaller than in Cl chondrite. In addition, distribution patterns of the average REE contents in garnets from peridotite xenoliths of diamondiferous kimberlites of Roberts Victor, Udachnaya, Aykhal and Mir pipes have a sinusoidal configuration.

Studies on the patterns of REE distribution in garnets, which are in the parageneses with diamonds in kimberlites and the xenoliths of mantle peridotite contained in them, in recent years received increasing attention. These garnets by their chemical composition correspond with pyropes and usually have specific sinusoidal REE patterns, which have been described for the first time by [17]. The

most important feature of these garnets is an anomalous enrichment in LREE with a relative depletion by medium and heavy elements, and this is due to the unusual sinusoidal shape of the patterns. Pyropes with similar REE patterns at different times were found in the diamond fields from Liqhobong, Lesotho, Jagersfontein and Premier (South Africa) provinces [5, 18–20], in xenoliths of megacrystalline peridotites from Udachnaya, Mir, Aykhal pipes and others (Yakutia) [6, 7, 18, 20, 21], in xenoliths of harzburgites and lherzolites from Roberts Victor pipe (South Africa) [15], in xenoliths of eclogites from Mbuji-Mayi deposit (Congo) [22], in xenocrysts of kimberlites from Camsell Lake (Canada). As mentioned above, the sinusoidal REE patterns have been also ascertained in many garnets, which are micro-inclusions in diamond crystals. However, there are examples when sinusoidal patterns, which are typical for inner zones of garnet crystals from micro-inclusions in diamonds, moving towards the peripheral zones were replaced by those more common for garnet patterns of simple form with a steep positive slope [23]. Apart from sinusoidal shape of patterns in the garnets associating with diamonds, other kinds of anomalous patterns were found: in particular, arched up or with an almost flat shape in the range between Sm and Lu.

The nature of sinusoidal shape of the REE patterns of garnets is still a subject of debate. Originally it was assumed that the origin of such patterns in garnets was caused by metasomatic change of mantle substrate that preceded the formation of garnets and diamonds in peridotite parageneses [17]. Later it was suggested that peridotites, containing garnets with a sinusoidal REE distribution, right after its formation have undergone a metasomatic recycling under the influence of deep-seated melts that were geochemically similar to carbonatite and that this process was a really time-consuming one [6]. It is the proximity of the REE compositions of garnets from micro-inclusions in diamond crystals and their varieties, which are parts of peridotite xenoliths from Roberts Victor and Akwatia pipes, that allowed to assume that the garnets from harzburgites and lherzolites, presented in the xenoliths, were formed from protolith, which had previously been depleted during partial melting in stability field of spinel [4]. There is also a hypothesis that subcalcium pyropes from deep-seated xenoliths were formed during the metasomatic transformation of spinel harzburgites in the stability field of diamond, and the process involved carbon-bearing fluids or melts [24]. It was also assumed that zoning in the distribution of REE and other impurities in subcalcium garnets, associating with diamonds, could be due to the continuous growth of grains on the background of the changes in *PT*-conditions of crystallization [19]. It was taken into account that the inner zones of garnet grains, apparently, were originally crystallized under nonequilibrium conditions, which have been replaced by the equilibrium conditions till the moment of crystallization of the peripheral zones, and it was considered that the growth of zonal garnet crystals and associating diamonds occurred shortly before they got into the kimberlite matrix. According to [23], a similar mechanism of formation of garnet can explain the transformation from the sinusoidal patterns of REE distribution to ordinary patterns as we move from the inner zones of garnet crystals towards the peripheral.

Apparently, for a more accurate study of the proposed mechanisms of arising for sinusoidal patterns of REE distribution in garnets, associating with diamonds, an additional research is needed. However, it is already obvious that namely this multistage and different by *PT*- parameters history of garnet crystals growth was the most important reason that even within a single manifestation the garnet samples of identical petrographic composition of the mantle xenoliths do often differ on the basis of the REE pattern configuration. The examples of such geochemical heterogeneity can be the garnets from diamondiferous Roberts Victor, Udachnaya, Aykhal and Mir kimberlite pipes. It is important to mention that the sinusoidal REE pattern, identified in the garnets containing more than 12 wt % Cr_2O_3 and having a higher content of knorringite (more than 30 %), are currently supposed to be the most important search criteria for assessing the potential diamond-bearing of kimberlite provinces [25].

It is well known that on the periphery of garnet segregations presented in the form of xenocryss in kimberlites those were often observed kelyphitic rims of complex structure, the formation of which is usually associated with exposure of kimberlite melts and fluids. Special studies showed that this kind of rims by their REE composition are close to the garnet crystals surrounded by them and differ significantly from their host kimberlites. These observations suggest that the formation of kelyphitic rims around the garnet crystals is not causally associated with exposure of the kimberlite melts which have pass them to the surface, but is caused by some earlier abyssal metasomatic processes [26].

Researchers studying the geochemistry of garnets are constantly paying attention to the regularity of distribution of REE and other trace elements between this mineral and coexisting melts, and solid phases [27, 28]. In order to obtain estimates of coefficients of distribution of REE between garnet and melt (hereinafter – D (garnet/melt)) there are usually used both natural and experimental systems involving ultramafic, basaltic, andesitic, dacitic, rhyodacitic and rhyolitic melts. To date, the biggest number of

D estimates is obtained for Sm, Yb, Lu and Ce, very little data for Gd, Tb, Ho and almost no data for Pr and Tm (Table 5). Among the first there were obtained the estimates of upon the analysis of REE in garnet phenocrystals and containing them poorly crystallized matrix of dacites from volcanic complexes in Japan [29]. In this case, the values of D (garnet / dacitic melt) for La, Ce and Nd range between 0,3 and 0,4, then, increasing for Sm, have a distinct minimum for Eu, after which the curve gets a steeper positive slope with increasing D values in the series from Gd (10.5) to Yb (26.0) and Lu (24.6). Over time, the results of experimental studies were mainly used to determine the values of D(garnet / melt) [30, 31]. The effect of such parameters as the chemical composition of the garnets, the total REE content in the system, the silica content in the melts, as well as temperature and pressure during crystallization, is usually taken into account during these studies [32–34]. The data obtained by these experiments confirmed earlier observations that indicated that the majority of the diagrams of D (garnet / melt) values have a steep positive slope, but sometimes they are complicated by anomalies for several elements. There was also a trend found in increasing of D values for all REE while changing of the chemical composition of melts from high-Mg ultramafic to basaltic and high-Si, and this tendency is more significant for D values for HREE. The function of values of D on the temperature and pressure of crystallization of the mineral was studied in the experiments in garnet-ultramafic melt system [35, 36]. In particular, it was shown that with decreasing pressure in the range of 20-5.5 GPp the values of D (garnet / ultramafic melt) vary in the following ranges: La (0.03-0.08); Sm (0.04-0.20); Gd (0.03-0.39); Yb (0.32-2.36). In another experiment it was determined that during the crystallization of garnet at 1420°C the value of D (garnet / andesitic melt) for Yb is 12, and at a temperature of 940°C - about 44 [37]. Moreover, according to the results of these experiments, in almost all the cases the values of D (garnet / melt) for the LREE are less than 1, while for the elements from Sm to Lu, they are usually > 1.

Judging by the shape and slope of diagrams of change in the values of D (garnet / melt) for the ultramafic and mafic melts, these values are close to a straight and inverse logarithmic function on the ionic radii of the REE. In contrast to the diagrams of changes of D (garnet / melt) for the ultramafic and mafic melts, such graphics for high-Si melts are usually complicated by the minimum for Eu. In this case, the available data give grounds to conclude that during the crystallization of garnet from a melt of any composition their residual fractions have been intensively depleted in HREE and, conversely, enriched with LREE. Based on the fact that D (garnet / melt) for the heavy REE with smaller ionic radii tend to have values > 1, and for light elements with large ionic radii - < 1, it can be assumed that LREE in the garnet structure represented incompatible elements, and the heavy REE possessed the properties of fully compatible trace elements.

The D(Yb)/D(Ce) parameter values, calculated from the experimental studies on the distribution of REE between coexisting garnets and melts of different composition, describing the fractionation intensity of these impurities during the crystallization of garnet, vary within very wide limits (Table 5). Thus, for ultramafic melts the range of variation of this parameter is 120-500, for basaltic melts it is much wider - 30-1320, and for melts of dacite, rhyodacite and rhyolite composition, by contrast, it is much narrower - 25-64.

Available data on D (garnet / melt) values are often used in solving inverse problems, i.e. determining the REE compositions of model parental melts, from which garnets were crystallized. Similar calculations were performed using the average REE compositions of garnets from the ultramafic xenoliths from Roberts Victor, Udachnaya, Aykhal and Mir kimberlite pipes, and have shown that the REE compositions of the model parental melts for ultramafites of these xenoliths were very similar, both by the overall level of REE accumulation and by the relations between individual elements; the greatest similarity is observed for the contents of Sm. Assuming that the calculated model REE composition is close enough to the real one, we can conclude that the REE in these melts were rapidly fractionated. Level of accumulation of elements in them repeatedly decreased from La (30-100 t.ch.) to Lu (0.02-0.2 t.ch.). Such calculations of REE distribution in the model melts, which are crystallized into garnets presented in ultramafic xenoliths from basalts of Vitim province, suggest that the REE in the parental melt of these ultramafites were relatively low fractionated. Unlike all the previous ones, REE compositions of model melts for the garnets from eclogites presented in the xenoliths from kimberlites of Bobbejaan pipe, in gabbros from Ivrea Verbano complex, as well as from basanites of Dutsen Dushowo, are characterized by a certain Eu excess.

Estimates of REE distribution coefficients between garnets and coexisting melts of different composition are an important geochemical characteristic of both the garnet and those of magmatic systems, in which they crystallized [27]. The values of D (garnet / melt) for all REE and for parental melts of different compositions are consistently increasing from light to heavy elements, thus, their graphs tend to have a positive slope. It was also found that the values of D (garnet / melt) for all REE increase from ultramafic to basaltic, andesite, dacite and rhyolite melts. At the same time, the values of D of REE increase with decreasing temperature and pressure of the

Table 5. The coefficients of REE distribution (D) between garnets and coexisting ultramafic, basaltic, hawaiitic, basanitic, andesitic, dacitic, rhyodacitic, and rhyolitic melts (experimental data).

	Ultramafic melt														
	[129]										[48]				
Element	M6943	M6946	M6954	M12952	O8952	O8953	O8951	O12953	O12951	BK7973	950608	950517	950613	SB2501	SB2778
La	N.d.	N.d.	N.d.	N.d.	N.d.	N.d.	N.d.	N.d.	N.d.	N.d.	0,080	0,020	0,020	0,050	0,030
Ce	0,018	0,013	0,015	0,049	0,012	0,037	0,012	0,016	0,015	0,014	N.d.	N.d.	N.d.	N.d.	N.d.
Nd	0,059	0,011	0,069	0,155	0,091	0,148	0,082	0,063	0,063	0,066	»	»	»	»	»
Sm	0,220	0,318	0,286	0,520	0,337	0,490	0,290	0,232	0,232	0,237	0,080	0,060	0,130	0,050	0,040
Gd	N.d.	N.d.	N.d.	N.d.	N.d.	N.d.	N.d.	N.d.	N.d.	N.d.	0,390	0,160	0,230	0,120	0,030
Er	2,54	3,13	2,97	4,22	3,58	5,04	3,51	2,70	4,14	2,58	N.d.	N.d.	N.d.	N.d.	N.d.
Yb	4,02	5,17	4,55	6,07	6,07	8,47	6,07	4,75	7,03	5,06	2,36	1,77	1,73	0,800	0,320
Lu	5,01	6,44	5,76	11,2	7,68	9,46	7,60	5,65	8,45	6,82	N.d.	N.d.	N.d.	N.d.	N.d.
D(Yb)/ /D(Ce)	223	398	303	124	506	229	506	297	469	361	»	»	»	»	»

	Basaltic melt															
	[102]									[143]	[96]		[39]		[50]	
Element	N-4883	N-4890	N-4934	N-4935	N-4863	N-4867	N-4869	N-4872	N-4861	SK-75	Mys-1	Mys-2	Harr-1	Harr-2	Kakan-1	
Ce	N.d.	N.d.	N.d.	N.d.	N.d.	N.d.	N.d.	N.d.	N.d.	0,020	0,071	0,077	0,009	0,009	0,007	
Nd	»	»	»	»	»	»	»	»	»	0,090	N.d.	N.d.	N.d.	N.d.	0,026	
Sm	»	»	1,00	»	»	0,700	»	»	»	0,220	2,71	3,52	0,293	0,321	0,131	
Eu	»	»	N.d.	»	»	N.d.	»	»	»	0,320	N.d.	N.d.	N.d.	N.d.	0,187	
Gd	»	»	»	»	»	»	»	»	»	0,500	»	»	»	»	0,680	
Dy	»	»	»	»	»	»	»	»	»	1,10	»	»	»	»	1,94	
Ho	»	3,90	»	»	»	»	3,50	»	3,300	N.d.	»	»	»	»	N.d.	
Er	»	N.d.	»	»	»	»	N.d.	»	N.d.	2,00	»	»	»	»	4,70	
Tm	»	»	»	»	»	»	»	»	»	N.d.	9,55	9,55	1,27	1,31	N.d.	
Yb	8,70	»	»	8,00	5,90	»	»	5,60	»	»	N.d.	N.d.	N.d.	N.d.	8,00	
D(Yb)/ /DCe)	N.d.	»	»	N.d.	N.d.	»	»	N.d.	»	»	»	N.d.	»	»	1443	

	Basaltic melt			Hawaiitic melt	Basanitic melt			Andesitic melt						
					Binge Point, Austral.	Dutsen Dushawo Nigeria								
	[54]	[20]	[142]	[42]	[142]	[50]	[102]							
Element	Joh-1	Cox -1	E113033	E113036	1430o	E113054	BBP-5	DD-2	N-4082	N-4079	N-4083	N-4091	N-4253	N-4252	N-4513
La	0,002	N.d.	0,236	0,188	0,0164	0,121	0,026	0,001	N.d.	N.d.	N.d.	N.d	N.d.	N.d.	N.d.	Ce 0,005 0,020
0,223	0,193	0,065	0,144	0,051	N.d.	»	»	»	»	»	»	»	»			
Nd	0,052	N.d.	0,286	0,257	0,363	0,232	N.d.	»	»	»	»	»	»	»	»	
Sm	0,250	0,220	0,635	0,566	1,100	0,541	0,600	0,101	2,00	1,70	1,10	1,00	0,700	1,00	1,30	
Eu	0,400	0,320	0,845	0,719	2,02	0,623	1,000	0,185	N.d.	N.d.	N.d.	N.d.	N.d.	N.d.	N.d.	
Gd	N.d.	N.d.	1,43	1,27	N.d.	1,190	2,10	N.d.	»	»	»	»	»	»	»	
Tb	»	»	N.d.	N.d.	»	N.d.	4,10	0,540	»	»	»	»	»	»	»	
Dy	2,200	»	3,23	2,89	4,13	2,56	N.d.	N.d.	25,0	16,6	13,4	13,9	9,50	»	»	
Ho	N.d.	»	N.d.	N.d.	N.d.	N.d.	13,2	2,11	N.d.	N.d.	N.d.	N.d.	N.d.	»	»	
Er	3,60	»	5,21	5,30	3,95	4,24	N.d.	N.d.	»	»	»	»	»	»	»	
Yb	6,60	4,00	6,48	7,90	3,88	5,73	35,6	6,40	44,6	34,9	37,6	37,0	23,0	20,0	»	
Lu	7,10	N.d.	6,64	8,53	3,79	6,30	41,0	8,50	N.d.	N.d.	N.d.	N.d.	N.d.	N.d.	»	
D(Yb)/ /D(Cc)	1320	200	29,1	40,9	59,7	39,8	698	N.d.	»	»	»	»	»	»	»	

	Andesitic melt							Dacitic melt	Rhyo-dacitic	Rhyolitic melt		
								Mt. Nijo, Japan	Tumut	Black Spur, Australia	Mt. Koburn, USA	
	[102]							[50]	[135]	[50]		
Element	N-5292	N-5301	N-5322	N-4697	N-4693	N-4694	N-4192	MN-7	GSFC2	T-8	BS-9	CM-10
La	N.d.	N.d.	N.d.	N.d.	N.d.	N.d.	N.d.	0,370	N.d.	0,370	0,278	0,540
Ce	»	»	»	»	»	»	»	0,530	0,348	0,510	0,790	0,930
Nd	»	»	»	»	»	»	»	0,810	0,525	N.d.	0,270	0730
Sm	1,30	0,900	0,600	0,800	»	»	0,600	5,50	2,66	0,760	0,840	1,04
Eu	N.d.	N.d.	N.d.	N.d.	»	»	N.d.	1,37	1,50	0,214	0,167	0,310
Gd	»	»	»	»	»	»	»	13,6	10,5	5,30	5,30	3,70
Tb	»	»	»	»	»	»	»	19,6	N.d.	8,90	11,9	7,20
Dy	»	»	»	»	»	»	»	N.d.	28,6	N.d.	N.d.	N.d.
Ho	»	»	»	»	5,500	»	»	31,1	N.d.	18,4	34,5	28,2
Er	»	»	»	»	N.d.	»	»	N.d.	42,8	N.d.	N.d.	N.d.
Tm	»	»	»	»	»	»	»	»	N.d.	»	»	»
Yb	»	»	10,6	»	»	10,0	11,7	26,0	39,9	26,0	67,0	54,0
Lu	»	»	N.d.	»	»	N.d.	N.d.	23.5	29,6	24,6	64,0	47,0
D(Yb) /D(Ce)	»	»	»	»	»	»	»	49,0	115	51,0	84,8	58,1

crystallization of mineral. Considering the fact that the values of D (garnet / melt) for LREE are usually less than 1, while for medium and especially heavy elements they are always barely greater than 1, we can assume that, unlike the incompatible LREE, medium and heavy elements found in garnet structure had properties of quite compatible trace elements. In the graphs of change of D (garnet / melt) for melts with high SiO_2 content of, Eu minimums are commonly observed, contrasting to its absence on graphs of ultramafic and mafic melts. Model parental melts for garnets from ultramafic xenoliths of Roberts Victor, Udachnaya, Aykhal and Mir kimberlite pipes are similar in many respects, both by the content of REE and by the nature of their distribution.

Since parageneses of garnets and clinopyroxenes is widely represented in the rocks of different composition and genesis, the data on the REE distribution coefficients between these coexisting minerals is also of great interest. Estimates of D (garnet / clinopyroxene) reveal some important trends in the behavior of trace elements during crystallization of these minerals from melts, including the involvement of fluids. Representative estimates of D (garnet / clinopyroxene) for clinopyroxene-bearing harzburgites, lherzolites and eclogites, as well as for some other garnet-bearing rocks are systematized in Table. 6. Largest amount of data was obtained for peridotites from xenoliths from Udachnaya-Vostochnaya kimberlite pipe, as well as for eclogites from xenoliths of Roberts Victor and Bobbejaan pipes, while for the peridotites, lherzolites, clinopyroxenites and eclogites from other occurrences there are only single estimates of D values. Due to the fact that the garnets almost always accumulate in its structure mainly HREE, while clinopyroxenes - medium and light elements, the values of D (garnet / clinopyroxene) for LREE in most cases do not exceed 1, for medium elements they are close to 1, and for heavy REE are almost always greater than 1, only in some cases reaching 50-100. Parageneses of garnets and clinopyroxenes from xenoliths of Udachnaya-Vostochnaya and Roberts Victor pipes is characterized by approximately the same ranging of D (garnet / clinopyroxene) for most REE, excluding the values for La and Ce from eclogites of Roberts Victor pipe, as well as from several other pipes. Graphs of change of D for a significant part of these samples are close to each other and have a similar configuration. Many of them are positively inclined and almost straight lines, which reflect the inverse relationship between the logarithms of the values of D (garnet / clinopyroxene) and ionic radii of REE. A significant part of parageneses of these minerals in peridotites has a less steep slope of these lines. Accordingly, the value of the D(Yb) / D(Ce) parameters in them is about 100 or slightly more, while for the same parageneses of eclogites the values of this parameter reach 1000, and in garnet-bearing gabbros, represented in Ivrea Verbano complex, their values reach up to several thousand. The lowest values of the D(Yb) / D(Ce) parameters are ascertained for the garnet-clinopyroxene parageneses of the eclogites from Atbashi metamorphic complex (Table 6). What is more, the distinguisher for the graphs of change of the values of D (garnet / clinopyroxene) for all of eclogites from Bobbejaan pipe, as well as for the graphs for some eclogites from Roberts Victor pipe, is the minimum for Dy observed in them.

The given data show that the D (garnet / clinopyroxene) values are to certain in some degree correlated with the composition and genesis of garnet-clinopyroxene rocks. In particular, it was ascertained that for diamondiferous eclogites those values of D that are close to unity are typically observed for Sm or Eu, while for non-diamondiferous eclogites such D values are frequently observed for Gd [26]. There was also revealed a dependence between the values of D (garnet / clinopyroxene), on the one hand, and the contents of Mg and Ca in the parental melts of garnet-bearing rocks, on the other [38].

According to the results of physical experiments, during the crystallization of basaltic melts, generated in the process of partial melting of garnet lherzolite at $P = 35$ kbar and $T = 1580$-1635°C, the D (garnet / clinopyroxene) values for Ce, Sm and Tm were increasing with the reduction of the temperature in the system and, correspondingly, with the decrease in the degree of partial melting of lherzolite (Table 7). Apparently, such dependence of D is not really connected with partial change in the ratio of concentrations of these elements in garnets and clinopyroxenes, crystallized from basaltic melts, but associated with the change in the overall concentration of REE in the parental basaltic liquids that arises due to different degrees of partial melting of garnet lherzolite. As mentioned above, various types of garnet-clinopyroxene rocks differ in the intensity of REE fractionation between coexisting garnets and clinopyroxenes. Taking this into account, such parameters as D(Yb) / D(Ce), D(Yb) / D(La), D(Lu) / D(Ce) and some others can be used as geochemical indicators for classification of rocks of this kind of composition. For example, it was found that fractionation of REE between garnet and clinopyroxene in eclogites from Soazza metamorphic complex, as well as from Roberts Victor kimberlite pipe, is more intensive in comparison with these minerals, which were synthesized by physical experiments with basaltic systems.

Contiguous location, as well as conformality of the graphs of changing D (garnet / clinopyroxene) values in the garnet-clinopyroxene rocks from the same manifestation give grounds to conclude that such rocks were formed in a geochemical equilibrium of garnets and clinopyroxenes,

Table 6. The coefficients of REE distribution (D) between coexisting garnets and clinopyroxenes from different provinces and parageneses.

	Udachnaya-Vostochnaya pipe (Yakutia, Russia)									Thaba Putsoa pprovince
	[148]									[143]
Element	267/89	228/89	115/89	107/89	61/91	417/89	100/91	25/91	306/89	1611
	Garnet peridotites									*Lherzolite*
La	0,045	0,037	0,028	0,181	0,091	0,009	8,33	0,004	0,057	N.d.
Ce	0,068	0,090	0,082	0,343	0,187	0,008	2,09	0,017	1,23	0,144
Pr	N.d.	N.d.	N.d.	N.d.	N.d.	N.d.	N.d.	N.d.	N.d.	N.d.
Nd	0,218	0,244	0,340	1,03	0,311	0,053	3,79	0,181	1,577	0,380
Sm	0,609	0,476	0,921	3,26	0,503	0,312	N.d.	0,748	1,41	1.03
Eu	1,02	0,685	0,849	3,86	0,626	0,537	1,32	0,863	0,892	1,43
Gd	N.d.	N.d.	N.d.	N.d.	N.d.	N.d.	N.d.	N.d.	N.d.	2,11
Tb	»	»	»	»	»	»	»	»	»	N.d.
Dy	2,40	1,66	1,53	7,83	1,56	3,37	3,12	2,73	3,85	4,78
Ho	N.d.	N.d.	N.d.	N.d.	N.d.	N.d.	N.d.	N.d.	N.d.	N.d.
Er	3,76	1,99	2,50	6,59	3,06	6,48	4,98	5,41	2,73	9,52
Tm	N.d.	N.d.	N.d.	N.d.	N.d.	N.d.	N.d.	N.d.	N.d.	N.d.
Yb	7,55	2,58	4,35	15,5	3,75	9,23	19,2	14,9	6,10	15,9
Lu	N.d.	N.d.	N.d.	N.d.	N.d.	N.d.	N.d.	N.d.	N.d.	N.d.
D(Yb)/ /D(Ce)	1121	28,5	53,2	44,6	20,0	1204	9,2	853	5,0	111

	Thaba Putsoa province	Bultfontein pipe		Motha province	Liqhobong province	Vitim province (Russia)				
	[143]					[49]				
Element	1925	G352	BUL 6	1566	2302	313-1	313-3	313-4	313-5	313-6
	Garnet lherzolites									
La	N.d.	N.d.	N.d.	N.d	N.d.	N.d.	N.d.	N.d.	N.d.	N.d.
Ce	»	0,041	0,045	0,256	0,158	»	»	»	»	»
Pr	»	N.d.	N.d.	N.d.	N.d	»	»	»	»	»
Nd	0,215	»	»	0,525	0,236	»	»	»	»	»
Sm	0,604	0,182	0,139	1,31	0,524	0,373	0,340	0,326	0,324	0,325
Eu	0,906	0,703	0,295	1,71	0,784	0,721	0,743	N.d.	0,689	N.d.
Gd	1,25	N.d.	N.d.	2,33	1,29	N.d.	N.d.	N.d.	N.d.	N.d
Tb	N.d.	1,21	0,573	N.d.	N.d.	2,73	2,25	2,44	2,19	2,37
Dy	3,59	2,20	0,926	4,76	2,61	N.d.	N.d.	N.d.	N.d.	N.d.
Ho	N.d.	N.d.	N.d.	N.d.	N.d.	»	»	»	»	»
Er	6,47	3,20	2,44	8,44	4,96	»	»	»	»	»
Tm	N.d.	N.d.	N.d.	N.d.	N.d.	»	»	»	»	»
Yb	12,6	»	»	11,6	15,0	»	»	28,7	26,3	»
Lu	N.d.	»	»	N.d.	N.d.	»	»	34,6	28,5	9,63
D(Yb)/ /D(Ce)	»	7,6	6,0	45,3	94,9	»	»	N.d.	N.d.	N.d.

	Vitim province (Russia)					Wesselton province (South Africa)				
	[49]					[160]				
Element	313-8	313-37	313-54	313-113G	314-580	959	960	965	966	968
	Garnet lherzolites					*Garnet peridotites*				
La	N.d.	N.d.	N.d.	N.d.	N.d.	0,008	0,007	0,003	0,022	0,013
Ce	»	»	»	»	»	0,009	0,008	0,006	0,034	0,030
Pr	»	»	»	»	»	0,032	0,016	0,022	0,078	0,081
Nd	»	»	»	»	»	0,064	0,052	0,047	0,191	0,172
Sm	0,330	0,371	0,362	0,361	0,409	0,344	0,319	0,273	0,832	0,722
Eu	0,733	1,04	0,693	0,759	0,750	0,486	0,643	0,597	1,000	0,955
Gd	N.d.	N.d.	N.d.	1,67	0,99	1,01	0,952	1,39	1,42	1,63
Tb	2,14	2,19	2,21	2,47	1,94	N.d.	N.d.	N.d.	N.d.	N.d.
Dy	N.d.	N.d.	N.d.	N.d.	N.d.	3,51	4,21	6,11	4,57	2,48
Ho	»	»	»	»	»	6,50	6,72	10,2	N.d.	1,16
Er	»	»	»	»	»	6,70	8,56	14,5	»	1,71
Tm	»	»	»	»	»	N.d.	N.d.	N.d.	»	N.d.
Yb	29.7	»	21.2	»	»	»	9,80	»	»	»
Lu	N.d.	45,4	15,0	71.0	6.85	3.47	4,87	»	»	3,33
D(Yb)/ /D(Ce)	N.d.	N.d.	N.d.	N.d.	N.d.	N.d.	1225	»	»	N.d.

	Massifs					Roberts Victor pipe (South Africa)				
	Beni Bousera (Morocco)		Lherz (Italy)		Freychinede (France)					
	[113]		[13]			[15]		[116]		
Element	GP87	GP147	70-291	70-385	70-357	SRV-4	XM-37	250	155	187
	Garnet clinopyroxenites					*Eclogites*				
La	0,042	0,733	0,620	N.d.	0,500	0,040	0,113	N.d.	N.d.	N.d.
Ce	0,028	0,153	0,333	»	0,444	0,153	0,318	0,340	0,214	0,078
Pr	N.d.	N.d.	N.d.	»	N.d.	N.d.	N.d.	N.d.	N.d.	N.d.
Nd	0,111	0,124	»	»	»	0,536	1,268	0,258	0,261	0,169
Sm	0,613	0,537	0,481	0,190	0,306	2,07	4,49	0,652	0,782	0,474
Eu	1,16	0,881	N.d.	0,387	0,706	4,04	7,29	1,03	1,31	0,863
Gd	1,80	1,23	»	N.d.	N.d.	N.d.	N.d.	1,82	2,07	1,47
Tb	N.d.	N.d.	4,65	0,740	1,81	10,8	18,1	N.d.	N.d.	N.d.
Dy	»	»	N.d.	N.d.	N.d.	2,42	15,9	5,69	5,75	4,97
Ho	»	»	»	»	»	N.d.	N.d.	N.d.	N.d.	N.d.
Er	20,8	12,3	»	»	»	»	»	13,4	12,6	10,6
Tm	N.d.	N.d.	»	»	»	»	»	N.d.	N.d.	N.d.
Yb	50,0	17,6	38,4	2,59	25,1	86,3	80,0	29,0	21,4	21,1
Lu	N.d.	N.d.	77,5	2,95	32,4	66,8	147	29,7	26,7	27,3
D(Yb)/ /D(Ce)	1808	115	115	N.d.	56,4	564	252	85,4	99,7	271

	Roberts Victor pipe (South Africa)									
	[40]									
Element	30-6	244	67	4	G6	175	RV-6	277	313	98
	Eclogites									
La	0,077	1,000	0,500	0,024	0,500	2,000	0,009	0,885	0,040	0,008
Ce	0,095	0,200	0,500	0,027	1,00	0,667	0,032	2,22	0,094	0,013
Pr	N.d.	N.d.	N.d.	N.d.	N.d.	N.d.	N.d.	N.d.	N.d.	N.d.
Nd	0,405	0,304	0,667	0,140	1,08	0,800	0,127	8,60	0,451	0,108
Sm	1,72	0,824	2,22	0,447	2,73	2,13	0,583	21,8	1,82	0,381
Eu	3,00	1,38	2,83	0,839	4,43	3,89	0,771	47,7	3,14	0,556
Gd	N.d.	N.d.	N.d.	N.d.	N.d.	N.d.	N.d.	N.d.	N.d.	N.d.
Tb	8,25	5,80	19,0	2,23	14,5	14,2	2,93	»	11,0	0,563
Dy	12,9	7,63	20,8	4,19	22,4	22,0	5,34	149	13,4	0,814
Ho	20,0	10,8	23,0	7,46	31,4	38,9	9,40	N.d.	40,0	2,50
Er	29,7	14,9	53,3	11,4	52,5	62,1	17,5	80,0	30,5	2,12
Tm	N.d.	N.d.	N.d.	N.d.	N.d.	N.d.	N.d.	N.d.	N.d.	N.d.
Yb	»	»	»	»	»	»	»	»	»	»
Lu	29,0	33,0	33,0	39,5	40,7	84,3	86,7	»	»	»
D(Yb)/ /D(Ce)	N.d.	N.d.	N.d.	N.d.	N.d.	N.d.	N.d.	»	»	N.d.

	Kakanui volcano	Bobbejaan pipe (South Africa)								
	[116]	[15]								
Element	21	SBB-2II	SBB-3II	SBB-7P	SBB-25	SBB-34	SBB-37	SBB-39	SBB-61	RV-1
		Eclogites								
La	N.d.	0,268	0,032	0,072	0,273	0,222	0,041	0,073	0,469	0,683
Ce	0,03	0,424	0,055	0,078	0,202	0,171	0,024	0,088	0,314	1,34
Pr	N.d.	N.d.	N.d.	N.d.	N.d.	N.d.	N.d.	N.d.	N.d.	N.d.
Nd	0,10	0,679	0,274	0,262	0,129	0,082	0,036	0,084	0,436	4,26
Sm	0,41	4,07	0,471	0,451	0,475	0,401	0,170	0,444	1,78	15,9
Eu	0,74	4,93	0,888	0,883	0,715	0,721	0,317	0,714	3,05	18,0
Gd	1,22	N.d.	N.d.	N.d.	N.d.	N.d.	N.d.	N.d.	N.d.	N.d.
Tb	N.d.	3,46	1,25	2,60	2,68	2,18	1,14	2,99	6,99	25,2
Dy	4,05	4,34	0,290	0,563	2,13	2,95	1,10	0,334	3,75	3,62
Ho	N.d.	N.d.	N.d.	N.d.	N.d.	N.d.	N.d.	N.d.	N.d.	N.d.
Er	90,3	»	»	»	»	»	»	»	»	»
Tm	N.d.	»	»	»	»	»	»	»	»	»
Yb	14,7	29,0	29,5	23,5	19,4	18,8	18,3	20,2	57,2	59,6
Lu	N.d.	23,7	39,0	21,3	27,2	23,7	29,1	27,4	47,8	34,3
D(Yb)/ /D(Ce)	480	68,4	536	302	95,8	110	762	230	182	44,5

	Soazza province (Switzerland) [12]			Atbashi complex (Kyrgyzstan) [data F. Lesnov]				Ivrea Verbano complex (Italy) [86]		
Element	M-12	M-6	M-48	AT2-5	AT4-5	AT2-7	AT4-7	MP1c	MP1r	MP3
	Eclogites							Garnet gabbros		
La	N.d.	N.d.	N.d.	0,793	1,018	0,778	0,998	N.d.	N.d.	N.d.
Ce	0,015	0,029	0,091	0,779	0,975	0,775	0,970	0,013	0,057	0,024
Pr	N.d.	N.d.	N.d.	0,777	1,00	0,749	0,967	N.d.	N.d.	N.d.
Nd	0,128	0,081	0,417	0,777	1,024	0,740	0,975	0,042	0,075	0,063
Sm	1,12	0,825	1,94	0,775	1,05	0,684	0,928	0,345	0,286	0,357
Eu	2,59	4,12	5,59	0,848	1,17	0,644	0,885	0,667	0,417	0,769
Gd	5,00	15,4	15,2	0,964	1,249	0,802	1,04	N.d.	N.d.	N.d.
Tb	N.d.	N.d.	N.d.	2,06	2,04	1,753	1,731	»	»	»
Dy	27,0	200	111	4,19	4,15	4,20	4,17	1.00	1,67	5,00
Ho	N.d.	N.d.	N.d.	6,35	6,68	7,60	7,99	N.d.	N.d.	N.d.
Er	76,9	333	143	7,91	9,35	9,35	11,1	1,14	3,70	16,7
Tm	N.d.	N.d.	N.d.	7,79	9,78	10,5	13,1	N.d.	N.d.	N.d.
Yb	125	200	111	7,91	10,0	10,5	13,3	1,43	5,00	33,3
Lu	N.d.	N.d.	N.d.	8,25	10,3	10,9	13,5	N.d.	N.d.	N.d.
D(Yb)/ /D(Ce)	8389	6803	1222	10,2	10,3	13,5	13,7	107	88,5	1372

	Ivrea Verbano complex (Italy) [86]							
Element	MP5	MO95	MP6	MP9	MZ145	MP12	MP13	MP18
	Garnet gabbros							
La	N.d.	N.d.	N.d.	N.d.	N.d.	N.d.	N.d.	N.d.
Ce	0,017	0,036	0,011	0,014	0,006	0,009	0,003	0,003
Pr	N.d.	N.d.	N.d.	N.d.	N.d.	N.d.	N.d.	N.d.
Nd	0,047	0,072	0,091	0,122	0,125	0,058	0,061	0,048
Sm	0,250	0,357	0,625	0,556	1,00	0,412	0,412	0,333
Eu	0,526	0,714	0,769	0,909	1,00	0,833	0,833	0,667
Gd	N.d.	N.d.	N.d.	N.d.	N.d.	N.d.	N.d.	N.d.
Tb	»	»	»	»	»	»	»	»
Dy	5,00	5,00	10,0	10,0	10,0	5,00	10,0	10,0
Ho	N.d.	N.d.	N.d.	N .d.	N.d.	N.d.	N.d.	N.d.
Er	14,3	7,69	25,0	16,7	33,3	16,7	25,0	20,0
Tm	N.d.	N.d.	N.d.	N.d.	N.d.	N.d.	N.d.	N.d.
Yb	50,0	9,09	50,0	25,0	100	50,0	50,0	50,0
Lu	N.d.	N.d.	N.d.	N.d.	N.d.	N.d.	N.d.	N.d.
D(Yb)/ /D(Ce)	2890	254	4386	1838	15625	5882	19231	16667

Table 7. The coefficients of Ce, Sm, and Tm distribution (D) between garnets and coexisting clinopyroxenes from basalts (experimental data).

Element	Degree of melting of garnet lherzolite, %	REE compositions, ppm		D
		Melt	Garnet	Clinopyroxene	garnet / clinopyroxene
Ce	2,29	55,169	0,477	11,337	0,042
	8,00	19,649	0,173	4,705	0,037
Sm	2,29	16,148	4,732	4,036	1,172
	8,00	11,538	3,704	3,569	1,038
Tm	2.29	1,370	1,794	0,296	6,061
	8.00	1,281	1,625	0,286	5,623

Note. The coefficients were calculated according to the results of analyses of products of crystallization of basaltic melts, received by experiments at partial melting of garnet lherzolite [39].

which haven't been unbalanced by later processes. On the contrary, in cases, when the graphs of these D values are significantly fragmented and have different configurations, a geochemical equilibrium between garnet and clinopyroxene was not achieved initially, or it has been unbalanced as a result of a later redistribution of the elements. In particular, a considerable spread of values of D (garnet / clinopyroxene) for LREE, which is observed in the graphs for the eclogites from Roberts Victor kimberlite pipe, might indicate that in this case the geochemical equilibrium be-

tween garnet and clinopyroxene might have been partially unbalanced by later processes. These statements might be illustrated by the example of REE distribution between zonal garnet crystals and coexisting omphacite crystals from eclogites of Atbashi metamorphic complex. For example, graphics of D (garnet / clinopyroxene) for internal and external zones of garnet crystals in LREE area up to Gd have the shape of straight horizontal lines, matching on by location, but in heavy elements area they differ significantly, both in the position and the shape. We can assume that at the stage of formation of marginal zones of the garnet crystals their initial geochemical balance, which was achieved during the formation of inner zones of these crystals, has been upset, and therefore garnets turned out to be much poorer in HREE [12].

The crystal structure of garnets, regardless of their chemical composition and genesis, is able to accumulate a higher amount of REE, mainly of heavy elements. Parameters of their distribution in this mineral contain very important, but not meaningful enough genetic information. At this stage of study of this question we can assume with a sufficient confidence that one of the determinants of preferential accumulation of isomorphous admixture of HREE in the crystal structure of garnets are intrinsic properties of the structure, which is characterized by a relatively small size of a unit cell. Another important factor that plays an essential role in this isomorphism is apparently some of the properties of trivalent ions of HREE, namely the smaller size of their ionic radii compared with the trivalent ions of LREE. In this regard, the opinion that the crystal structure of garnets is the "perfect place to find heavy lanthanides" is quite legitimate [39].

As evidenced by the above presented data on the REE distribution in the zoned garnets, the REE composition of real crystals is largely caused by their common chemical composition. The level of HREE accumulation in garnets increases regularly with increasing of Ca content in them and of some other components in the direction from the core of the crystals to the peripheral zone [23]. According to other sources, variations in the level of REE accumulation in the garnet structure are connected not only with changes in their chemical composition, but also with concomitant changes in the geometry of the unit cell of mineral structure, as well as with the size of ionic radii and charge balance of some other elements involved in the process of heterovalent isomorphous substitution in garnets [40].

It is commonly believed that Ca^{2+} ions due to their crystal-chemical properties, especially the size of ionic radius, are the most likely contenders for the isomorphic substitution of trivalent REE ions in the structural points of lattice of calcium-bearing silicate minerals [41]. Data obtained while studying the properties of synthetic garnets are the evidence that this assertion is reasonable [34]. This work particularly shows that with decreasing of the pyrope content from 84 to 9% in synthetic garnets the values of D (garnet / melt) for La are increasing from 0,004 to 0,2, i.e., by 50 times. These data allowed the authors to assume that the values of D (garnet / melt) for all REE have an inverse relationship with the magnitude of Mg/(Mg+Ca) parameter.

While doing statistic calculations based on overall database to determine REE in garnets of the various occurrences, different composition, and genesis, we managed to determine a positive correlation between the Eu concentrations in garnet, on the one hand, and the content of mineral-forming elements such as Ca, Al, Fe, Mn, on the other hand. A positive correlation was also observed between pairs of components such as Yb-FeO and Sm-FeO. In addition, between the contents of Sm, on the one hand, and the contents of Si and Mg - on the other hand, there was found a negative correlation. However, as believed by some researchers, we should not oversimplify the relationship between the general chemical composition of garnets and their REE compounds, because there are cases when with sufficiently large variations in REE content the overall chemical composition of garnets is almost the same [23].

The possible options for coordinating the positions of REE in the structure of this mineral were discussed in several works on the crystallochemistry of garnets. In particular, it was shown that the HREE, as well as Li, Na, Sc and Y, can be localized in the structure of garnets in the eightfold coordination [42]. Another study ascertains that in the structure of synthetic yttrium garnets the trivalent La, Nd, Dy and Yb substituting Y^{3+} ions are in eightfold coordination [43]. In addition, while studying the crystal-chemical properties of synthetic pyropes and grossulars, it was found that Yb^{3+} ions in them, being located in the dodecahedral position, substitute the divalent Ca and Mg ions [44]. According to the results of research, M. Gaspar et al. concluded that the heavy REE predominantly accumulate in garnets of grossular-andradite series, where the grossular component is dominant, in turn, light REE predominantly accumulate in those varieties of garnets, in which andradite is dominant.

Identified at this stage of research garnet differences in the level of REE accumulation, as well as in the quantitative relationship between light and heavy elements, are presumably based on the end result of complex heterovalent isomorphous substitution, in which the number of network-forming elements could be involved, mainly Ca, Fe, Mg and Al cations. The intensity of the substitution of these cations by REE ions was increasing with the de-

crease in the pyrope content of garnet crystals, as well as with lowering the temperature of mineral crystallization. Preferential accumulation of HREE in the garnet structure, most likely due to the relatively smaller sizes of the radii of their trivalent ions compared with ions of LREE, which in turn contributed to a better compatibility of these REE with the crystal structure of this mineral. However, in garnets with a high content of andradite component the isomorphism of LREE could play a more significant role.

3. Chrome-spinels

As an accessory phase, chrome-spinels are almost always present in the dunites, harzburgites, lherzolites, wehrlites, pyroxenites, olivine and some non-olivine gabbroids constituting the mafic-ultramafic massifs within the folded regions and platforms, as well as presented in abyssal xenoliths of alkali-basalts and kimberlites. As a part of many massifs they form deposits of various scale and schlieren of massive and densely disseminated ores, as well as cross veins, most often localized among the dunites and harzburgites. Chrome-spinels are yet little examined with respect to the distribution of lithophile trace elements, REE included, contained in relatively low concentrations. Application of methods of analysis of REE in the individual grains, in particular, the method of LA ICP-MS, slightly expanded opportunities for studying the features of the impurities' distribution in it. Below is a rare earth element chrome-spinels composition characterized by the example of a limited collection of specimens that are represented as an accessory phase in the spinel and garnet peridotites of some abyssal xenoliths in alkaline basalts and kimberlites, in dunites from Dovyrensky mafic-ultramafic massif (Northern Baikal region, Russia) of the ultramafites from Ergak massif (West Sayan, Russia), a number of kimberlite occurrences of Brazil, as well as the ore chromitites present in harzburgites of Voykar-Syn'insky massif (Polar Urals, Russia).

According to [45], chrome-spinels of the Voykar-Syn'insky massif's ore deposits summarily contain REE concentrations in the range from 1.2 to 14.1 ppm (Table 8), and their REE patterns have a flatter negative slope: $(La/Yb)_n$ = 1.2-3.6. At the same time, we can observe positive Eu anomalies on the patterns of specimens from the high-chromous deposits, while it is absent on the patterns of the minerals from low-chromous deposits. Approximately the same level of REE concentrations is established for accessory chrome-spinels of dunite in Dovyrensky massif, but in this case its fractionation is more intense. Lower chondrite-normalized REE contents - from 0.1 to 1.0 t.ch., are recorded in the accessory chrome-spinels from xenoliths of garnet peridotites in kimberlites and alkaline basalts. The REE patterns of these specimens have a complex configuration, which is, perhaps, partly due to analytical errors in the determination of Ce, Nd, Ho and Lu. Accessory chrome-spinels from peridotite xenoliths of alkaline basalt province Dreiser Weiher (Germany) have a more homogeneous REE composition in comparison with specimens from other occurrences [46, 47]. According to the research, chrome-spinels from kimberlites and kamafugites of Alto Paranaíba province (Brazil) are characterized by low total REE concentrations, but they contain relatively high amounts of La, Tm and Lu in relation to other elements. The REE composition of chrome-spinels from Ergak ultramafic massif, which is located in Ergak-Targak-Tayga ridge (West Sayan) has been investigated in detail and structurally confined to the junction between Kurtushibinsky and North Sayan ophiolite belts. The massif manifested the indigenous bedding of single ore chromitite veins ranging from a few to tens of centimeters, as well as their eluvial lumps sized up to 3.5 m [48, 49]. In 15 grains chrome-spinels were determined REE LA ICP-MS method [50, 51]. Total REE content in the chrome-spinel grains from ultramafic of this massif vary in a fairly wide range. At the same time, like in other minerals from ultramafic massifs, chondrite-normalized light REE concentration in this chrome-spinels was higher than the concentration of medium and in particular heavy items. Their REE patterns have a shape of sinuous lines with a common negative slope. Patterns that are based on the average, maximum and minimum contents of elements in the studied specimens. The REE patterns of some chrome-spinel grains show different intensity anomalies of Tm and Er. On the basis of 15 performed analyses on chrome-spinels we calculated the coefficients of correlation between REE contents, on the one hand, and the contents of major and minor components - on the other. The values of these coefficients, except for a pair of Gd-NiO, were below the limits of statistical significance for this sample (r_{01} = 0.53). Nevertheless, the values obtained for the coefficients indicate the presence of trends in an inverse relationship between the contents of REE and the contents of Cr_2O_3, FeO_{tot} and TiO_2. In addition, the evidence of a direct relationship between the content of the majority of REE, on the one hand, and the contents of Al_2O_3, NiO, and MgO, on the other, were found out.

On the example of chrome-spinels from spinel peridotites and websterites of Ronda massif (Spain), the estimates of D (chrome-spinel / clinopyroxene) were obtained for REE and some other trace elements [30]. Judging by the graph from that paper, the average values of D consistently reduced in number from La (~0.02) to Ho and then

Table 8. REE compositions of chrome-spinels from peridotites, kimberlites, kamafugites, and chromitites from some provinces and manifestations (ppm).

	Dreiser Weiher province (Germany)						Australia			Shavarin Tsaram paleovolcano (Mongolia)		
	[157], RNAA			[156], RNAA			[24], LA ICP-MS			[77], LA ICP-MS		
Element	Ia/236	Ib/2	Ib/K1	D-42/1	D-42/2	D-45	402/1	402/2		A-17	A-31	A-42
	Spinel lherzolites											
La	0,008	0,007	0,007	0,0009	0,0002	0,0007	<0,0009	0,006	0,027	N.d.	0,001	
Ce	0,016	0,010	0,008	N.d.	N.d.	N.d.	<0,0007	0,014	0,063	»	0,001	
Pr	N.d.	N.d.	N.d.	»	»	»	N.d.	N.d.	0,006	»	0,001	
Nd	»	0,0186	»	»	»	»	<0,0024	0,008	N.d.	»	N.d.	
Sm	0,0012	0,0013	0,001	0,0002	0,0001	0,0001	<0,0019	0,005	0,004	0,003	»	
Eu	0,0006	N.d.	0,001	N.d.	N.d.	N.d.	<0,0010	0,012	0,003	N.d.	»	
Gd	N.d.	»	N.d.	»	»	»	<0,0023	0,005	N.d.	0,001	»	
Tb	»	»	0,0003	»	»	»	N.d.	N.d.	0,001	N.d.	0,001	
Dy	»	»	N.d.	»	»	»	<0,0018	0,006	N.d.	0,001	0,001	
Ho	»	»	0,0005	»	»	»	N.d.	N.d.	»	0,001	N.d.	
Er	»	»	N.d.	»	»	»	<0,0014	»	»	0,004	»	
Tm	»	»	»	»	»	»	N.d.	»	»	0,001	0,002	
Yb	0,002	0,001	0,002	0,0005	0,0006	0,0008	<0,0016	0,003	0,003	0,005	N.d.	
Lu	N.d.	0,0003	0,0003	0,0002	0,0002	0,0002	<0,0003	N.d.	N.d.	0,002	»	
Total	»	N.d.	N.d.	N.d.	N.d.	N.d.	N.d.	»	»	»	»	
$(La/Yb)_n$	3,18	3,37	2,18	1,12	0,18	0,63	0,38	1,31	7,37	»	»	

	Yubileynaya pipe (Yakutia, Russia) [2], LA ICP-MS		Dovyrensky (Russia) [69], RNAA	Massifs Voykar-Syn'insky (Urals, Russia) [161], ICP-MS							Alto Paranaiba province (Brazil) [91]	
Element	Asch-11	Asch -12	L-14	3660*	3730*	3943*	3992	4047	4334	8536	Lim-1	PO-2
	Garnet peridotites		*Dunite*	*Chromitites high-Cr*			*Chromitites high-Al*				*Kimberlite*	*Kamafugite*
La	0,024	0,05	5,88	0,193	0,456	1,38	1,31	0,114	0,460	2,09	0,439	0,055
Ce	0,052	0,25	13,2	0,462	1,100	3,27	2,80	0,293	1,15	4,97	0,022	0,037
Pr	0,009	0,01	N.d.	0,070	0,169	0,506	0,442	0,046	0,182	0,689	N.d.	N.d.
Nd	0,035	0,14	2,04	0,360	0,772	2,40	1,92	0,234	0,885	3,11	0,017	»
Sm	0,025	0,07	1,50	0,104	0,232	0,669	0,487	0,067	0,244	0,663	N.d.	»
Eu	0,024	0,02	0,52	0,043	0,110	0,203	1,22	0,110	0,199	0,338	0,014	0,009
Gd	0,081	0,09	1,86	0,126	0,276	0,482	0,624	0,081	0,269	0,524	N.d.	N.d.
Tb	0,010	0,011	0,30	0,020	0,046	0,154	0,094	0,014	0,042	0,090	0,004	»
Dy	0,025	0,07	N.d.	0,124	0,297	0,902	0,535	0,078	0,253	0,575	0,013	0,038
Ho	0,060	0,13	»	0,025	0,067	0,200	0,121	0,017	0,053	0,121	0,003	0,002
Er	0,025	0,02	»	0,072	0,204	0,617	0,386	0,054	0,170	0,372	0,01	0,008
Tm	0,003	0,004	0,13	0,011	0,034	0,100	0,064	0,009	0,029	0,060	0,021	0,012
Yb	0,014	0,02	1,02	0,075	0,249	0,673	0,463	0,063	0,196	0,396	0,018	0,047
Lu	0,004	0,10	0,15	0,012	0,041	0,106	0,075	0,010	0,033	0,061	0,02	N.d.
Total	0,391	0,985	N.d.	1,70	4,05	11,7	10,5	1,19	4,16	14,1	N.d.	»
$(La/Yb)_n$	1,16	1,69	»	1,74	1,24	1,38	1,91	1,22	1,58	3,56	16,5	0,8

to the rest of the heavy REE (~0.003). Contrasting to the previous work the values for D (chrome-spinel / clinopyroxene) are lower and for some elements were obtained from the chrome-spinels from peridotites provided in the xenoliths from alkaline basalts of Dreiser Weiher province (Germany): Eu – 0.0007, Sm – 0.0006 [52].

Structural position that REE ions can take up in the crystal lattice of chrome-spinel haven't been elucidated yet. However, on the assumption of the size of the REE ionic radii, which are in eightfold coordination [53], among the cations, which are included into the structure of the chrome-spinels, as the most likely candidates for the isomorphic substitution of trivalent ions of heavy REE ($^{VIII}Tm^{3+}$ – 0,994 Å ; $^{VIII}Yb^{3+}$ – 0,985 Å; $^{VIII}Lu^{3+}$ – 0,977 Å) can be expected to be called ion $^{VIII}Fe^{2+}$ (0,920 Åp).

4. Ilmenites

Ilmenites as an accessory phase are represented in many varieties of magmatic rocks, including normal and calc-alkaline gabbroids, diorites, pyroxenites, subvolcanic and volcanic mafic rocks of normal and high alkalinity, kimber-

lites, carbonatites and some schist and other formations. In gabbroids and pyroxenites from some massifs there is a dense impregnation of ilmenites observed, as well as deposits of their massive ores.

Currently the REE composition of ilmenites from many massifs and species composing them is studied only by single samples. More representative data were obtained from the ilmenites from the rocks of mafic-ultramafic Skaergaard massif (Greenland), from a set of kimberlite pipes located on the territory of Yakutia (Russia), Tigrovy (Primorie province, Russia) and some others. Among the investigated ilmenites there are samples of such rocks as gabbro, gabbronorites, wehrlites, pyroxenites, kimberlites, basalts, as well as monzonites, rhyolites, some metamorphic and other species [31, 54]- [63].

According to available data the total REE contents in ilmenites of different types of magmatic rocks vary within the following ranges: kimberlites – 0.02-298 ppm, pyroxenites in xenoliths of alkaline basalts – 0.13-0.66 ppm, websterites - 5 3-17.6 ppm, gabbronorites and gabbro – 5.1-40 ppm. In ilmenites from metamorphic schists of Polar Urals REE total content reaches 107 ppm, and in sample of ilmenite from rhyolite - 1700 ppm. In the mineral from the gabbros of Skaergaard massif REE total content varies in the range of 1.94-9.05 ppm (Table 9). In picroilmenites of Frank Smith, Monastery (South Africa) and Mir (Yakutia, Russia) kimberlite pipes there were observed increased chondrite-normalized REE contents of LREE and to a smaller extent Yb and Lu compared with MREE, while the patterns of REE distribution in these samples have a common negative slope (Fig. 3-1, 2, 3, 4). In turn, the patterns of ilmenites from Yubileynaya kimberlite pipe (Yakutia, Russia) and from the pyroxenites presented in the xenoliths indicate their enrichment with medium and heavy REE. At the same time the patterns of picroilmenites of kimberlites from Yubileynaya pipe have a shape close to sinusoidal (Fig. 3-5). Unlike previous ones, the ilmenites from pyroxenites presented in the xenoliths from basalts of Bayuda (Sudan) and Kakanui volcano (New Zealand) volcanoes are depleted in LREE relative to HREE, respectively, their patterns have the same positive slope (Fig. 3-6, 7). The patterns of some ilmenites have positive or negative Eu anomalies of different intensity (Fig. 3-10, 12). We have investigated the collection of samples of accessory ilmenites from gabbro-norites and websterites composing the Tigrovy massif (Primorie province, Russia) [62], which as well as Ariadninsky, Kedimiysky, Uonchoysky massifs and the others, is situated in the southern part of Khabarovsk territory, in Sikhote Alin ridge [64, 65]. Numerous indigenous occurrences of disseminated and massive ilmenite ores and ilmenite placers are connected to all these massifs spatially and genetically. The ilmenite content in the massive ore sometimes reaches 50%. In the accessory ilmenites of Tigrovy massif the TiO_2 content varies in the range of 47.0-53 wt. %, FeO_{tot} - 46-49 wt. %, MnO – 0.7-1.6 wt. %, and the presence of impurities of MgO and Cr_2O_3 was identified only in some of the cases. Determination of REE in these ilmenites was carried out by INAA method and in the certain grains was duplicated by ICP-MS method. According to the method of INAA, the total REE content in ilmenites of Tigrovy massif varies in the range of 5.81-6.98 ppm, and the differences between ilmenites from websterites and gabbronorites on this basis have not been identified. All ilmenites in this collection demonstrate a relative enrichment with LREE: $(La/Yb)n$ = 3.0-4.8, respectively, their patterns have a common negative slope (Fig. 3-8, 9). Analyses of those ilmenites from gabbro-norites, which were performed by ICP-MS method, indicated the presence of a substantial surplus of Eu in them (Fig. 3-10). According to the data obtained by the mentioned method for the ilmenites from gabbronorites the values $(Sm/Eu)n$ = 0.19-0.28, which is slightly less than in its samples from websterites (0.38-0.48). Determination of REE in the three samples of ilmenites made by INNA method and duplicated by ICP-MS showed results comparable both on the basis of the content of certain elements and their total content (Table 9). Positive Eu anomalies on the REE pattern of ilmenites from websterite (sp. Sch-095D*, Fig. 3-8) and gabbro-norite (analyses Sch-093g*, 1a, b, c; Fig. 3-10) which were identified according to ICP-MS method, also show a slight excess of this element in the samples stated. According to observations made under an optical microscope, the ilmenite grains from these and other samples from the Tigrovy massif are mostly xenomorphic regarding coexisting crystals of pyroxene and plagioclase, which indicates their belated crystallization relative to these silicate phases. It is obvious that in these two silicate phases during the crystallization have focused the vast majority of available Eu in parent melt. Therefore, the residual portion of the latter, which then became the material of crystallization of ilmenite, should be exhausted with respect to Eu, so its excess in this ilmenite was not supposed to take place. Considering the possible causes of the observed positive Eu anomalies in these ilmenites, one would assume that they are caused by the presence of some amounts of micro-inclusions of plagioclase in their grains. However, the phase X-ray analysis of these ilmenites had shown that the admixture of plagioclase has not been detected. Thus, the reason for the positive Eu anomalies in the patterns of these ilmenites has not been ascertained yet. What is more, a very intense negative Eu anomaly was found on the spectrum of ilmenite from the rhyolite, which is characterized by very high concentrations of REE (Fig. 3-12).

Table 9. REE compositions of ilmenites from kimberlites, peridotites, pyroxenites, troctolites, gabbros and other rocks from some provinces, complexes and pipes (ppm).

	Frank Smith pipe (South Africa) [106], INAA		Monastery pipe (South Africa) [56], INNA			Mir pipe (Russia) [90], INNA	Yubileynaya pipe (Russia) [2], LA ICP-MS		Alto Paranaiba province (Brazil) [91], LA ICP-MS	
Element	3241-1	3241-2	MON-1	2626R	2626R1	2633C	VII-34/2	Asch-6	Asch-7	Ind-c-1	Ind-c-2
	Kimberlites										
La	0,060	0,160	0,250	0,720	0,660	0,200	1,50	0,030	0,020	0,013	0,013
Ce	0,090	0,340	0,500	0,690	0,350	0,290	2,000	0,044	0,043	0,054	0,028
Pr	0,010	0,030	0,060	N.d.	N.d.	N.d.	N.d.	0,008	0,005	0,005	0,007
Nd	0,080	0,120	0,220	0,330	0,250	0,130	»	0,059	0,041	0,032	N.d.
Sm	0,020	0,020	0,050	0,065	0,061	0,026	0,180	0,06	0,032	0,008	0,02
Eu	0,010	0,010	0,010	N.d.	0,022	0,010	0,050	0,034	0,011	0,007	N.d.
Gd	0,020	0,010	0,040	0,080	0,063	0,030	N.d.	0,073	0,046	N.d.	0,025
Tb	N.d.	N.d.	N.d.	N.d.	N.d.	N.d.	»	0,016	0,005	0,003	N.d.
Dy	0,020	0,020	0,050	0,079	0,062	0,041	»	0,068	0,025	0,031	0,028
Ho	N.d.	N.d.	N.d.	N.d.	N.d.	N.d.	»	0,011	0,003	0,004	0,012
Er	0,010	0,010	0,030	0,045	0,042	0,028	»	0,034	0,006	0,021	0,032
Tm	N.d.	N.d.	N.d.	N.d.	N.d.	N.d.	»	0,004	0,001	0,001	0,005
Yb	0,020	0,020	0,040	0,187	0,064	0,051	0,190	0,017	0,020	0,075	0,048
Lu	N.d.	N.d.	N.d.	N.d.	N.d.	N.d.	0,140	0,005	0,007	0,011	0,03
Total	0,340	0,740	1,25	2,20	1,57	0,806	N.d.	0,463	0,445	0,265	0,248
$(La/Yb)_n$	2,02	5,40	4,22	2,60	6,96	2,65	5,33	0,03	0,02	0,12	0,18

	Bayuda province (Sudan) [169], INAA		Kakanui volcano (New Zealand) [14]			Ukraine Urals (Russia) [14]				Urals (Russia) [14]	
Element	C59	C42	K2b	K 4	K7	BL-1	BL-2	BL-3	BL-4	BL-5	BL -6
	Pyroxenites					*Peridotite Pl-bearing*	*Wehrlite*	*Pyroxenite (4)*	*Troctolite (2)*	*Gabbro (13)*	*Gabbro*
La	<0,02	0,0017	<0,01	0,004	0,009	0,05	0,15	0,14	0,18	0,24	0,80
Ce	0,0081	0,016	<0,01	0,006	0,010	0,13	0,60	0,37	0,36	0,52	1,85
Pr	<0,01	0,0033	<0,01	0,006	0,003	N.d.	N.d.	N.d.	N.d.	N.d.	N.d.
Nd	<0,18	0,068	0,01	0,014	0,034	»	»	»	»	»	»
Sm	<0,11	<0,05	0,012	0,007	0,002	0,012	0,20	0,18	0,071	0,11	0,59
Eu	<0,03	0,0065	0,0077	0,002	0,005	0,003	0,084	0,072	0,020	0,039	0,16
Gd	<0,13	<0,07	<0,10	0,014	0,028	N.d.	N.d.	N.d.	N.d.	N.d.	N.d.
Tb	<0,05	<0,01	0,0086	0,005	0,007	0,036	0,39	0,055	0,038	0,031	0,083
Dy	<0,09	<0,04	<0,07	0,022	0,053	N.d.	N.d.	N.d.	N.d.	N.d.	N.d.
Ho	<0,02	N.d.	<0,01	0,002	0,011	»	»	»	»	»	»
Er	N.d.	N.d.	N.d.	N.d.	N.d.	»	»	»	»	»	»
Tm	<0,03	<0,01	0,0065	0,003	0,010	»	»	»	»	»	»
Yb	<0,14	0,082	<0,04	0,025	0,050	0,56	0,059	0,075	1,49	0,18	0,14
Lu	<0,03	<0,04	<0,02	0,013	0,006	0,15	0,021	0,019	0,38	0,053	0,028
Total	0,66	0,38	0,26	0,126	0,228	N.d.	N.d.	N.d.	N.d.	N.d.	N.d.
$(La/Yb)_n$	<0,02	0,0017	0,13	0,11	0,12	0,06	1,72	1,26	0,08	0,90	3,86

	Ukraine Urals (Russia) [14], RNAA						Ukraine Urals (Russia) [32]		Tigrovy massif (Sikhote Alin', Primorie, Russia) [70], INAA		
Element	BL-7	BL-8	BL-9	BL-10	BL-11	BL-12	Gol-1		Sch-085c	Sch-095d	Sch-095D
	Gabbro (2)	Gabbro-norite (5)	Gabbro-anortosite (3)	Gabbro-amphi-bolite (5)	Monzonite	Rapakivi granite	Schist (3)		Websterites		
La	0,72	1,85	2,61	0,20	9,43	9,05	19,26		4,30	3,80	0,848
Ce	1,53	3,52	4,85	0,40	21,6	18,9	36,30		7,20	5,70	1,772
Pr	N.d.	N.d.	N.d.	N.d.	N.d.	N.d.	N.d.	N.d.	N.d.	0,252	
Nd	»	»	»	»	»	»	»		4,50	3,00	1,037
Sm	0,18	0,39	0,54	0,05	2,51	2,29	4,93		1,00	0,760	0,266
Eu	0,024	0,046	0,060	0,005	0,20	0,06	0,730		0,230	0,130	0,144
Gd	N.d.	N.d.	N.d.	N.d.	N.d.	N.d.	N.d.	N.d.	N.d.	0,271	
Tb	0,030	0,083	0,119	0,014	0,36	0,36	0,700		0,100	0,040	0,036
Dy	N.d.	N.d.	N.d.	N.d.	N.d.	N.d.	N.d.	N.d.	N.d.	0,226	
Ho	»	»	»	»	»	»	»		»	»	0,037
Er	»	»	»	»	»	»	»		»	»	0,121
Tm	»	»	»	»	»	»	»		»	»	0,024
Yb	1,04	1,18	1,27	0,072	1,02	1,68	1,12		0,260	0,140	0,184
Lu	0,34	0,34	0,35	0,014	0,24	0,22	0,160		0,036	0,025	0,032
Total	N.d.	N.d.	N.d.	N.d.	N.d.	N.d.	N.d.	N.d.	N.d.	5,25	
$(La/Yb)_n$	0,16	0,22	1,39	1,88	6,24	3,64	11,61		11,16	18,32	3,11

	Tigrovy massif (Sikhote Alin', Russia)								Twin Peaks [101]	Skaergaard mas. [111]
	[70], INAA									
Element	Sch-084g	Sch-093g	Sch-095c	Sch-096c	Sch-93 g(1a)	Sch-093g(1b	Sch-093g(1c)	Sch-096C	Nash-1	4312
	Gabbro-norites							*Rhyo-lites*	*Gabbro*	
La	5,30	8,00	5,80	10,0	1,13	1,30	1,29	1,06	423	3,70
Ce	9,60	14,0	9,00	18,0	1,72	2,06	1,93	1,68	900	9,60
Pr	N.d.	N.d.	N.d.	N.d.	0,240	0,260	0,240	0,232	N.d.	N.d.
Nd	5,50	8,00	6,00	9,00	0,800	0,900	0,830	0,782	325	8,40
Sm	0,920	1,30	1,10	2,30	0,160	0,170	0,190	0,193	39,0	2,90
Eu	0,240	0,480	0,300	0,170	0,380	0,400	0,280	0,210	1,38	0,690
Gd	N.d.	N.d.	N.d.	N.d.	0,160	0,210	0,190	0,201	N.d.	2,90
Tb	0,120	0,130	0,100	0,180	0,020	0,020	0,020	0,037	3,80	0,450
Dy	N.d.	N.d.	N.d.	N.d.	0,210	0,240	0,240	0,226	19,5	N.d.
Ho	»	»	»	»	0,050	0,050	0,050	0,048	N.d.	0,440
Er	»	»	»	»	0,140	0,140	14,0	0,157	N.d.	N.d.
Tm	»	»	»	»	N.d.	N.d.	N.d.	0,028	»	»
Yb	0,500	0,280	0,290	0,260	0,160	0,190	0,170	0,217	11,9	1,09
Lu	0,080	0,058	0,056	0,050	0,020	0,020	0,020	0,042	1,66	N.d.
Total	N.d.	N.d.	N.d.	N.d.	5,19	5,96	19,45	5,11	N.d.	»
$(La/Yb)_n$	7,15	19,29	13,50	25,96	4,77	4,62	5,12	3,29	24,0	3,70

	Skaergaard massif (Greenland)									
	[53], ICP-MS									
Element	Sk-783	Sk-782	Sk-776	Sk-795	Sk-797	Sk-813	Sk-815	Sk-778	Sk-50	Sk-51
	Gabbros									
La	0,36	0,39	0,23	0,27	0,24	0,38	0,33	0,37	0,27	0,31
Ce	0,79	0,94	0,47	0,59	0,40	0,65	0,50	0,62	0,44	0,47
Pr	0,11	0,12	0,05	0,07	0,05	0,07	0,09	0,09	0,05	0,06
Nd	0,59	0,69	0,21	0,36	0,24	0,36	0,32	0,34	0,31	0,21
Sm	0,16	0,16	0,06	0,11	0,05	0,09	0,07	0,10	0,08	0,09
Eu	0,05	0,05	0,03	0,03	0,03	0,04	0,03	0,04	0,03	0,03
Gd	0,18	0,19	0,08	0,12	0,08	0,11	0,09	0,10	0,12	0,12
Tb	0,04	0,04	0,02	0,03	0,02	0,03	0,02	0,02	0,03	0,02
Dy	0,29	0,27	0,13	0,19	0,16	0,21	0,13	0,15	0,18	0,15
Ho	0,07	0,07	0,04	0,05	0,05	0,06	0,03	0,04	0,04	0,06
Er	0,39	0,35	0,21	0,26	0,26	0,35	0,19	0,21	0,22	0,26
Tm	0,10	0,08	0,05	0,06	0,06	0,07	0,04	0,05	0,05	0,07
Yb	0,82	0,81	0,44	0,51	0,52	0,58	0,37	0,45	0,48	0,46
Lu	0,21	0,20	0,09	0,12	0,11	0,12	0,08	0,10	0,13	0,13
Total	4,16	4,36	2,11	2,77	2,27	3,12	2,29	2,68	2,43	2,44
$(La/Yb)_n$	0,30	0,32	0,35	0,36	0,31	0,44	0,60	0,55	0,38	0,45
$(Eu/Eu^*)_n$	0,90	0,88	1,32	0,79	1,44	1,23	1,16	1,21	0,93	0,88

	Skaergaard massif (Greenland)									
	[53], ICP-MS									
Element	Sk-805	Sk-803	Sk-802	Sk-801	Sk-800	Sk-107	Sk-110	Sk-753	Sk-755	Sk-756	Sk-757
	Gabbros										
La	0,32	0,31	0,24	0,23	0,79	0,27	0,30	0,28	0,32	0,27	0,58
Ce	0,70	0,61	0,50	0,55	1,77	0,49	0,68	0,65	0,66	0,75	1,19
Pr	0,10	0,07	0,07	0,06	0,25	0,07	0,08	0,08	0,09	0,09	0,19
Nd	0,54	0,45	0,31	0,28	1,27	0,29	0,45	0,40	0,33	0,48	0,89
Sm	0,14	0,13	0,08	0,07	0,36	0,10	0,12	0,11	0,10	0,12	0,26
Eu	0,04	0,04	0,03	0,03	0,12	0,03	0,05	0,05	0,05	0,05	0,09
Gd	0,16	0,11	0,09	0,10	0,41	0,09	0,12	0,13	0,14	0,16	0,33
Tb	0,03	0,03	0,02	0,02	0,09	0,02	0,03	0,03	0,04	0,04	0,07
Dy	0,27	0,22	0,18	0,20	0,63	0,15	0,20	0,32	0,22	0,28	0,49
Ho	0,11	0,07	0,05	0,07	0,20	0,04	0,09	0,07	0,07	0,08	0,15
Er	0,38	0,30	0,26	0,34	0,96	0,25	0,36	0,35	0,38	0,46	0,76
Tm	0,09	0,07	0,06	0,08	0,22	0,06	0,09	0,08	0,10	0,09	0,17
Yb	0,64	0,53	0,63	0,74	1,59	0,61	0,60	0,56	0,59	0,89	1,29
Lu	0,18	0,14	0,12	0,15	0,39	0,12	0,19	0,19	0,15	0,20	0,33
Total	3,70	3,08	2,64	2,92	9,05	2,59	3,36	3,30	3,24	3,96	6,79
$(La/Yb)n$	0,34	0,39	0,26	0,21	0,34	0,30	0,34	0,34	0,37	0,20	0,30
$(Eu/Eu^*)n$	0,81	1,00	1,08	1,10	0,95	0,95	1,26	1,28	1,29	1,10	0,94

Yakutia (Russia)

	Aykhal pipe							Komsomol'skaya pipe		
	[3], LA ICP-MS									
Element	Ay-1	Ay-2	Ay-4	Ay-9	Ay10	Ay-11	Ay-22	Koms-1	Koms-2	Koms-3
	Kimberlites									
La	4,98	4,96	17,69	0,44	0,0027	0,32	0,30	0,087	0,35	0,94
Ce	10,58	7,42	28,99	0,76	0,0083	0,51	0,56	0,053	0,56	2,17
Pr	1,16	0,79	2,95	0,047	0,0006	0,052	0,041	0,011	0,045	0,12
Nd	4,02	3,04	12,21	0,20	0,0024	0,17	0,15	0,05	0,18	0,45
Sm	0,67	0,44	1,79	0,037	0,0008	0,027	0,02	0,032	0,028	0,102
Eu	0,15	0,099	0,40	0,0085	0,0003	0,0066	0,0066	0,002	0,008	0,015
Gd	0,42	0,28	1,16	0,032	0,0013	0,023	0,023	0,004	0,014	0,036
Tb	0,042	0,027	0,11	0,0038	0,0003	0,0021	0,003	0,0004	0,002	0,004
Dy	0,20	0,12	0,50	0,022	0,0014	0,012	0,018	0,004	0,011	0,023
Ho	0,025	0,017	0,068	0,004	0,0004	0,0019	0,0026	0,002	0,003	0,005
Er	0,053	0,036	0,14	0,01	0,0013	0,0071	0,0079	0,005	0,016	0,009
Tm	0,0048	0,0031	0,013	0,0017	0,0001	0,0009	0,0012	0,0008	0,001	0,001
Yb	0,026	0,017	0,070	0,01	0,0011	0,007	0,0066	0,012	0,008	0,012
Lu	0,0031	0,0017	0,007	0,0014	0,0001	0,001	0,0013	0,001	0,002	0,001
Total	22,32	16,86	64,11	1,57	0,02	1,15	1,13	0,26	1,23	3,88
(La/Yb)*n*	128,2	178,1	171,5	29,65	1,60	30,62	30,87	4,89	29,78	52,7

Yakutia (Russia)

	Ozernaya pipe						Zarnitsa pipe		Ukrainskaya pipe			
	[3], LA ICP-MS											
Element	Oz-15	Oz-16	Oz-17	Oz-18	Oz-19	Oz-20	Zrn-12	Zrn-13	Ukr-3	Ukr-4	Ukr-5	Ukr-6
	Kimberlites											
La	0,17	0,56	17,14	0,051	18,72	0,084	10,10	28,57	1,54	6,93	3,51	8,81
Ce	0,15	0,92	34,84	0,12	31,79	0,19	12,62	63,36	2,26	9,75	6,65	13,52
Pr	0,022	0,12	3,54	0,027	2,72	0,032	1,35	3,75	0,25	1,31	0,75	2,42
Nd	0,22	0,32	14,30	0,29	10,42	0,17	5,15	17,74	0,93	0,48	1,73	7,38
Sm	0,074	0,11	2,51	0,065	0,77	0,088	0,76	4,01	0,094	1,15	0,26	0,86
Eu	0,037	0,028	0,691	0,036	0,093	0,034	0,63	0,49	0,03	0,25	0,12	0,25
Gd	0,13	0,13	1,19	0,13	0,37	0,16	0,51	1,21	0,067	0,64	0,20	0,73
Tb	0,022	0,017	0,19	0,020	0,040	0,015	0,040	0,15	0,0060	0,089	0,014	0,02
Dy	0,11	0,11	0,94	0,097	0,19	0,085	0,24	0,59	0,050	0,33	0,10	0,32
Ho	0,023	0,026	0,20	0,017	0,028	0,020	0,038	0,089	0,0068	0,048	0,020	0,051
Er	0,063	0,10	0,38	0,038	0,096	0,038	0,16	0,29	0,021	0,13	0,049	0,20
Tm	0,0076	0,023	0,051	0,0054	0,021	0,0095	0,022	0,075	0,0059	0,019	0,0074	0,024
Yb	0,057	0,17	0,37	0,038	0,13	0,083	0,073	0,57	0,019	0,063	0,046	0,067
Lu	0,024	0,021	0,031	0,0047	0,042	0,0070	0,0094	0,070	0,0033	0,010	0,0057	0,0090
Total	1,12	2,67	76,38	0,93	65,42	1,02	31,69	120,9	5,69	26,08	13,45	34,72
(La/Yb)*n*	2,08	2,22	31,33	0,91	99,72	0,68	93,07	34,12	54,65	74,84	51,16	89,11

Yakutia (Russia)

	Festival'naya pipe						Dal'naya pipe				Udachnaya pipe	
	[3], LA ICP-MS											
Element	Fest-8	Fest-9	Fest-10	Fest-11	Fest-12	Fest-13	Daln-11	Daln-12	Daln-13	Daln-14	Ud-1402	Ud-1293
	Kimberlites											
La	3,13	3,00	0,81	0,038	1,91	0,020	0,023	0,032	0,033	0,075	0,45	0,013
Ce	2,80	4,81	1,63	0,051	3,15	0,059	0,074	0,038	0,066	0,079	0,39	0,040
Pr	0,22	0,80	0,12	0,0069	0,52	0,0098	0,015	0,0056	0,012	0,0085	0,038	0,0050
Nd	0,76	2,33	0,38	0,028	1,17	0,037	0,079	0,041	0,11	0,065	0,16	0,018
Sm	0,15	0,49	0,083	0,026	0,22	0,029	0,032	0,018	0,047	0,030	0,027	0,0050
Eu	0,017	0,12	0,018	0,0001	0,076	0,0083	0,014	0,0083	0,019	0,015	0,010	0,0020
Gd	0,13	0,31	0,031	0,0078	0,16	0,036	0,032	0,029	0,076	0,054	0,033	0,0080
Tb	0,013	0,067	0,0084	0,0006	0,026	0,0022	0,0048	0,0052	0,010	0,0071	0,0070	0,0030
Dy	0,068	0,47	0,044	0,0054	0,13	0,0066	0,027	0,0167	0,025	0,032	0,036	0,024
Ho	0,019	0,085	0,010	0,0006	0,019	0,0019	0,0045	0,0036	0,0064	0,0068	0,0070	0,0040
Er	0,069	0,24	0,015	0,0018	0,052	0,0076	0,012	0,0090	0,017	0,022	0,033	0,017
Tm	0,012	0,036	0,0018	0,0003	0,0072	0,0015	0,0036	0,0016	0,0039	0,0049	0,0030	0,0020
Yb	0,084	0,21	0,029	0,0021	0,048	0,014	0,035	0,012	0,039	0,041	0,024	0,022
Lu	0,011	0,027	0,0035	0,0005	0,0058	0,0045	0,0056	0,0029	0,043	0,017	0,0040	0,0040
Total	7,49	13,0	3,18	0,17	7,49	0,42	0,36	0,22	0,50	0,46	1,22	0,17
(La/Yb)*n*	25,06	9,55	18,74	12,07	26,89	9,89	0,44	1,85	0,57	1,26	12,63	0,40

Yakutia (Russia)												
	Udachnaya pipe					Mir pipe						
	[3], LA ICP-MS											
Element	Ud-1504	Ud-1240	Ud-1506	Ud-1505	Ud-1507	Mir-9	Mir-13d	Mir-23	Mir-26	Mir-29	Mir-13	Mir-13a
	Kimberlites											
La	0,12	0,28	0,077	0,0010	0,0040	1,54	42,75	0,53	0,020	0,0020	25,28	23,92
Ce	0,12	0,32	0,016	0,0090	0,017	1,74	68,58	0,46	0,16	0,018	33,20	32,13
Pr	0,012	0,032	0,0020	0,0020	0,0017	0,17	8,08	0,042	0,017	0,0020	3,50	3,45
Nd	0,040	0,18	0,13	0,19	0,0040	0,69	30,52	0,15	0,075	0,010	13,08	13,49
Sm	0,010	0027	0,0050	0,0040	0,0010	0,093	4,38	0,019	0,024	0,012	1,88	1,85
Eu	0,0040	0,013	0,0020	0,0010	0,0005	0,020	0,99	0,0070	0,011	0,0030	0,38	0,40
Gd	0,015	0,051	0,011	0,0060	0,0030	0,091	2,95	0,024	0,016	0,0090	1,31	1,44
Tb	0,0035	0,010	0,0020	0,0030	0,0010	0,012	0,26	0,0040	0,0020	0,0020	0,14	0,14
Dy	0,036	0,040	0,022	0,022	0,014	0,068	1,12	0,027	0,016	0,031	0,64	0,64
Ho	0,0060	0,0090	0,0040	0,0040	0,0030	0,014	0,15	0,0060	0,0050	0,0060	0,093	0,15
Er	0,019	0,026	0,017	0,012	0,012	0,036	0,037	0,016	0,012	0,019	0,22	0,22
Tm	0,0030	0,0040	0,0030	0,0030	0,0020	0,0060	0,033	0,0040	0,0030	0,0030	0,024	0,024
Yb	0,0022	0,037	0,015	0,019	0,010	0,038	0,18	0,022	0,017	0,025	0,15	0,15
Lu	0,0040	0,0060	0,0030	0,0030	0,0030	0,0090	0,019	0,0040	0,0040	0,0030	0,019	0,019
Total	0,41	1,04	0,19	0,11	0,08	4,53	160,4	1,30	0,38	0,15	79,91	77,98
(La/Yb)*n*	3,53	5,14	3,46	0,04	0,27	27,41	154,4	16,17	0,79	0,05	116,9	107,7

Yakutia (Russia)										
	Internatsional'naya pipe						Niurbinskaya pipe			
	[3], LA ICP-MS									
Element	Int-16	Int-19	Int-21	Int-22	Int-27	Int-28	Nur-1	Nur-2	Nur-3	Nur-4
	Kimberlites									
La	0,016	0,0040	0,024	0,27	0,0020	0,010	0,15	0,11	74,17	5,83
Ce	0,034	0,0070	0,032	0,30	0,017	0,014	0,15	0,040	132,7	10,13
Pr	0,0040	0,0035	0,0063	0,024	0,0020	0,0050	0,0034	0,025	16,01	1,05
Nd	0,021	0,024	0,035	0,095	0,021	0,029	0,048	0,0048	59,0	3,68
Sm	0,030	0,035	0,016	0,027	0,0018	0,020	0,0062	0,019	8,00	0,48
Eu	0,012	0,017	0,0084	0,0094	0,0090	0,0060	0,0099	0,0040	1,59	0,11
Gd	0,066	0,086	0,039	0,045	0,020	0,015	0,012	0,0057	3,98	0,35
Tb	0,013	0,015	0,012	0,010	0,013	0,012	0,014	0,0021	0,40	0,031
Dy	0,070	0,083	0,088	0,094	0,082	0,076	0,020	0,0076	1,71	0,18
Ho	0,014	N.d.	0,015	0,016	0,015	0,016	0,010	0,0017	0,22	0,024
Er	0,037	0,031	0,025	0,034	0,029	0,029	0,035	0,0051	0,40	0,069
Tm	0,0049	0,0041	0,0032	0,0041	0,0071	0,0061	0,0093	0,0014	0,037	0,0093
Yb	0,030	0,020	0,018	0,026	0,032	0,034	0,042	0,0067	0,18	0,047
Lu	0,0035	0,0040	0,0030	0,0040	0,0030	0,0040	0,011	0,0024	0,026	0,0082
Total	0,36	0,33	0,32	0,95	0,25	0,28	0,25	0,23	298,5	21,99
(La/Yb)*n*	0,36	0,13	0,90	7,01	0,04	0,20	0,25	10,54	284,7	83,10

Yakutia (Russia)									
	Niurbinskaya pipe		Novinka pipe	Trudovaya pipe					
	[3], LA ICP-MS								
Element	Nur-5	Nur-7	Nov-1	Tru-02	Tru-03	T ru-04	Tru-07	Tru-08	Tru-11	Tru-12
	Kimberlites									
La	0,13	0,62	0,057	1,17	0,11	0,093	0,41	0,14	25,64	13,07
Ce	0,25	0,88	0,13	2,65	0,23	0,17	0,48	0,15	42,85	39,06
Pr	0,017	0,10	0,017	0,24	0,024	0,016	0,067	0,034	4,58	5,51
Nd	0,045	0,20	0,051	0,59	0,12	0,056	0,20	0,072	15,83	13,95
Sm	0,012	0,036	0,020	0,11	0,012	0,010	0,077	0,011	1,97	1,86
Eu	0,0057	0,013	0,0050	0,027	0,0029	0,0042	0,013	0,0043	0,38	0,33
Gd	0,014	0,027	0,011	0,066	0,0086	0,012	0,038	0,018	1,00	1,18
Tb	0,0017	0,0040	0,0020	0,012	0,0016	0,0019	0,0053	0,0025	0,097	0,090
Dy	0,0060	0,025	0,0080	0,056	0,011	0,0095	0,026	0,011	0,43	0,41
Ho	0,0014	0,0061	0,0020	0,012	0,025	0,0016	0,0063	0,0016	0,055	0,046
Er	0,0038	0,017	0,0045	0,031	0,0060	0,0045	0,018	0,0039	0,088	0,10
Tm	0,0026	0,0022	0,0010	0,0037	0,0009	0,0005	0,0027	0,0006	0,010	0,0087
Yb	0,014	0,011	0,010	0,026	0,013	0,0039	0,018	0,0065	0,063	0,059
Lu	0,0027	0,0006	0,0013	0,0043	0,0029	0,0006	0,0040	0,0011	0,0092	0,0083
Total	0,51	1,95	0,32	4,99	0,54	0,39	1,37	0,46	93,02	75,70
(La/Yb)*n*	6,65	38,71	3,85	30,69	5,53	16,35	15,80	14,79	276,7	150,37

Note. The analyses Sch-0959D, Sch-93g(1a), Sch-093g(1b), Sch-093g(1c), and Sch-096C in addition were done by method ICP-MS; analyses VII-34/2, 4312, and Nash-1 – by INNA method. In brackets – number of analyses for calculation of average rock compositions. The ilmenites from Yakutian pipes (data [Aschepkov et al., 2007]) were done using megacrysts from heave mineral separates of kimberlites.

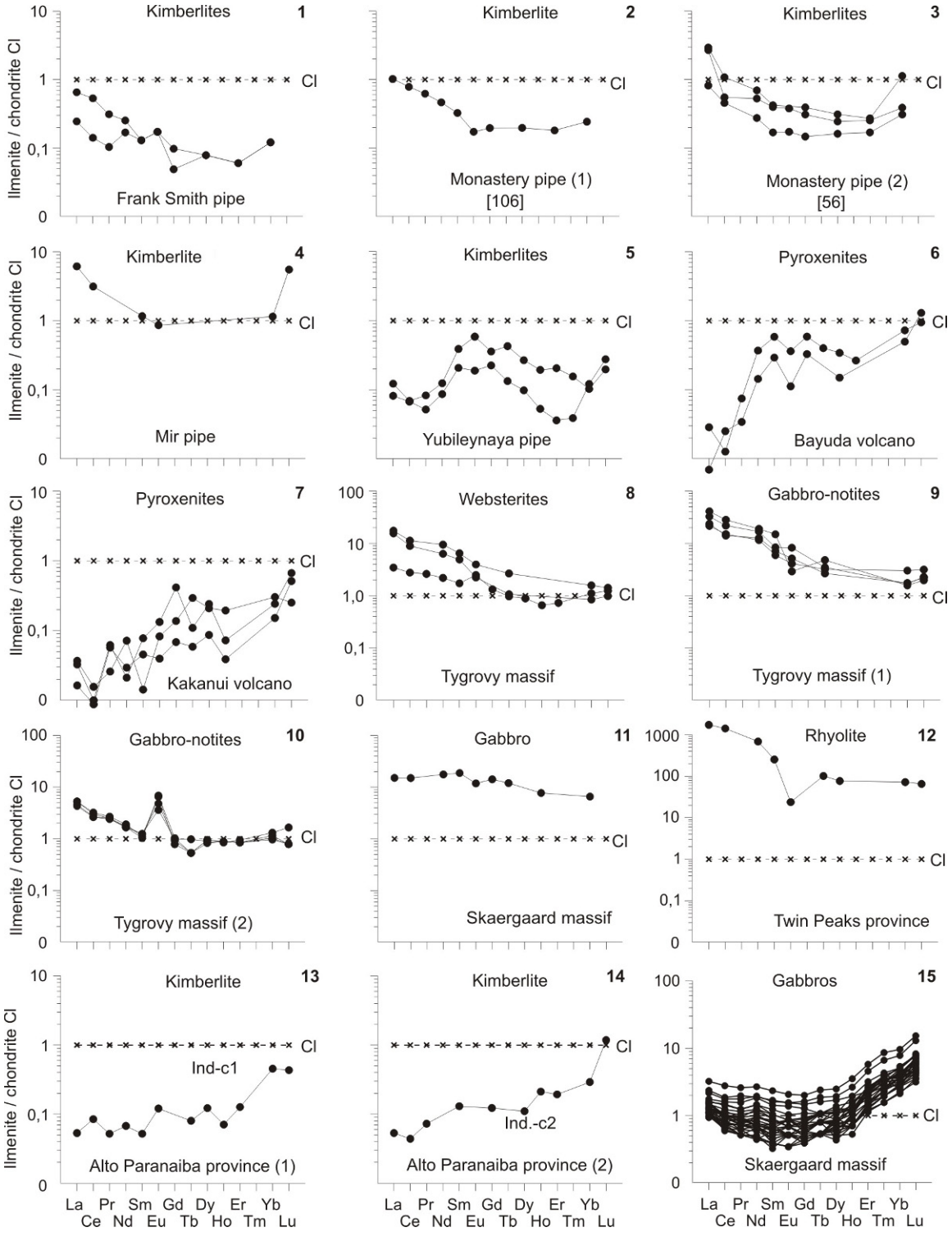

Figure 3. Chondrite-normalized REE patterns for ilmenites from some rocks. 1-5 - phenocrysts, 6-15 - accessory grains.

According to the analysis of ilmenites of kimberlites from Indaia manifestation (Alto Paranaíba province, Brazil) it was ascertained that the overall level of accumulation of REE in them is significantly lower than in Cl chondrite, while the chondrite-normalized contents of HREE in them is higher than the content of LREE (Fig. 3-13, 14).

Judging by the configuration of REE pattern, all the researched ilmenites from gabbros of Skaergaard massif demonstrate a slight enrichment with LREE and a more significant enrichment with HREE compared with the MREE, and many of these patterns show very weak positive or negative Eu anomalies (Fig. 3-15).

Aschepkov et al. [66] investigated the REE composition of great collections of ilmenite megacrystals from 50 pipes from six regions of the kimberlite magmatism in Yakutia (Russia). In this work it was shown that ilmenites from the researched kimberlite pipes both as a whole and from each of the pipe are characterized by very wide variations of REE composition, as can be seen both in the total content of elements and the configuration and slope of their distribution (Table 9). Thus, the total REE content within this entire collection of the ilmenite samples ranged from 0.02 to 298 ppm, and values (La/Yb)*n* - from 0.04 to 477. The highest average total REE content, as well as the increased values of the parameter (La/Yb)*n* define ilmenites from Ozernaya, Zarnitsa, Mir, International'naya and Khardakh pipes. The overwhelming majority of the patterns of ilmenites from this collection have a negative slope. The patterns of ilmenites from Yubileynaya, Dal'nyaya and Nebaybit pipes have a specific sinusoidal configuration, which is comparable to one that is typical for the patterns of already described garnets from diamond-bearing parageneses. Note that all the analyzed ilmenites from Komsomolskaya, Yubileynaya, Zarnitsa, Ukrainskaya, Dalnyaya and Trudovaya kimberlite pipes are almost identical, both in configuration and in slope of REE patterns. Contrasting to them, the patterns of the ilmenites from Aykhal and Udachnaya pipes and especially from Sytykanskaya, Mir and Nyurbinskaya pipes are characterized by significant variations in the shape and slope angle, especially in the LREE area. Based on data on concentrations of LREE, the ilmenites from these kimberlite pipes can be divided into two groups: 1) with a moderate amount of LREE, and 2) dramatically increased content of LREE. As we assume, in those samples of ilmenite, which proved to be anomalously enriched with LREE, a significant portion of these elements might be presented not as an isomorphous (structural) impurity, but in the form of unstructured impurity, localized in the microcracks of ilmenite crystals, as well as in solid or fluid microinclusions.

In generalizing the data on representative samples of kimberlites analyses in order to identify the correlations between the contents of petrogenic components and REE, it has been shown that in these rocks between the contents of TiO_2 and FeO, on the one hand, and the HREE, on the other hand, there is a directly proportional dependence [60, 67, 68]. Proceeding from the fact that both of these major kimberlite components are mainly concentrated in accessory segregations and phenocrystals of picroilmenite, it was suggested that picroilmenites accumulate mainly the HREE in their structure. This assumption was later confirmed by the analysis of picroilmenite phenocrystal from Mir kimberlite pipe by using INNA method [89]. In addition to the REE in this picroilmenite phenocrystal there have been found elements in form of impurity such as (ppm): Hf (28.8), Ta (351), Sc (45.2), Co (207), Cr (14789) and Zn (176). The ilmenites are known to accumulate rather significant amounts of Zr in their structure. Thus, in some of their samples from alkaline mafic rocks the content of this element reaches 3850 ppm [69]. The average content of Zr in ilmenites of gabbro from Skaergaard massif is 485 ppm. It was also noted that the average content of Zr in the accessory ilmenites consistently decreases in the sequence from mafic rocks to rocks rich in silicon [70]. In this regard, it is important to mention that in the grains of accessory ilmenites from anorthosite rocks of Eastern Canada complexes there were discovered rim width from 1 to 100 microns, formed by microsegregations of zircon [71]. Taking into account these observations we can assume that such rims consisting of microsegregations of zircon might be present also around grains of accessory ilmenite and in other rock complexes, and that they were not identified because of their submicroscopic size. Given the fact that the structure of zircon, as it will be shown in the following chapter, is very favorable for the accumulation of REE, especially heavy items, we can assume that the observed uneven enrichment with REE ascertained in some studied ilmenites is due to the presence around their grain and in their microcracks of very narrow zones, which are composed of submicroscopic segregations of later zircon.

As of today there are limited data on estimation of the D (REE) between ilmenites and coexisting phases, including the melts (Table 10), and [99]. Thus, in experiments using ilmenites from garnet pyroxenite it was determined that the values of D (ilmenite / melt) successively increase from La (~0.00003) to Yb (0.2) and then slightly decrease towards Lu (0.1) [58]. A similar trend in the values of these D from light to HREE was ascertained in the course of another experiment, but in this case the obtained values were slightly different: from 0.0072 - for La to 0.029 - for Lu [103]. Based on the results of the determination of

REE composition of ilmenites from Skaergaard massif, it was found that the average D (ilmenite / melt) decreases in the sequence from La to Sm, and then slightly increases in the sequence from Sm to Lu. These data are consistent with available information on the strong positive correlation between contents of HREE and contents of FeO_{tot} and TiO_2 in ilmenites. Using experimental data [58], it was found that the values of D (ilmenite / clinopyroxene) for La (~0.00054) and Ce (0.00063) by nearly three orders of magnitude are smaller than those for Tm (0.22), Yb (0.40) and Lu (0.19) (Table 10). On this basis we can assume that the contents of HREE in ilmenites might be approximately 20-40% of their amount in the coexisting clinopyroxenes. In this regard, it should be mentioned that according to the data obtained in the study of ilmenites from Skaergaard massif, the values of D (ilmenite / gabbro), D (ilmenite / clinopyroxene) and D (ilmenite / magnetite) obtained for REE were determined as unusually high [54]. Moreover, according to [72] the estimates of the values of D (ilmenite / melt of basic composition) for Zr are 0.28 and for Nb – 0.8. In addition, according to data obtained from ilmenites from Skaergaard massif it follows that the contents of Ce and Yb in them increase with increasing content of Zr and Nb, as well as with reducing content of V. Given the fact that the D (ilmenite / melt) for the LREE have lower values compared with the D for HREE, it is logically assumed that the latter are more compatible with the structure of this mineral compared with the first one.

5. Zircons

Zircon is one of the most prevailing accessory minerals of magmatic, metamorphic and some metasomatic formations of different composition. Due to its mechanical strength, during the disintegration of indigenous sources the zircons sometimes accumulate in the sedimentary rocks up to the formation of placer deposits. This mineral is presented in high amounts in the granites, diorites, nepheline syenites, lamproites, carbonatites and alkaline metasomatic rocks, more rarely it occurs in the gabbros, eclogites, kimberlites, minettes, lamproites, carbonatites, gneisses, amphibolites and other metamorphic rocks. Recently, the zircons were found in ultramafites from some mantle xenoliths in alkali basalts in several provinces of China and Russia [73, 74], in ore chromitites occurring among phlogopite-bearing peridotites of Finero massif (Southern Alps) [75], as well as in dunites and ore chromitites of Voykar-Syn'insky massif (Polar Urals, Russia) [76, 77]. In the latter case, as the authors assume, zircons crystallized from the residual portions of fractionated basic melts that infiltrated into peridotites. Zircons with Archean U-Pb isotopic age have recently been identified in the dunites of the Nizhnetagilsky massif, which is a part of Platinum-bearing belt of the Urals (Russia) [78]. Note that in some gabbroid rocks the crystals of accessory ilmenites were identified surrounded by narrow (1-100 microns) rims that consist of microcrystals of zircon. The formation of the latter, as suggested by the researchers, was due to a later infiltration of high-temperature interstitial fluids enriched with Zr [72].

The main trace elements in zircons might be Hf, REE, Y, U, Th, the total amount of them can reach first weight percents. In recent decades, the zircons have been widely used for isotope dating of magmatic and metamorphic rocks using U-Pb-method, which considerably increased interest in a more detailed geochemical study of this mineral, including the study of REE distribution in it [79]. Note that previously we presented a brief review of materials published in recent decades on REE distribution in zircons from rocks of different composition and origin [64], as well as on some features of their isomorphism in this mineral [80].

First of all, it should be noted that to date the regularities of REE distribution in zircons have been studied much better in comparison with other accessory minerals. In particular, a fairly representative data have been published on the distribution of REE in zircons from kimberlites, eclogites, minettes, granitoids, gabbros, and ultramafic rocks, some of the effusive and metamorphic rocks.

Kimberlites. Sufficiently large amount of analytical data on the REE composition of zircons was published on the results of their study in the kimberlites of several provinces in Australia, South Africa and Yakutia (Russia) [81]. This work shows that zircons from kimberlites of these provinces are more or less different both in the general level of REE accumulation and in the concentration of some other trace elements. The authors concluded that the zircons from kimberlites in its geochemical properties are very different from zircons presented in lamproites, carbonatites and some mafic rocks. In general, the zircons from the studied kimberlites are characterized by relatively low total REE content (less than 50 ppm), including heavy elements, and their REE patterns often have a more or less gentle positive slope. A low content of U (6-20 ppm) and Y (6-200 ppm) is observed in these zircons. In addition, E. Belousova et al. drew attention to the fact that the zircons from kimberlites differ from the zircons from most other magmatic rocks crystallized in the earth's crust and the former has higher values of Hf (wt %)/Y (ppm) parameter.

While studying the geochemistry of zircons from kimberlites of Timber Creek province (Northern Australia) it was found that by their REE composition they are very simi-

Table 10. The coefficients of REE distribution (D) between ilmenites and coexisting phases.

	D (ilmenite / melt)			D (ilmenite / clinopyroxene)		D (ilmenite / gabbro)	D (ilmenite / / magnetite)
Element	[169]	[104]	[53]	[169]	Calculated by data [111]		
La	0,000029	0,0072	0,015	0,00054	1,61	0,276	6,85
Ce	0,000054	N.d	0,012	0,00063	0,417	0,234	6,76
Pr	0,00019	»	N.d.	0,0013	N.d.	N.d.	N.d.
Nd	0,00048	»	0,010	0,0026	0,467	0,255	5,25
Sm	0,00059	0,0091	0,009	0,0020	0,164	0,293	7,25
Eu	0,0011	N.d.	0,010	0,0036	0,377	0,238	4,06
Gd	0,0034	0,0077	0,011	0,0085	0,341	0,242	7,63
Tb	0,006	N.d.	0,018	0,016	0,341	0,273	7,63
Dy	0,009	»	N.d.	0,022	N.d.	N.d.	N.d.
Ho	0,01	0,012	0,035	0,024	0,306	0,270	8,00
Er	N.d.	N.d.	0,067	N.d.	N.d.	N.d.	N.d.
Tm	0,1	»	0,102	0,22	»	»	»
Yb	0,2	»	0,13	0,40	0,352	0,454	9,48
Lu	0,1	0,029	0,19	0,19	N.d.	N.d.	N.d.

lar to zircons from kimberlites of several other provinces of Australia, as well as provinces in Southern Africa and Yakutia, but differ in slightly reduced overall level of REE accumulation [82]. Thus, the total REE contents in zircons from the Timber Creek province range from 3.4 to 43.6 ppm (with an average of 12 ppm) (Table 11), which corresponds to the lower limit of this parameter for zircons from kimberlites in general. Zircons from kimberlites of Timber Creek province are depleted in lanthanum, the average chondrite-normalized content of which is ~0.19 t.ch., while they are moderately enriched with HREE. Thus, the average chondrite-normalized Yb content in them is about 22 t.ch., which causes a relatively low average value of (La / Yb)*n* - around 0.02. On REE patterns of almost all of these zircons there are positive Ce anomalies of various intensity. The values of (Ce/Ce*)*n*parameter in them range between 1.2 and 7.6 with an average of 3.1. Finally, it should be noted that the zircons from kimberlites of Timber Creek province mostly have relatively low average contents of U (~8 ppm) and Th (~4 ppm).

The study of zircons from kimberlites of Kampfersdam province (Africa) showed that their crystals are characterized by a zonal distribution of REE: in the kernels the contents of REE are higher compared to the peripheral zones of the crystals, and the chondrite-normalized contents of elements increase manifold in the row from La (2 t.ch.) to Lu (400 t.ch.) [83]. In the peripheral zones of crystals the REE are less fractionated; respectively, their chondrite-normalized contents vary in a narrow range – from 0.15 t.ch. (La) to 50 t.ch. (Lu). The REE patterns of internal and peripheral zones of zircon crystals from kimberlites of the province, having the form of almost straight lines with positive slope, are complicated by intense positive Ce anomalies.

Eclogites. While isotopic dating of eclogites from some metamorphic provinces of Norway by using U-Pb zircon method in the latter there have also been estimated REE contents [84]. It was ascertained that the total REE content in these zircons vary in the range of 28 - 54 ppm with the average of 42 ppm. The zircons from eclogites of Flatraket province (Norway) that were studied in more detail turned out to be almost identical, both in the general level of REE accumulation and the configuration of REE patterns, that in each case are complicated by positive Ce anomalies. The average value of the intensity index of these anomalies - (Ce/Ce*)*n* parameter - is 5.6. For the heavy REE the patterns of these zircons have a form of shallow lines, indicating a weak fractionation of these elements. D. Root et al. suggested that the characteristics of REE composition of zircons they studied are caused by the presence in their crystals of syngenetic or later microinclusions of garnet, enriched with pyrope component. The zircons from eclogites of Norwegian province called Verpeneset differ from the mineral of the other provinces by a much more significant enrichment with HREE and less intense positive Ce anomalies.

In the zircons from eclogites of Monte-Rosa complex (Western Alps) the content of LREE, excepting Ce, is below the limits of detection by the analytical method used. In addition, chondrite-normalized contents of Yb and Lu in them exceed 100 t.ch. [85]. In order to finish the description of zircons from eclogites, we should add that in their samples from eclogites exposed in Kuru-Vaara manifestation (Kola Peninsula, Russia) [86] the total REE contents range from 10 to 176 ppm and the value of (Ce/Ce*)*n* pa-

rameter varies in the range of 2.4-3.7. Moreover, their patterns often show intense negative Nd anomalies, which were not observed in the patterns of zircons from eclogites described above.

Minettes. Zircons from these rocks are studied by the example of dikes samples that are cutting the metamorphic complex within Kirovograd block (Ukraine) [87]. Note that this minettes have previously been described as lamproites [81]. The minette samples were selected from the core of several holes drilled in order to estimate the prospects for diamond-bearing of these rocks. They usually have a porphyric structure due to the presence of phenocrysts of phlogopite, biotite, hornblende, diopside, rarely - of olivine, which are immersed in the fine- and medium-granular matrix. In the content of the latter there are micro-crystals of zircon, common potash feldspar, pseudo-leucite, plagioclase and quartz. The zircons presented in minettes are heterogeneous in size, shape and color of grains. The dominating ones are well-faceted crystals of different habit; the rarely seen are fragments of crystals, as well as grains of irregular shape with evidence of melting with observed fluid microinclusions. The values of Zr/Hf parameter in zircons from this collection vary in a relatively narrow range. Additionally, the contents of most trace elements, including REE, vary widely. At the same time the contents of Y are higher than the contents of U, and the latter are higher than in zircons from kimberlites.

By the general level of REE accumulation the analyzed zircons from minettes of Kirovograd block were divided into four types. The grains of zircons that are prevailing in this collection were assigned to the 1st type and the total REE content in them ranges from 160 to 1400 ppm. Zircons of this type have almost identical by configuration REE patterns, which usually show positive Ce anomalies of moderate intensity and intense negative Eu anomalies. They are also characterized by very low values for $(La/Yb)n = 0{,}0005\text{-}0{,}007$. Based on the assumptions that the zircons of this type were crystallized on conditions of equilibrium with the minette parent melt, and that afterwards the trace elements in them have not undergone a substantial redistribution, the calculations on the model REE composition of the minette parent melt were made. Results of the calculations showed that this minette parent melt was significantly enriched with LREE, especially with Ce, and at the same time had some Eu deficiency. The estimated model REE composition of minette parent melt gives grounds to consider them as geochemical analogues of lamproites, although in the latter there is usually a less severe Eu deficiency.

The REE composition of the zircon crystals from the considered minettes, which were assigned to the 2^{nd}, 3^{rd} and 4^{th} types, was studied on the example of single grains. It was ascertained that zircons of the 2^{nd} type, being close to zircons of the 1^{st} type by total REE content, differ from them by higher values of $(Ce/Ce^{*})n$ parameter. Meanwhile, the zircons of 3^{rd} and 4^{th} types show an anomalous enrichment with LREE, while their patterns have no positive Ce anomalies. Apart from this, the pattern of zircon, which is referred to the 4^{th} type, has no negative Eu anomaly.

The identified geochemical features of zircons from minettes of Kirovograd block give grounds to consider these zircons to by heterogeneous. Their crystals that are referred to the 1^{st} type are characterized by typical for this mineral significant enrichment with HREE, depletion by LREE, as well as excess content of Ce with Eu deficit. Additionally, the unusual for zircons REE distribution observed in the grains, that are assigned to other three types, melting signs observed in their crystals as well as the presence of fluid microinclusions, lead to the conclusion that these crystals at a late stage of its crystallization have undergone different intensity effects of the residual portions of the parent melt, resulting in partial redistribution of these trace elements, REE included.

Ultramafic rocks. In these rocks the accessory zircons are much rarer present and in much smaller quantities than in most other varieties of magmatic and metamorphic rocks, so they are still the least studied with respect to the geochemistry of REE and other trace elements. Thus, in this concern there have been recently studied in detail the zircons from peridotites forming massifs in the Northern Tibet [88] and Sulu provinces (China) [89], from ultramafic xenoliths in kimberlites of Gibeon province (Southern Namibia), as well as from ultramafic xenoliths of some diatremes of Hinyang province (North China) [75]. According to the research, in the zircons from Hinyang province the total REE contents, except for Tb and Tm, vary in the range from 435 to 1483 ppm. Also there have been identified the contents of Y (572-1933 ppm), P (202-586 ppm), Pb (1.35-23.5 ppm), and HfO_2(1.2-2.49 wt %). The zircons from ultramafites of Hinyang province by the values of $(La/Yb)n$ parameter can be divided into two geochemical types - with lower (0.0001-0.0003) and with relatively higher (0.0016-0.0074) values of this parameter. On REE patterns of the first type of zircons the positive Ce anomalies have a higher intensity compared to zircons of the second type. It can be assumed that the relative enrichment of the second type of zircon with LREE and specificity of their patterns are due to the presence in the microcracks of their crystals of small amounts of unstructured LREE impurities, brought by epigenetic processes. The configurations of the multielemental patterns of the observed zircons also indicate their anomalous enrichment

with uranium and thorium. The average value of U/Th parameter in them is 3.3.

Saltykova et al. [74] studied zircons with melt, fluid and mineral (apatite, sillimanite and quartz) inclusions from garnet spinel lherzolites from Vitim province. These fell into four groups. The first had the oldest zircon U-Pb ages, two of which (1694 and 1506 Ma) had low La, intense positive Ce anomalies and negative Eu anomalies; a third zircon crystal from this group (age 1088 Ma) was enriched in the LREE, lacked a Ce anomaly and had only a weak Eu anomaly. The samples from the second, third and fourth groups showed significantly lower values of the isotopic age (277-139 Ma). All of them have patterns complicated by intense positive Ce anomalies, while the intensity of negative Eu anomalies consistently decreases in them from the second group to the fourth group, which has Eu anomaly completely neutralized. We assume that such a "reduction" of the isotopic ages of zircons and the accompanying changes of their REE composition were caused by later processes of redistribution of impurities and disturbances in the original U-Pb isotopic system in the process of thermal and isotopic-geochemical influence of those fluids that were separated from basaltic melts, subtracting xenoliths of garnet-spinel lherzolites from the upper-mantle level to the surface and seeped into the xenoliths and their minerals by the systems of microcracks. Such an assumption correlates with the presence of fluid microinclusions in some zircons, as well as the appearance of a brownish color, which indicates their relative enrichment with LREE.

Gabbros, diorites, pyroxenites. The REE composition of zircons from these rocks is studied by the example of samples of pegmatite gabbros forming Khayalygsky massif (South-Western Tuva, Russia) [75, 76]. These zircons are represented by idiomorphic short-columnar crystals of 0.2-1 mm in size and of a color from pink to colorless. According to the results of U-Pb isotopic dating the age of these zircons is 447.4±1.3 Ma (Late Ordovician). Using the microprobe technique it was determined that the content of ZrO_2 in them is 66.4-66.9 wt %, HfO_2 – 0.85-0.99 wt %. The value of ZrO_2/HfO_2 vary in the range of 67-78. The total REE content varies in the range of 128-156 ppm, the values of (La/Yb)*n* - in the range of 0.004-0.012. On the REE patterns of the studied zircons there are relatively weak in intensity positive Ce anomalies and negative Eu anomalies. At the same time, their multielemental patterns show intense positive anomalies for Zr, Hf, and U, less obvious - for Th and Pb, as well as negative anomalies for Sr, Rb and Nb. Note that by the configuration of the multielemental patterns of the zircons from gabbros of Khayalygsky massif are rather similar to those zircons described above, that are from peridotites represented in deep xenoliths of North China provinces, although the latter are somewhat richer in Ce, medium and heavy REE, Th, U, Ta and Nb, and poorer in Pb and Sr.

While isotopic dating of hornblende gabbros of Chernoistochninsky and Reftinsky massifs (Urals, Russia) by accessory zircons in individual samples of the latter their, REE composition was determined [90]. In these zircons the chondrite-normalized HREE contents predominate over the contents of LREE, as indicated by the steep positive slope of the REE patterns. The zircons from the rocks of Chernoistochninsky massif have higher overall level of REE accumulation (La - 40 t.ch., Lu - 3000 t.ch.) compared with the mineral from rocks of Reftinsky massif (La – 0.6 t.ch., Lu - 1300 t.ch.). Nevertheless, a positive Ce anomaly on patterns of zircon from Chernoistochninsky massif has a much lower intensity than this anomaly in the mineral from rocks of Reftinsky massif. In the spectrum of the latter the positive Eu anomaly is of minimal importance, while it is very clearly shown in the spectrum of zircon from Chernoistochninsky massif.

Ronkin & Nesbit [91] studied the REE composition of zircons from certain kinds of rocks that form the Berdyaushsky massif (Urals, Russia), including gabbro. It was ascertained that in the zircons from this gabbro the chondrite-normalized La contents are around 0.015-03 t.ch., which is about the same level as the Pr content. The determined Ce content in these zircons is about 1-8 t.ch., which causes the presence of Ce positive anomalies in their patterns. At the patterns intervals between Pr and Lu they have a form of almost straight positively inclined lines complicated by weak negative Eu anomalies.

Interesting data was obtained during studies on REE composition of zircons from gabbros that underwent brittle-plastic deformation and are dredged in Markov depression (Mid-Atlantic Ridge) [92] (Table 11, Fig. 4-1, 2). According to the U-Pb isotope dating of zircon grains from the gabbros, it was determined that their age varies from 2.3 to 0.7 Ma. The authors of this paper concluded that under the plastic deformation, accompanied by infiltration of the intergranular fluids of unknown nature, the studied zircon crystals have undergone an uneven enrichment with several trace elements, including REE, U, Th, Hf, P and Y. On the example of zircon crystals from particular sample of gabbro it was found that the $^{238}U/^{206}Pb$ parameter varies significantly even within individual grains of the mineral. At the same time, the values may differ in order, to some extent correlated with the intensity of brittle-plastic deformations experienced by these grains. Thus, in a weakly deformed zircon crystal (f) the values for $^{238}U/^{206}Pb$ ranged from 287 to 670. While in a strongly deformed and recrystallized zircon crystal (g) the value of the parameter was in the range of 4363-5473, but data on

Table 11. REE compositions of zircons from kimberlites, lherzolites, gabbros, gabbro-norites, anorthosites from some provinces (ppm).

Timber Creek province (North Australia)
[10], LA ICP-MS

Element	1-V-t	1-V-b	2-V-t	2-V-b	3-V-t	3-V-b	4-V-t	4-V-b	5-V-t	5-V-b	6-P-t	6-P-b	7-P
	Kimberlites												
La	0,020	0,040	0,020	0,030	0,070	0,050	0,030	0,060	0,190	0,030	0,020	0,030	0,060
Ce	0,260	0,920	0,330	0,370	0,270	1,030	0,530	0,370	0,430	0,390	0,370	0,380	0,550
Pr	0,030	0,040	0,020	0,030	0,040	0,100	0,030	0,040	0,030	0,040	0,020	0,030	0,060
Nd	0,170	0,730	0,310	0,410	0,220	0,500	0,750	0,230	0,330	0,220	0,140	0,330	0,790
Sm	0,180	0,730	0,270	0,460	0,420	0,570	0,700	0,530	0,680	0,330	0,700	0,160	0,630
Eu	0,080	0,500	0,140	0,050	0,060	0,150	0,260	0,070	0,120	0,250	0,100	0,200	0,280
Gd	0,180	2,820	0,680	0,970	0,460	0,940	1,22	0,420	1,38	1,12	1,20	1,020	1,500
Tb	N.d.	N.d.	N.d.	N.d.	N.d.	N.d.	N.d.	N.d.	N.d.	N.d.	N.d.	N.d.	N.d.
Dy	0,640	8,46	1,66	1,42	1,01	2,52	3,60	0,960	1,75	1,79	3,89	3,37	3,65
Ho	0,160	2,470	0,460	0,750	0,320	0,630	0,950	0,220	0,570	0,610	0,830	1,10	1,12
Er	0,720	10,18	1,82	2,49	0,990	2,26	4,31	0,510	1,41	1,45	3,58	3,79	3,31
Tm	N.d.	N.d.	N.d.	N.d.	N.d.	N.d.	N.d.	N.d.	N.d.	N.d.	N.d.	N.d.	N.d.
Yb	0,800	13,9	1,76	3,26	2,18	3,26	5,60	0,910	3,19	2,33	4,58	5,04	5,17
Lu	0,120	2,79	0,470	0,570	0,330	0,630	1,050	0,240	0,560	0,530	0,830	0,890	1,01
Total	3,36	43,6	7,94	10,8	6,37	12,6	19,0	4,56	10,6	9,09	16,3	16,3	18,1
$(La/Yb)_n$	0,017	0,002	0,008	0,006	0,022	0,010	0,004	0,045	0,040	0,009	0,003	0,004	0,008
$(Eu/Eu^*)_n$	1,35	0,93	0,95	0,22	0,42	0,62	0,85	0,44	0,37	1,13	0,33	1,14	0,84
$(Ce/Ce^*)_n$	2,08	5,00	3,58	2,68	1,21	2,61	3,84	1,76	1,24	2,28	4,02	2,75	1,99

Tolstik manifestation and Yavrozero district (Kola Peninsula, Russia)
[58], LA ICP-MS

Element	742-51a	742-51b	742-51c	742-51c	763-1a	763-1b	763-1c	GKR-7a	GKR-7b	GKR-7c	A-3-1	A-3-2	A-3-3
	Gabbros				*Gabbro-anorthosites*			*Gabbro-norites*			*Anorthosites*		
La	0,5	0,2	1,8	0,4	0,2	0,1	0,2	0,1	0,5	0,1	0,1	0,03	0,04
Ce	35	39	40	23	33	34	27	1.4	1.2	1,0	3,0	1.0	2.0
Pr	1.3	0.7	1,0	1.1	0,2	0,2	0,1	0.01	0,02	0.01	0,05	0,04	0.01
Nd	14	9	10	12	2	3	2	0,1	0,1	0,1	0,4	0,3	0,1
Sm	13	12	11	10	4	6	4	0,3	0,3	0,3	0,5	0,5	0,1
Eu	2,7	1,2	1,0	1,7	0,2	0,2	0,1	0,1	0,2	0,1	1,3	1,0	0,1
Gd	70	58	54	43	20	25	15	2	3	2	2	2	0.4
Tb	N.d.	N.d.	N.d.	N.d.	N.d.	N.d.	N.d.	N.d.	N.d.	N.d.	N.d.	N.d.	N.d.
Dy	248	202	200	132	64	75	53	14	18	13	3	3	1
Ho	N.d.	N.d.	N.d.	N.d.	N.d.	N.d.	N.d.	N.d.	N.d.	N.d.	N.d.	N.d.	N.d.
Er	510	425	435	252	121	134	97	38	51	36	2	3	1
Tm	N.d.	N.d.	N.d.	N.d.	N.d.	N.d.	N.d.	N.d.	N.d.	N.d.	N.d.	N.d.	N.d.
Yb	842	741	748	428	203	216	177	96	135	94	3	4	3
Lu	130	121	122	66	32	34	29	18	26	18	0,3	0,4	0,2
Total	1866	1609	1624	971	481	528	404	169	234	165	15	14	8
$(Yb/La)_n$	2178	6066	575	1381	1262	3384	1466	2546	3836	1988	59	151	113
$(Eu/Eu^*)_n$	0,2	0,1	0.1	0,2	0,1	0,04	0,04	0,4	0,4	0,4	3,5	3,2	1,3
$(Ce/Ce^*)_n$	7	16	7	6	35	48	41	16	11	12	13	6	27

Tolstik manifestation and Yavrozero district (Kola Peninsula, Russia)
[58], LA ICP-MS

Element	A-3-4	A-3-5	A-3-6	A-3-7	A-2-1	A-2-2	A-1	A-3	U-1a	U-1b	U-1c
	Anorthosites								*Lherzolites*		
La	0,03	0,03	0,01	0,02	0,01	0.01	0,003	0,02	0,04	0,01	0,1
Ce	1	1	1	1	10	6	2	9	4	4	5
Pr	0,03	0,01	0,01	0,01	0,1	0,1	0,03	0,3	0,02	0,02	0,04
Nd	0,2	0,1	0,04	0,04	1,3	0,8	0,3	3	0,2	0,1	0,4
Sm	0,3	0,3	0,1	0,1	1,7	0,9	0,7	3	0,3	0,3	0,4
Eu	0,8	0,7	0,2	0,2	0,7	0,4	0,1	1,8	0,1	0,1	0,1
Gd	1	1	0,3	0,4	5	3	2	6	1	1	1
Tb	N.d.	N.d.	N.d.	N.d.	N.d.	N.d.	N.d.	N.d.	N.d.	N.d.	N.d.
Dy	2	3	1	1	16	12	5	8	5	5	6
Ho	N.d.	N.d.	N.d.	N.d.	N.d.	N.d.	N.d.	N.d.	N.d.	N.d.	N.d.
Er	3	3	1	1	34	38	6	6	12	10	13
Tm	N.d.	N.d.	N.d.	N.d.	N.d.	N.d.	N.d.	N.d.	N.d.	N.d.	N.d.
Yb	5	3	1	2,1	82	103	9	4	26	24	30
Lu	0,5	0,4	0,1	0,2	14	19	1	1	5	4	5
Total	14	12	4	6	164	184	26	42	53	48	62
$(La/Yb)_n$	0,004	0,007	0,006	0,006	0,0006	0,0009	0,003	0,03	0,001	0,0004	0,001
$(Eu/Eu^*)_n$	3.6	3,0	2,8	2,9	0.7	0,6	0.3	1,3	0,3	0.5	0.4
$(Ce/Ce^*)_n$	7	12	10	14	24	13	19	7	39	44	26

Markov depression (Mid-Atlantic Ridge)
[172], LA ICP-MS

Element	L1153-49							L1097-1					
	Grain's number												
	a-1	a-2	b-1	b-2	c-1	c-2	d-2	e-1	e-2	f-2	g-1	h-1	i-1
	Gabbros												
La	0,04	0,06	1,11	0,15	0,09	0,03	0,49	0,01	0,01	0,02	0,12	0,02	0,02
Ce	6,71	5,92	9,43	5,82	10.13	30,23	45,92	1,75	3,68	7,97	22,09	21.96	24,83
Pr	0,08	0,27	1,21	0,09	0,25	0,18	0,68	0,04	0,05	0,12	0,12	0,10	0,13
Nd	2,09	5,90	13,18	1,43	4,93	4,66	12,31	0,85	0,98	2,07	2,26	2,34	2,72
Sm	5,80	12,58	14,26	3,96	11,94	15,04	30,79	1,83	2,18	5,15	6,30	6,52	7,37
Eu	1,57	3,76	4,37	1,13	2,75	2,69	5,12	0,52	0,67	0,97	0,60	0,57	0,67
Gd	33,53	72,97	49,31	27,36	73,46	105,74	189,69	9,16	17,08	30,86	41,30	41,81	47,83
Tb	13,96	27,24	15,24	10,71	27,20	39,98	69.63	3,51	7,02	12,39	17,25	17,84	19,98
Dy	150,89	317,13	170,90	138,45	342,27	516,98	823,73	38,81	89,91	148,96	210,30	223,00	244,37
Ho	60,01	125,66	63,88	56,02	136,15	200,29	325,71	13,89	36,68	59,79	85,89	91,14	100,81
Er	296,87	553,91	284,06	260,24	613,79	895,53	1456,14	58,25	156,45	271,97	401,18	429,54	457,55
Tm	68,37	115,11	57,24	59,67	131,88	197,45	305,86	12,89	34,52	62,58	90,58	95,22	103,72
Yb	623,27	977,95	469,84	520,83	1065,79	1638,11	2547,81	117,78	302,58	533,39	777,40	775,96	904,41
Lu	106,38	160,40	101,46	95,82	217,63	312,22	457,53	20,07	48,00	87.15	128,62	128.54	150,44
Total	1370	2379	1255	1182	2638	3959	6271	279	700	1223	1784	1835	2065
$(La/Yb)_n$	0,00004	0,00004	0,002	0,0002	0,00006	0,00001	0,0001	0,00006	0,00002	0,00003	0.0001	0,00002	0,00001
$(Eu/Eu^*)_n$	0,27	0,30	0,45	0,24	0,22	0,15	0,16	0,32	0,24	0,18	0,09	0,08	0,08
$(Ce/Ce^*)_n$	21.2	6,1	1,7	11.8	10,7	47,6	15,9	12,0	20.6	18.8	39.9	61,5	54,4

Northern Catena Costiera area (Southern Italy)
[81], LA ICP-MS

Element	M53								M57				
	Grain's number												
	Zrn-7	Zrn-10a	Zrn-10b	Zrn-13a	Zrn-14	Zrn-18a	Zrn-35a	Zrn-16a	Zrn-1	Zrn-7	Zrn-8	Zrn -13	Zrn-14
	Gabbros												
La	<0,021	<0,020	<0,019	<0,019	N.d.	<0,024	N.d.	<0,023	0,01	N.d.	0,08	0,03	0,01
Ce	0,70	3.48	5,58	2,49	0,84	1,41	2,94	2,85	0,72	0,77	1,86	1.40	1,73
Pr	0,02	0,02	0,04	<0,014	0,02	<0,017	0,06	<0,023	0,07	<0,015	0,09	0,02	<0,016
Nd	0,56	0,49	0,50	0,63	0,11	0,15	0,63	0,47	1,22	<0,094	0,73	0,65	0,50
Sm	0,97	0,75	1,60	0,57	0,21	0,31	1,59	1,17	5,15	0,93	1,69	1,35	1,58
Eu	0,50	0,46	0,51	0,71	0,12	0,36	0.72	0,50	0,31	0,12	0,54	0,08	0,21
Gd	4,47	4,68	8,37	3,47	1,37	2,66	6,42	5,94	25,28	6,54	8,80	9,65	10,30
Tb	1,85	1,87	2,92	1,84	0,77	0,96	2.10	1,79	5,88	2,08	5,36	3,33	3,62
Dy	23,36	24,59	35,69	23,19	11,70	11,16	23,42	19,72	29,62	26,71	64,79	49,70	46,49
Ho	9,39	9,70	13,29	9,65	4,65	4,33	9,26	7,44	4,77	10,08	29,00	20,52	19,16
Er	46,19	51,09	62,20	51,01	25.18	19,92	44,81	34,91	10,42	48,21	149.52	101,52	86,33
Tm	10,08	11,47	15,43	12,67	6,14	4,78	9,66	7,86	1,10	9,66	33,76	23,93	18,55
Yb	103,22	131,73	148,82	144,09	62,13	47,42	104,49	80,56	6,52	96,30	337,01	274,41	188,17
Lu	22.86	30,38	33,80	34,74	16.06	10,25	22.92	19,03	1,12	19,69	76,44	55.16	37,44
Total	224	271	329	285	129	104	229	182	92	221	710	542	414
$(Yb/Gd)_n$	27.94	34,05	21,51	50,24	54,87	21,57	19,69	16.41	0,31	17,81	46,33	34,40	22.10
$(Eu/Eu^*)_n$	0,73	0,75	0,43	1,54	0,67	1,19	0,69	0,58	0,08	0,15	0,43	0,07	0,16

age of zircons with such values of parameter $^{238}U/^{206}Pb$ in the article are not available. These data led to the conclusion that redistribution of trace elements, including REE, U, Hf and Th, accompanying the plastic deformations of zircon crystals of the gabbro, had a significant effect on the parameters of U-Pb isotopic system, which, in turn, affected the reliability of the estimates of isotopic age obtained on the basis of these zircons.

We obtained the first data on REE composition (LA ICP-MS method), as well as on the isotopic age (U-Pb method, SHRIMP II) of zircons from gabbros, gabbro-diorites, gabbro-pyroxenites, pyroxenites and some other rocks that form Beriozovsky mafic-ultramafic massif, which is a part of Eastern-Sakhalin ophiolite association (Sakhalin Island, Russia) (Table 11). In the gabbros of this complicated massif there were numerous xenoliths of ultramafites found. Due to the active influence of mafic melts and their fluids on the rocks of earlier ultramafic protrusion, as well as on the surrounding terrigenous-volcanic rocks, along their boundaries there were formed contact-reaction zones composed of heterogeneous in quantitative-mineral composition and often banded hybrid rocks (wehrlites, plagioclase-bearing wehrlites, pyroxenites, gabbro-pyroxenites, gabbro-diorites, diorites and others). These observations led us to the conclusion that the gabbro intrusion have formed later in relation to protrusion of ultramafic restites it was spatially brought together with and that Beriozovsky massif is polygenic [80, 93].

Based on the performed isotope studies it was ascertained that zircons from rocks of gabbro intrusion, which is a part of Beriozovsky massif, have an average age of about 158 Ma (late Jurassic). However, some grains of zircon from the hybrid pyroxenites and gabbro-pyroxenites have

Beriozovsky massif, Sakhalin Island (Russia)
[data F. Lesnov], LA ICP-MS

Element	1606-1										1597				
	Grain's number														
	1	2	3	4	5	6	7	8	9	10	1	2	3	4	5-1
	Gabbro-pyroxenite										*Pyroxenite*				
La	0,60	0,31	0,05	0,06	0,02	0,06	0,01	0,05	0,02	0,02.	0,06	0,08	0,03	0,09	0,68
Ce	14,98	19,32	7,00	18,07	11,63	7,46	23,38	16,26	8,54	6,94	3,10	28,5	5,5	96,4	24,0
Pr	0,49	0,97	0,29	0,72	0,15	0,18	0,28	0,20	0,12	0,06	0,05	0,80	0,09	0,39	0,45
Nd	3,38	12,53	4,27	9,63	2,42	2,75	3,11	3,44	1,40	1,20	1,30	6,30	1,60	5,00	4,60
Sm	4,97	15.43	6,92	15,09	4,90	4,92	7,43	4,73	3,19	1.49	2,80	12,2	2,30	11.3	5,10
Eu	0,19	1,53	0,47	1,25	0,67	0,31	1,88	1,19	1,09	0,50	0,30	2,53	1,18	2,04	0,52
Gd	18,7	40,2	21,4	47,5	13,0	20,4	26,0	17,4	19,37	5,86	14,1	41,6	11,1	34,0	25,2
Tb	6,37	12,2	6,98	18,1	5,23	7,52	9,18	6,52	8,82	2,38	5,40	15,6	4,30	13,7	8,30
Dy	74	129	77	209	60	96	99	75	121	31	63	181	54	129	107
Ho	24	41	23	71	22	32	32	26	52	13	19	64	19	42	36
Er	115	177	104	349	105	158	158	119	311	72	94	311	98	174	172
Tm	26	35	23	80	24	38	36	29	80	20	21	76	22	36	35
Yb	248	315	210	755	243	351	347	286	975	236	207	762	232	331	340
Lu	33	40	28	103	36	45	46	40	168	40	29	112	34	37	46
Total	570	840	512	1678	527	764	789	625	1749	430	461	1613	486	911	805
$(La/Yb)_n$	0,0016	0,0007	0,0002	0,0001	0,0001	0,0001	0,00003	0,0001	0,00001	0,00005	0,0002	0,0001	0,0001	0,0002	0,0014
$(Eu/Eu^*)_n$	0,05	0,18	0,11	0,13	0,24	0,08	0,37	0,35	0,32	0,45	0,12	0,31	0,59	0,29	0,11
$(Ce/Ce^*)_n$	6,25	5,36	6,91	7,33	22,25	11,00	25,03	23,06	21,30	29,90	13,47	10,37	16,77	68,51	10,12
Age, Ma	623	601	1061	1412	626	1366	2121	518	154	716	2048	697	3096	974	2031

Beriozovsky massif, Sakhalin Island (Russia)
[data F. Lesnov], LA ICP-MS

Element	1597					1658									
	Grain's number														
	5-2	6	7	8	9	1	2	3	4	5	6	7	8	9	10
	Pyroxenite					*Gabbro-diorite*									
La	0,10	0,03	0,04	0,05	0,05	0,05	0,02	0,005	0,18	0,05	0,02	0,05	0,09	0,09	0,04
Ce	12,1	16,0	10,5	7,8	15,2	4,2	6,8	4,3	12.1	4,7	2,9	7,6	7,2	8,2	5,5
Pr	0,08	0,15	0,14	0,19	0,09	0,05	0,38	0,04	0,15	0,23	0,11	0,06	0,37	0,39	0,25
Nd	1,90	2,40	1,50	2,70	1,00	2,30	4,00	0,70	2,40	3,50	1,40	1,70	4,50	4,60	3,30
Sm	1,70	4,10	2,80	5,10	3,60	2,90	6,80	2,10	3,70	5,70	2,80	3,00	7,10	8,60	6,50
Eu	0,18	0,90	1,00	0,41	0,64	1,28	2,04	0,44	1,16	1,58	0,69	0,84	2,23	2,99	2,02
Gd	8,10	13,8	8,50	16,8	11,0	11,4	27,5	8,50	21,9	20,2	9,00	17,9	29,4	35,1	27,0
Tb	3,10	5,10	3,30	6,40	4,20	4,30	10,40	3,80	11,3	8,50	3,60	8,40	11,7	11,5	9,40
Dy	39	57	37	75	54	59	120	52	170	100	46	117	146	143	113
Ho	14	20	15	26	21	24	47	24	75	37	18	51	55	54	41
Er	73	107	77	121	110	141	250	140	410	201	106	301	290	296	221
Tm	17	27	20	27	26	42	70	40	104	51	30	80	79	80	59
Yb	188	293	223	273	295	577	798	484	1189	633	367	941	861	1015	718
Lu	27	46	37	36	39	105	135	83	193	104	62	155	140	162	119
Total	384	592	437	596	580	974	1478	842	2195	1170	649	1685	1633	1821	1326
$(La/Yb)_n$	0,0004	0,0001	0,0001	0,0001	0,0001	0,0001	0,00002	0,00001	0,0001	0,0001	0,00003	0,00004	0,0001	0,0001	0,00004
$(Eu/Eu^*)_n$	0,12	0,33	0,58	0,12	0,28	0,59	0,39	0,27	0,30	0,40	0,38	0,27	0,40	0,45	0,40
$(Ce/Ce^*)_n$	30,5	29,1	19,9	11,1	42.6	17,4	5,4	30,1	16,6	5,6	7.2	28,3	5.4	5,8	6,3
Age, Ma	2045	2267	647	1683	668	153	156	160	161	163	156	161	160	159	160

an older age - from about 1000 to about 2500 Ma and more. On this basis we can assume that these older zircons are xenogeny and that they were captured by mafic melt during the process of its interaction with more ancient mantle ultramafic restites.

Table 11 shows a representative REE analysis of zircons only from certain types of rocks from Beriozovsky massif. According to the general results of these studies the total REE content of zircons from different rocks of this massif vary over a very wide range - from ~100 to ~17000 ppm. On those REE patterns of zircons from rocks of this massif that show a very steep positive slope some intense positive Ce anomalies are observed, as well as less intense negative Eu anomalies. In the interval from Yb to Lu the steep slope of these patterns usually becomes less steep (Fig. 4-3, 4, 5). The contents of the main components in the zircons from rocks of the massif are (% wt): ZrO_2 (63.8-66.3), HfO_2 (0.86-2.15), the parameter ZrO_2/HfO_2 ranges from 29.9 to 76.9.

Hoskin & Ireland [94] published their own summary and literature data on the REE composition of zircons from the many varieties of magmatic and metamorphic rocks, including diorites, plagiogranites, aplites, gabbros, kimberlites, carbonatites, charnockites and metamorphic rocks from many parts of the world. Before giving any comments on the materials presented it should be noted that in one of authors studied samples of gabbro (weighing about 2 kg), forming Blind massif (Australia), they discovered about 1000 zircon crystals ranging in size from 50 to 250 microns. In the collection of zircon samples, outlined

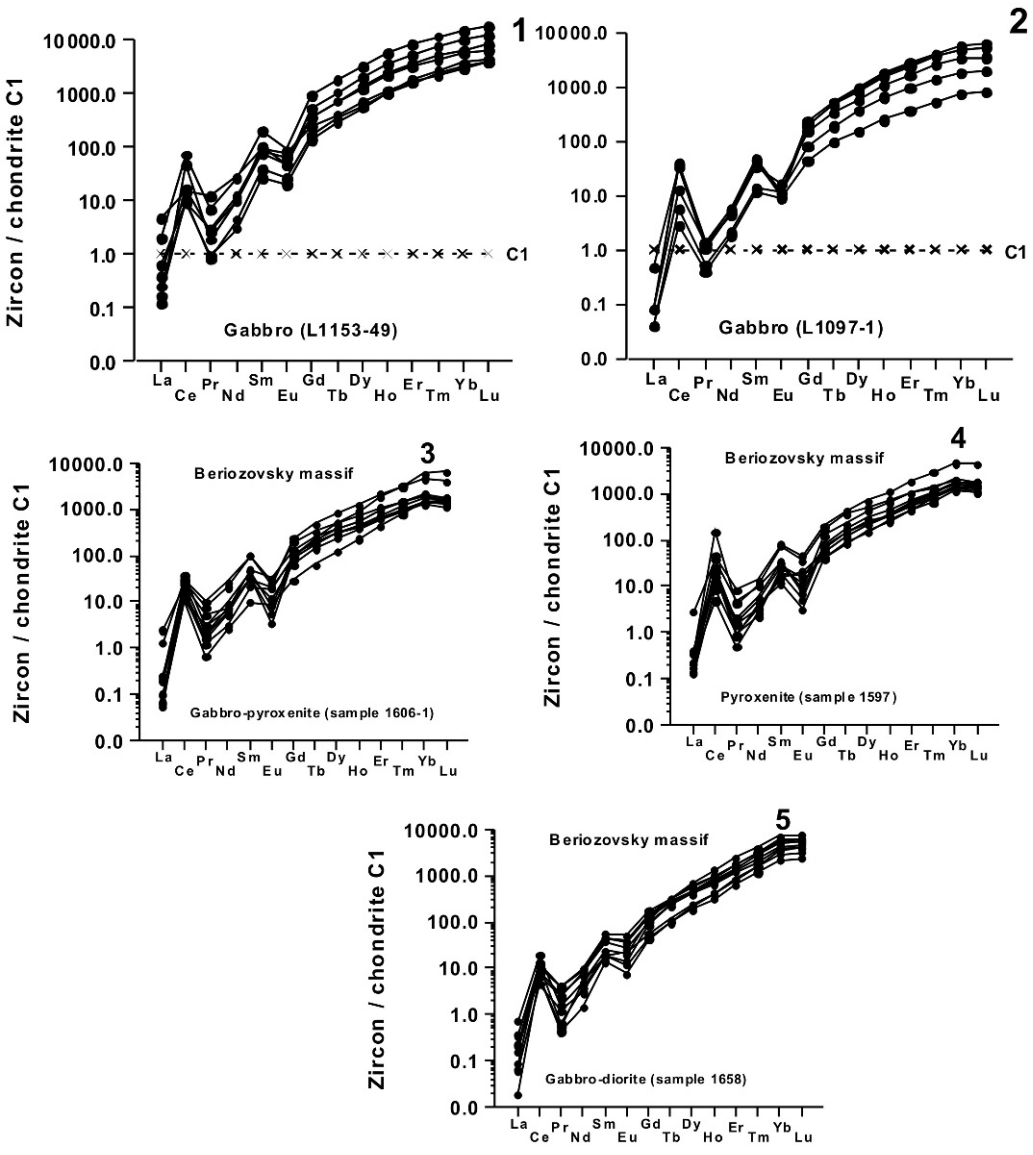

Figure 4. Chondrite-normalized REE patterns for zircons from gabbro, gabbro-diorite, gabbro-pyroxenite, pyroxenite: 1, 2 - dredged in Markov depression (Mid-Atlantic Ridge); 3-5 – Beriozovsky massif (Sakhalin Island).

in this paper, the chondrite-normalized REE contents are significantly increasing in the row from La (0.1-1.0 t.ch.) to Yb (1000-10000 t.ch.). Their REE patterns in almost all cases are complicated by positive Ce anomalies of various intensities, as well as less intense negative Eu anomalies. Moreover, summing up the results of their studies, P. Hoskin & T. Ireland emphasized that they didn't manage to detect any significant correlation between the REE composition of zircons and the petrographic types, as well as the genesis of the rocks containing them. These observations led them to conclude that the parameters of REE distribution in zircons shouldn't be used as criteria in determining the sources of ablation of the material during the formation of terrigenous rock mass. An exception was made only for zircons from kimberlites and carbonatites, for which they have identified some specific features, in particular, a significantly reduced overall level of REE accumulation, very gentle slope of REE patterns in the area of heavy elements, as well as the absence of negative Eu anomalies in the patterns of these zircons.

In several works along with the data on the REE composition of zircons there are results of studies on the coefficients of REE distribution between this mineral and melts and coexisting minerals of different composition (Table 12).

Among the first, the data on the values of D (zircon / dacite matrix) and D (zircon / granite) were published by [96], according to which the D of all REE for these rocks have values > 1, while the values for the light elements were the first units and for heavy elements - 366-389 (Fig. 5-3). Later, E. Watson relying on the results of physical experiments with felsitic melts executed at T = 800°C and P = 2 kbar, determined that the value of D (zircon / melt) vary within the following ranges: La (1.4-2.1); Sm (26-40); (Ho > 340); Lu (72-126) (Fig. 5-7). Data on the REE composition of zircons from syenites and charnockites containing them allowed [95] to calculate the values of D for some elements. For a zircon-syenite system they were: La ~0.035 and Lu ~100, for zircon-charnockite system: La ~3 and Lu ~2000 (Fig. 5-5, 6). According to the calculations made using the estimations of REE in zircons and the basanite matrix containing them [51], the following values of D (zircon / basanitic melt) were obtained: La ~0.09, Lu - 300 (Fig. 5-1). While studying the zircons from amphibole-biotite diorites of Quottoon complex (British Columbia, Canada), the values of D (REE) in zircon-dioritic melt system was determined. For this purpose there were used the results of analysis of REE in melt microinclusions contained in these zircons [?]. According to these estimates, the values of D for La ranged from 0.02 to 0.26 (average - 0.05); for Ce – from 0.43 to 2.06 (average - 0.99); for Nd the average D was 0.5; for all the rest elements the average values of D increased consistently: Sm – 3.56, Dy – 22.45, Er – 52.72 (Fig. 5-8). The D values obtained by [96] indicate that under the crystallization of zircons from the diorites of Quottoon complex La, Ce and Nd had the geochemical properties of the incompatible trace elements, while the rest REE had the properties of compatible elements.

Hinton & Upton [97] discussed the values of D (zircon / melt) on the basis of the analysis of REE in the individual large crystals of zircon from basanites and syenites. According to them the values of D (zircon / syenite melt) are consistently increasing in the row from La (0.0083) to Lu (472), and that these values ??correlate with a successive decrease in the size of the radii of trivalent ions of these elements - from 1.16 Å for La to 0.977 Å for Lu. However, such a sequence disrupted in case of Ce, the mean value of D for which amounted to 718, which is much higher than that for Lu (Fig. 5-10). Given these observations, the authors concluded that such an anomaly for Ce is due to the fact that in the zircons they studied this element was in the form of Ce^{4+} ions, which are more favorable for the occurrence in the mineral structure as compared to Ce^{3+} ions, because they have a much smaller radius (0.970 Å) compared with Ce^{3+} ions (1.143 Å). These data suggest that Ce^{4+} ions in the zircon structure would prevail over the Ce^{3+} ions in cases where the zircons were crystallized under high oxygen fugacity. Add that in discussing the role of Ce^{4+} in generating the Ce anomaly considered in detail in some recent experimental studies: Trail et al. [98], and Trail et al. [99].

The level of REE in zircons, as in all other minerals, is largely due to their crystal-chemical properties. According to earlier data of [100], the size of the radius of Zr^{4+} ion as the main net-forming element of zircon is 0.82 Å, which is comparable with the size of the radii of the trivalent ion of heavy REE, especially the Yb^{3+} (0.82 Å) and Lu^{3+} (0.80 Å). However, the values represented by [?] were not precise enough. Later estimates of the size of the ionic radii of elements were slightly adjusted, resulting in the currently accepted values for Zr^{4+} - 0.84 Å; for Yb^{3+} - 0.985 Å; for Lu^{3+} - 0.977 Å [53]. It is likely that similar ionic radii of Zr^{4+} and HREE are an important determinant of particularly high values of D (zircon / melt) for them, and that these REE are characterized by a high degree of compatibility with the crystal structure of zircons.

In the study of synthetic zircon by using cathodoluminescence method it has been found that their patterns contain a series of narrow lines in the area of 200-500 nm that were attributed to the REE such as Sm, Eu, Tb, Dy and Er [16]. In addition, on a laser-fluorescent patterns of zircons from garnet amphibolites of the Cape Kamchatka (Kamchatka, Russia) there were also determined the lines, which were attributed to Er^{3+} ions [101].

It is assumed that in the structure of zircons there are two basic positions that can potentially be replaced by cations: tetrahedral position in which Si^{4+} ions are, and triangular (dodecahedral) position, which contains the Zr^{4+} ions, and the latter is the most favorable for the replacement of heavy REE by ions [96]. However, the relatively high level of compatibility with the zircon crystal structure of heavy and part of MREE, is obviously not only due to similar size of the radii of their trivalent ions and network-forming ions, but also because of an appropriate balance of their charges. According to the model that has been proposed to solve this problem, an isomorphic substitution of Zr^{4+} ions by trivalent ions of REE and Y is accompanied by the entrance of P^{5+} ions into positions of Si^{4+} ions, which compensates for the balance of charges [102]. According to this model, the authors suggested the following scheme of REE isomorphism in zircons, which takes into account the balance of ion charges:

$$Zr^{4+} + Si^{4+} \leftrightarrow REE^{3+} + P^{5+}.$$

However, while discussing the scheme of REE isomorphism in zircons, some doubts aroused related to the fact that the phosphorus content in natural zircons is generally much lower (202-586 ppm, see above) than the total

Table 12. The coefficients of REE distribution (D) between zircons and coexisting different melts.

	Melts											
	Basanitic	Alkaline basaltic		Dacitic			Granitic		Felsitic		Sienitic	Charnocitic
	Zircon / matrix			Zircon / rock					Zircon / melt		Zircon / rock	
	[51]	[44]		[97]					[164]		[95]	
Element	IrF-1(min)	Hmin-1	Hmax-2	1Za	1Zb	4Z	9Z	10Z	Wat-1	Wat-2	Mur-1	Mur-2
La	0,08	0,033	4,1	N.d.	N.d.	N.d.	N.d.	N.d.	1,4	2,1	0,035	0,3
Ce	0,13	0,4	4	3	7,38	2,29	0,27	0,31	N.d.	N.d.	0,1	0,25
Pr	N.d.	0,082	N.d.	N.d.	N.d.	N.d.	N.d.	N.d.	»	»	N.d.	N.d.
Nd	»	0,176	5	2,43	6,51	1,97	0,26	0,55	»	»	»	»
Sm	0,38	0,891	4,7	3,7	6,5	2,58	0,87	3,24	26	40	0,15	1,0
Eu	1,26	N.d.	4,7	5,22	3,96	1,07	0,18	1,57	N.d.	N.d.	0,5	0,5
Gd	N.d.	3,54	7,9	N.d.	N.d.	N.d.	N.d.	N.d.	»	»	N.d.	N.d.
Tb	»	23.4	24,4	»	»	»	»	»	»	»	4,0	20
Dy	»	26,5	52	53,5	51,5	37,8	25,2	105	N.d.	»	N.d.	N.d.
Ho	»	82	88,5	N.d.	N.d.	N.d.	N.d.	N.d.	340	340	»	»
Er	»	62.9	143	152	141	119	81,5	450	N.d.	N.d.	»	»
Tm	»	282	282	N.d.	N.d.	N.d.	N.d.	N.d.	»	»	»	»
Yb	138	304	304	299	296	242	178	890	»	»	50	500
Lu	172	N.d.	420	366	389	281	N.d.	1230	72	126	100	2000

	Tonalitic (dioritic) melt											Alkaline basaltic melt	Ionic radii, Å
	Zircon / melt												
	[159]											[44]	[139]
Element	#1	#1-1	#B-1	#B-2	#4	#7	#1-11	#35	#46	#I	#G	Average	Average (H-1)	
La	0,05	0,04	0,07	0,22	0,03	0,02	0,06	0,26	0,02	0,03	0,05	0,05	0,0083	1,16
Ce^{3-}	2,06	0,83	1,46	0,99	1,4	0,61	0,93	1,26	0,43	1,1	0,75	0,99	0,022	1,143
Pr	N.d.	N.d.	N.d.	N.d.	N.d.	N.d.	N.d.	N.d.	N.d.	N.d.	N.d.	N.d.	0,0635	1,126
Nd	1,58	0,2	0,5	0,53	0,77	0,11	0,56	0,81	0,35	0,31	0,16	0,5	0,176	1,109
Sm	11,6	2,7	3,56	4,14	5,02	2,49	4,58	3,26	0,75	11,2	1,27	3,56	1,06	1,079
Eu	N.d.	N.d.	N.d.	N.d.	N.d.	N.d.	N.d.	N.d.	N.d.	N.d.	N.d.	N.d.	2,30	1,066
Gd	»	»	»	»	»	»	»	»	»	»	»	»	5,01	1,033
Tb	»	»	»	»	»	»	»	»	»	»	»	»	10,9	1,040
Dy	73,0	20,1	22,5	16,8	19,4	36,6	12,4	52,0	19,3	52,3	26,4	22,5	23,7	1,027
Ho	N.d.	N.d.	N.d.	N.d.	N.d.	N.d.	N.d.	N.d.	N.d.	N.d.	N.d.	N.d.	48,6	1,015
Er	72,4	29	29,4	21,1	17.9	58,9	13,1	75,0	52,7	60,7	70	52,7	94	1,004
Tm	N.d.	N.d.	N.d.	N.d.	N.d.	N.d.	N.d.	N.d.	N.d.	N.d.	N.d.	N.d.	171	0,994
Yb	51,5	40,6	35,9	21,9	14,0	66,1	13,0	76,3	82,3	35,1	96,7	40,6	293	0,985
Lu	N.d.	N.d.	N.d.	N.d.	N.d.	N.d.	N.d.	N.d.	N.d.	N.d.	N.d.	N.d.	472	0,977
Ce^{4}	»	»	»	»	»	»	»	»	»	»	»	»	718	0,970

content of REE^{3+} (in atomic terms). Therefore, in order to maintain a real balance of charges during the isomorphous entrance of REE into the zircon structure, obviously, there should be involved some additional ions as charge compensators [97, 103]. In this context a theory emerged, according to which the function of compensating the charge could be carried out by such ions as Mo^{4+}, Li^{+} and others, and the heterovalent REE isomorphism in zircons could have the following form [104]:

$$2Zr^{4+} \leftrightarrow 2(Yb, Lu)^{3+} + R^{2+}(2R^{+}; 0.5R^{4+}),$$

where R^{2+} - Ti^{2+} ions, Fe^{2+}, $2R^{+}$ and $0.5R^{4+}$ - Li^{+} and Mo^{4+} ions.

During the reconstruction of the crystallization conditions of natural zircons a considerable attention is usually paid at positive Ce anomalies and negative Eu anomalies observed in many of their REE patterns. It is quite obvious that the appearance of anomalies of these elements, which can change its valence depending on the redox conditions of the environment, may be causally related to their valence state and the corresponding changes in the size of the radii of the ions that are involved in isomorphic substitution, and indirectly connected with the values of D (zircon / melt).Therefore, Zr^{4+} ions, the size of the radius of which is 0.84 Å, should be better replaced by Ce^{4+} ions, the size of the radius of which is 0.970 Å, compared with larger Ce^{3+} ions, the size of the radius of which is 1.143 Å. Such differences in the properties of Ce ions that are due to the degree of oxidation of the environment, seem to be the determining factor in a multiple increase of D (zircon / melt) values from 0.022 – for Ce^{3+} to 718 – for Ce^{4+}.

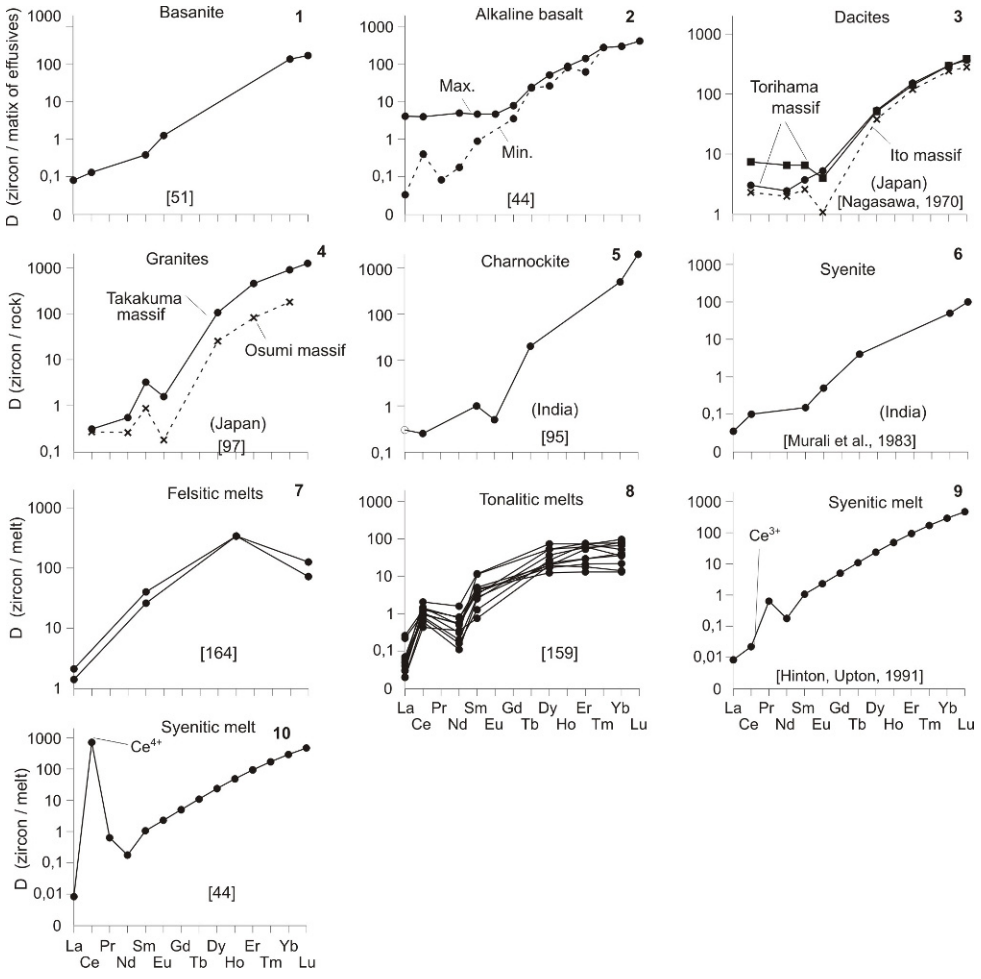

Figure 5. The graphs of coefficients of REE distribution (D) between zircons and the bulk matrix of the basanites (1), alkali basalts (2), dacites (3); between zircons and granites (4), charnockites (5), syenites (6); 7 - between zircons and experimental felsitic melt; 8 - between zircon and tonalite melts (in microinclusions); 9 - graph is made using D for Ce^{3+}; 10 - graph is made using D for Ce^{4+}.

The value of Ce^{4+}/Ce^{3+} in the zircons depends on the redox conditions of environment of their crystallization and varies widely. Increasing the degree of medium oxidation will stimulate the transition of certain amounts of Ce^{3+} ions into Ce^{4+} ions, as a result the ratio Ce^{4+}/Ce^{3+} will increase. The intensive positive Ce anomalies observed in the patterns of many zircons from the rocks of different composition and conditions of formation, indicate that in their structure Ce^{4+} ions prevail over Ce^{3+} ions, which may indicate that the crystallization of zircons was under a relatively high degree of medium oxidation. The validity of this conclusion can be proved by the fact that in zircons from lunar rocks that were crystallized in deliberately reducing conditions, Ce anomalies are not observed [44]. Another argument indicating that the crystallization of zircons from many terrestrial magmatic rocks with positive Ce anomalies on their patterns proceeded at a relatively high oxidation degree of crystallizing systems, are negative Eu anomalies, commonly observed in these patterns. The latter indicate the lower values of Eu^{2+}/Eu^{3+} ratio, which are indicative of oxidizing conditions of the zircon crystallization.

In conclusion, the results of experiments performed by [105] using natural and synthetic zircon crystals; it was found that the rate of REE diffusion in the crystal lattice of this mineral has very low values. These observations have led to the assumption that REE ions might be inactive during the metamorphic transformation of those protoliths, in which the zircons were initially present as accessory phases.

6. Apatites

In general, the regularities of REE distribution in apatites are studied a bit better compared to some other accessory minerals but samples from various petrographic and genetic types of rocks are characterized unevenly by these studies. The total REE content in apatites varies widely and the chondrite-normalized contents of LREE mostly prevail over HREE contents (Table 13). Among the first samples of apatite, which were determined to contain some REE, is the sample from gabbro of Skaergaard massif, the total REE content of which was 3000 ppm [54]. Chondrite-normalized contents of certain elements in it were (t.ch): La ~1300, Ce ~1550, Nd ~1800, Sm ~1800, Yb ~300. The REE pattern of the apatite was a relatively shallow negative sloping and slightly convex upward line complicated by weak negative Eu anomaly (Fig. 6-1). Slightly lower total REE content and a steep negative slope of REE patterns were determined in apatites from hawaiites from the State of Texas (USA) ~2700 ppm and from basanites from the State of Arizona (USA) ~2600 ppm [106]. The level of La in apatite from hawaiite was 2100 t.ch., from basanite - 2900 t.ch., while the level of Yb accumulation in them was slightly lower (70-120 t.ch.) than in minerals from gabbro of Skaergaard massif. REE patterns of apatites from hawaiites and basanites are almost straight lines with a steep negative slope, on which there are no Eu anomalies, while the value of $(Ce/Yb)n$ in the mineral from hawaiite was higher (~107) than in the sample from basanite (~79) (Fig. 6-3, 4). Apatites from kimberlites of Benfontein sill (South Africa) show much higher chondrite-normalized La contents in comparison with their samples from kimberlites of Wesselton province, while both have almost rectilinear patterns with a very steep negative slope [107]. These authors assumed that significant differences in the level of REE accumulation in apatites of these two kimberlite occurrences are due to the mineralogical-structural differences of rocks containing them. In particular, relatively large and fairly rare apatite grains from kimberlites of Benfontein sill are in parageneses with perovskite, while they are mainly concentrated in the cumulative layers enriched with oxides. Moreover, the apatites from kimberlites of Wesselton province are presented with numerous but smaller segregations and together with associating perovskite grains are evenly distributed in a homogeneous rock matrix enriched with carbonates.

A large amount of analytical data on the REE composition of apatites was obtained by E. Belousova et al. [108] in a study of this mineral from different types of magmatic rocks, including granites, granodiorites, tonalites, adamellites and granitic pegmatites (Australia, Norway, Ukraine), lherzolites (Australia and USA), dolerites (Ukraine), carbonatites (Norway, South Africa, Russia), larvikites and jacupirangites (Norway), as well as the rocks represented in iron-ore deposits (Mexico, Norway, Sweden) (Table 14, Fig. 7). As shown in this work, the apatites from granitoids have the most volatile REE composition. The relatively low average total REE content is typical of apatites from dolerites (3130 ppm), granitic pegmatites (4130 ppm) and carbonatites (4800 ppm). This index is slightly higher for the mineral from granitoids (5030 ppm), from rocks of iron-ore deposits (5890 ppm), as well as from some lherzolites (8030 ppm), jacupirangites (10 370 ppm) and larvikites (16 690 ppm). The vast majority of apatites from the collections studied by E. Belousova et al. have the values of $(La/Yb)n$ and $(Ce/Yb)n$ greater than 1 and the highest values were observed in the mineral from lherzolites and carbonatites. In apatites from granitic pegmatites there was a slight excess of chondrite-normalized HREE contents over the LREE contents, which is rarely observed in this mineral. The patterns of the vast majority of apatite samples from the collection showed negative Eu anomalies of various intensity. Judging by the average estimates of $(Eu/Eu^*)n$ parameter, the intensity of these anomalies was increasing in the following row of rocks: carbonatites (0.80) → jacupirangites (0.67) → metasomatic rocks of iron-ore deposits (0.45) → granitoids (0.33) → dolerites (0.32) → larvikites (0.28) → granitic pegmatites (0.19). For some apatites from granitoids the intensity of negative Eu anomalies was even higher - $(Eu/Eu^*)n$ = 0.01-0.06, while for the samples of lherzolites there were identified positive Eu anomalies: the mean value of $(Eu/Eu^*)n$ = 1.14. Thus, the observations show that variations of the REE composition of apatites significantly correlate with petrographic belonging and formation conditions of rocks containing them. Hallmarks of the overwhelming majority of the investigated apatites are, firstly, more or less significant predominance of chondrite-normalized LREE contents over the HREE, and, secondly, the presence on their REE patterns of negative Eu anomalies of various intensity. In addition, these results suggest that in-depth study of REE distribution in apatites from rocks that form separate magmatic massifs allows using such data to specify the taxonomy of rocks within these massifs, as well as to ascertain the postmagmatic transformations of apatite-bearing rocks. Therefore, a further detailed research of REE composition of apatites from rocks of different composition and origin is an urgent task.

Among the first the estimates of D (apatite / melt) values were obtained by the example of samples from the natural system - basanites [106], and later on – based on the results of experimental studies of basaltic melts [109]. These observations showed that all the REE have values of D (apatite / melt) > 1. In addition, for the values of

Table 13. REE composition of apatites from some rocks (ppm).

	Skaergaard massif, Greenland province	Aldan prov. (Russia)	Texas State (USA)	Arizona State (USA)	South Dakota State, (USA)			Koksharovsky massif (Russia)	
	[111]	[158]	[51]		[55]			[107], LA ICP-MS	
Element	EG4312	Tab-1	188/7	SC73	B2	G11f	B8	B12	Kok-19
	Gabbro	*Pyroxenite*	*Hawaiite*	*Basanite*	*Granitic pegmatites*				*Carbonatite*
La	320	290	517	712	N.d.	N.d.	N.d.	N.d.	1127
Ce	990	860	1205	1540	119	57	374	328	2442
Pr	N.d.	N.d.	N.d.	N.d.	N.d.	N.d.	N.d.	N.d.	260
Nd	870	1170	614	»	63	13	157	216	953
Sm	280	210	104	121	15	6,8	27	61	153
Eu	64	N.d.	30,9	34,9	33	3,7	18	29	37,5
Gd	320	165	81,7	N.d.	N.d.	N.d.	N.d.	N.d.	121
Tb	48	N.d.	10,3	14,2	»	»	»	»	16
Dy	N.d.	»	N.d.	N.d.	14	5,6	20	65	75,5
Ho	43	»	»	»	N.d.	N.d.	N.d.	N.d.	11,2
Er	N.d.	»	»	»	12	2,3	17	45	25,8
Tm	»	»	»	»	N.d.	N.d.	N.d.	N.d.	2,42
Yb	52	17	11,3	19,4	10	2,6	18	52	13,5
Lu	N.d.	N.d.	1,52	2,38	N.d.	N.d.	N.d.	N.d.	1,44
Total	2987	2712	2576	2444	266	91	631	796	5239
$(La/Yb)_n$	4,2	12	31	25	N.d.	N.d.	N.d.	N.d.	56
$(Ce/Yb)_n$	19	51	107	79	12	22	21	6,3	47

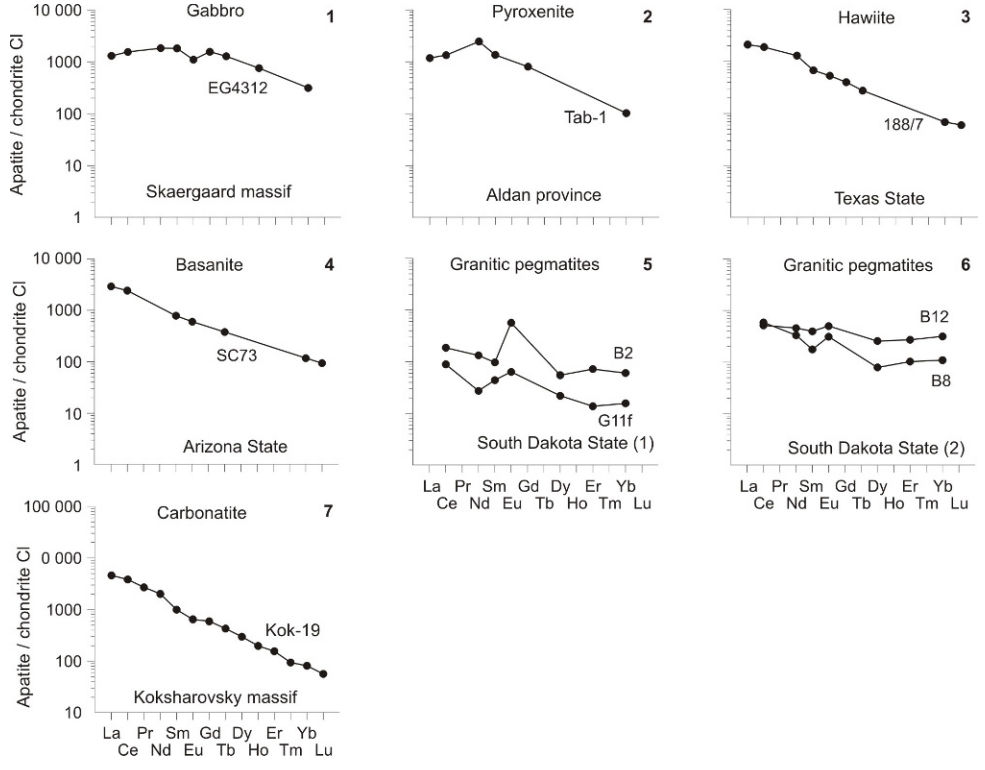

Figure 6. Chondrite-normalized REE patterns for apatites from gabbros (1), pyroxenites (2), hawaiites (3), basanites (4), granitic pegmatites (5, 6), and carbonatites (7).

Table 14. Maximum, minimum, and average REE composition of apatites from lherzolites, dolerites, granitoids, granite pegmatites, carbonatites, larvikites, jacupirangites, and iron ores from different manifestation (ppm).

[9] LA ICP-MS

Element	Lherzolites (*n* – 8			Dolerites *n* – 11			Granitoids *n* – 669			Granite pegmatites *n* – 52		
	Aver.	Min.	Max	Aver.	Min.	Max.	Aver.	Min.	Max.	Aver.	Min.	Max.
La	1761	679	4457	390	288	553	704	9,9	6722	211	46	419
Ce	4620	1198	7642	1081	794	1430	2165	20	13979	751	119	1258
Pr	392	109	803	149	114	199	265	1,8	1392	129	24	213
Nd	1036	305	2618	755	599	1047	1032	7,9	5756	723	137	1367
Sm	104	26	313	202	153	248	215	1,9	972	345	69	950
Eu	32	8,7	79	21	18	25	23	1,5	240	26	6	77
Gd	60	16	192	199	158	255	208	2,6	1057	489	121	1659
Tb	N.d.	N.d.	N.d.	N.d.	N.d.	N.d.	N.d.	N.d.	N.d.	N.d.	N.d.	N.d.
Dy	»	»	»	162	138	207	172	2,8	1483	600	121	1981
Ho	4,5	1,7	14	32	27	41	36	0,5	353	113	16	426
Er	9,9	4,5	14	78	65	99	97	1,8	1029	306	31	1185
Tm	N.d.	N.d.	N.d.	N.d.	N.d.	N.d.	14	0,6	151	46	3,8	176
Yb	6,2	3,7	8,1	51	49	66	85	2,3	1032	332	23	1244
Lu	0,86	0,51	1,0	6,6	5,4	8	13	0,4	150	58	2,7	197
Total	N.d.	N.d.	N.d.	3127	2408	4178	5029	54	34316	4129	720	11152
$(La/Yb)_n$	192	124	371	5,16	3,97	5,66	5,59	2,91	4,40	0,43	1,35	0,23
$(Ce/Yb)_n$	193	84	244	5,49	4,19	5,61	6,59	2,25	3,51	0,59	1,34	0,26
$(La/Sm)_n$	10.7	16,4	8,97	1,22	1,19	1,40	2,06	3,28	4,35	0,39	0,42	0.28

[9] LA ICP-MS

Element	Carbonatites *n* = 61			Larvikites *n* = 34			Jacupirangites *n* = 14			Iron ores *n* =35		
	Aver.	Min.	Max.	Aver.	Min.	Max.	Aver.	Min.	Max.	Aver.	Min.	Max.
La	959	549	3931	3423	2242	4188	2052	1452	3709	1301	161	4569
Ce	2060	1369	7728	8144	6278	9797	4585	3578	7542	2463	802	4965
Pr	261	178	920	880	672	1024	539	446	907	324	151	393
Nd	1081	741	3487	3070	2126	3665	2185	1685	3343	1140	723	1587
Sm	189	115	459	445	293	542	353	270	517	165	138	324
Eu	43	30	111	35	22	50	66	53	75	24	15	55
Gd	126	72	265	294	186	363	261	195	385	156	118	306
Tb	N.d.	N.d.	N.d.	N.d.	N.d.	N.d.	N.d.	N.d.	N.d.	N.d.	N.d.	N.d.
Dy	52	38	102	198	121	243	166	127	261	131	82	281
Ho	7,2	5,3	13	35	22	44	30	23	49	27	17	61
Er	13	8,7	24	85	50	106	70	51	115	70	41	166
Tm	N.d.	N.d.	N.d.	10	6,1	13	8.1	6	13,9	14	7.8	24
Yb	7,5	3,3	11	61	35	76	45	34	82	62	32	161
Lu	0,8	0,3	2,2	7,5	4,2	9,4	6	4,2	10,7	8,7	4,1	23
Total	4800	3110	17053	16688	12057	20120	10366	7924	17010	5886	2292	12915
$(La/Yb)_n$	86	112	241	38	43	37	31	29	31	14	3,40	19
$(Ce/Yb)_n$	71,1	107	182	34,6	46,4	33,4	26,4	27,2	23,8	10,3	6,49	7,98
$(La/Sm)_n$	3,19	3,01	5,39	4,84	4,82	4,86	3,66	3,39	4,52	4,96	0,73	8,88

basanitic melts the values of D(La, Ce) were significantly higher than the values of D (Lu), while for basaltic melts, on the contrary, values of D (La, Ce) were slightly lower than D (Lu). Therefore, the graphs of D (REE) values for basanitic melts have a steep negative slope, and for basaltic melts - a gentle positive slope.

E. Watson & T. Green [110] performed a series of experiments with melts of different composition and at different *PT*-conditions including the presence of water in order to determine the values of D (apatite / melt) for La, Sm, Dy and Lu. As a result of these studies the authors stated the following: 1) under all determined *PT*-conditions of experiments and for all studied melts the named four REE had values of D (apatite / melt)> 1; 2) the values of D (apatite / granite melt) and D (apatite / nepheline-hawaiite melt) in most cases were higher than the respective values of D (apatite / tholeiite-andesite melt); 3) in all experiments the values of D (La, Lu) were slightly lower than the values of D (Sm, Dy); 4) the values of D obtained in experiments with tholeiite-andesite and basanite melts at relatively low temperatures were higher than the values of D obtained at higher temperatures; and 5) the results of experiments with basanitic melts at T = 1080°C and P = 20 kbar determined that the values of D (La, Sm) are slightly lower than those values that were obtained at the same temperature but at a lower pressure (7.5 kbar) (Table 15, Fig. 8). On the respective graphs of the D (apatite / melt) values for La, Sm, Gd, Dy and Lu, as well as for Eu^{2+}, which are shown in the work of, there have been very intense negative Eu^{2+}anomalies observed. It follows

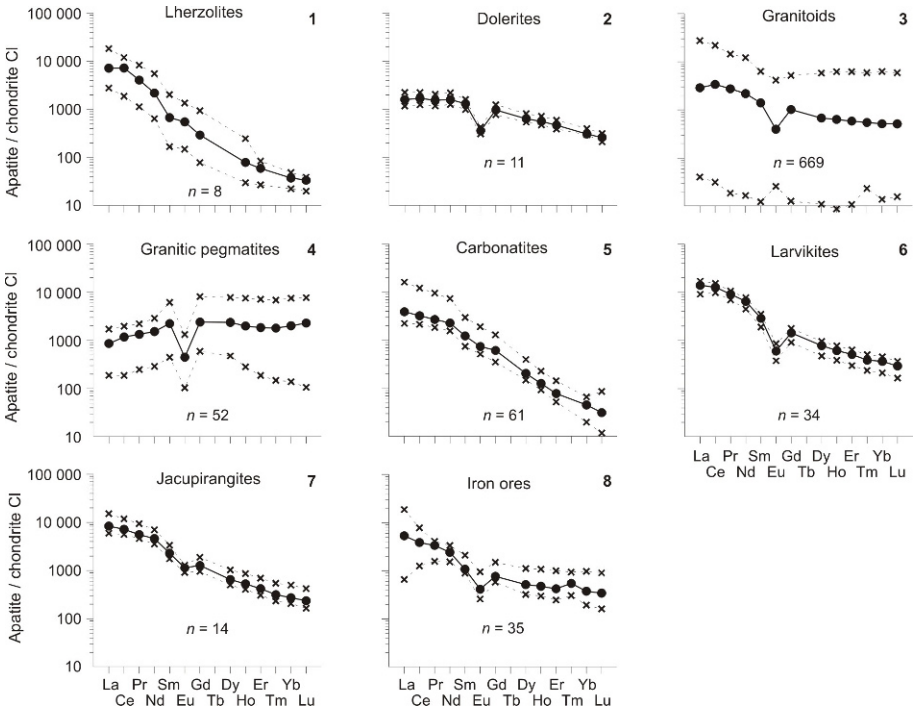

Figure 7. Chondrite-normalized REE patterns for average composition (solid line), as well as maximum and minimum composition (dashed lines) for apatites from lherzolites (1), dolerites (2), granitoids (3), granitic pegmatites (4), carbonatites (5), larvikites (6), jacupirangites (7), and iron ores (8) from some manifestations.

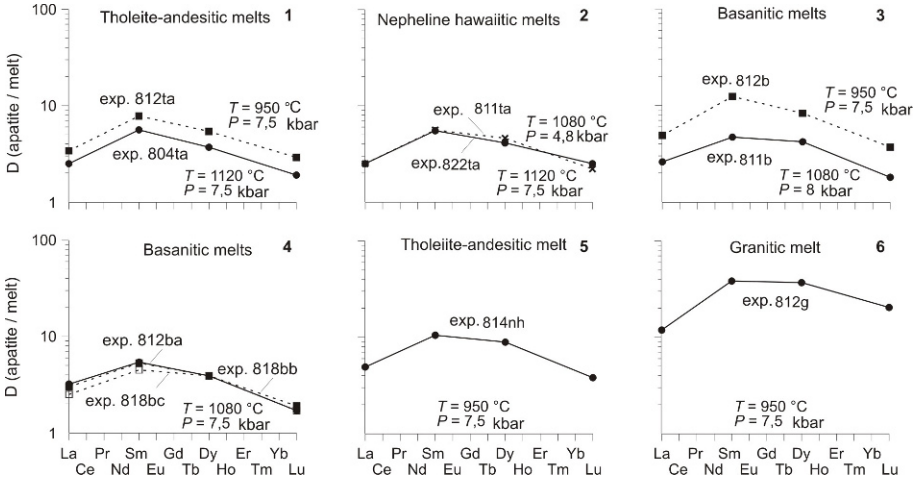

Figure 8. The graphs of coefficients of La, Sm, Dy, and Lu distribution (D) between apatites and melts of different composition and under different PT-conditions.

that the Eu^{2+}ions were significantly less compatible with the structure of apatites in comparison with the trivalent ions of La, Sm, Gd, Dy and Lu.

There were also obtained estimates of the coefficients of REE distribution between apatites and coexisting perovskites by example of samples from jacupirangites, ijolites and nepheline syenites forming xenoliths in tuffs of Oldoinyo Lengai volcano (Tanzania) [111]. It was shown in this study that in the absence of titanites in these rocks the values of D (apatite / perovskite) were: La ~0.11, Ce ~0.063, Nd ~0.105, while in titanite-bearing samples

Table 15. The coefficients of La, Sm, Dy, and Lu distribution (D) between apatites and melts of different composition and under different *PT*-conditions (experimental data).

[165]

No experiment	Melt composition	*T*, °C	*P*, kbar	La	Sm	Dy	Lu
804ta	ta	1120	7,5	2,5	5,6	3,7	1,9
811ta	ta	1080	4,8	2,5	5,5	4,1	2,5
812ta	ta	950	7,5	3,4	7,8	5,4	2,9
822ta	ta	1120	7,5	2,5	5,6	4,6	2,2
808a	a	950	7,5	6,4	19,1	15,2	8,1
815a	a	1080	20	4,4	9,8	8,1	4,0
811b	b	1080	8	2,6	4,7	4,2	1,8
812b	b	950	7,5	4,9	12,4	8,3	3,7
814b	b	950	7,5	4,6	9,9	7,3	3,4
815b	b	1080	20	2,8	4,5	4,2	1,8
818ba	b	1080	7,5	3,2	5,4	3,9	1,7
818bb	b	1080	7,5	3,0	5,3	3,9	1,9
818bc	b	1080	7,5	2,5	4,5	3,9	1,7
814nh	nh	950	7,5	4,9	10,5	8,9	3,8
812g	g	950	7,5	11,9	38,4	37,0	20,4
823g	g	1080	20	8,0	18,5	15,9	7,5

Note. Composition of melts: ta – tholeiite-andesitic; a – andesitic; b – basanitic; nh – nepheline-hawaiitic; g – granitic.

of these rocks the values of D for these elements were slightly higher.

As noted above, the apatites are one of the most important minerals concentrating REE in magmatic, metasomatic and metamorphic rocks. In this regard, from theoretical and practical points of view it is interesting to study the reasons for such an intense REE accumulation in apatites and mechanisms of their isomorphous incoming into crystalline structure of apatites, as well as the reasons that cause the Eu deficiency often observed in the mineral. According to some reports, the intensity of negative Eu anomalies in the apatites increased with increasing degree of minerals fractionation in the rocks of mafic and ultramafic composition. It is assumed that such dependence is due to the presence of plagioclase in these rocks, the structure of which is very favorable for the occurrence of a significant proportion of Eu in it, which was a part of crystallizing parental melt. Given the ability of Eu to change its valence state and to change from Eu^{2+} to the Eu^{3+} under oxidizing conditions, we can assume that this fact had a significant effect on the Eu accumulation in the structure of apatites, which were in parageneses with plagioclase. It is known that under oxidizing conditions the prevailing ions of Eu^{3+} have a much smaller ionic radius (0.947 Å) compared with the Eu^{2+} ions (1.17 Å) prevailing under reduced conditions [53]. Therefore, by isomorphic substitution of Ca^{2+} ions, the radius size of which is 1.00 Å, Eu^{3+} ions, apparently, became less compatible with the structure of apatite. Thus, these differences in ionic radii size seem to have caused the fact that for Eu^{3+} ions, which prevailed in oxidizing conditions, D (apatite / melt) have relatively low values, which leads to the appearance of frequently observed negative anomalies of this element on the REE patterns of apatites. In addition, the crystallization of apatites at reducing conditions was accompanied by an increase in the number of Eu^{2+} ions in the melt and increase of D (apatite / melt) values for Eu. Owing to this fact, the patterns of these apatites experienced decrease in intensity or complete levelling of negative Eu anomalies and sometimes appearance of positive anomalies.

7. Titanites

As accessory minerals, titanites are observed in many varieties of magmatic, metamorphic and some metasomatic rocks. Most often titanites are present in the granites, diorites, syenites, nepheline syenites, lamprophyres, in some volcanic rocks and rarely does it occur in the gabbros.

V. Liakhovich [112] showed that titanite presented in diverse granitoids plays the role of second-largest REE concentrator after monazite and according to him the average weight of titanite content in these rocks is about 640 ppm. According to the same data, the titanites from granitoids can concentrate up to 27% of the total REE present in them. The research of titanites from granodiorites of Peninsular Ranges batholith (South California) also showed that they contain a considerable part of the

amount of REE, which is present in them [113]. Titanites that were also described are present in gabbros of some mafic-ultramafic Urals massifs (Russia) [114, 115] and Tuva (Russia) [116]. Some general regularities of distribution of REE in titanites are considered earlier [?].

J. Russell et al. [117] studied the REE distribution in titanites from granitic pegmatites of Bisson Mountain (British Columbia, Canada). In addition to titanite, these rocks contain other accessory minerals enriched with REE: allanite, apatite, ilmenite, zircon and thorite. In different crystals of titanite from these granitic pegmatites the chondrite-normalized REE contents varied significantly (t.ch.): La (270-10 000), Ce (4000-12 000), Pr (3500-20 000), Nd (5500 - 15 000), Sm (2000-10 000). In addition to this, the titanites from granitoids of Shartashsky massif (Middle Urals, Russia) have the total REE content up to 7000 ppm [?]. According to [118], in dacites from the volcanic province in the Andes (Chile and Bolivia) the modal quantity of titanite segregations are from 0.1 to 0.4% of the rock bulk. Segregations of the mineral are presented as phenocrysts and as microinclusions in hornblende grains. In different zones of titanite phenocrysts the total REE contents increased with decreasing content of Ca in them, in this case dependence of REE contents from Ti contents has no been revealed. Mulroney & Rivers [93] studied the REE distribution in accessory titanites from some metamorphic rocks of San-Antonio complex (Newfoundland Islands, Canada). In these rocks small idiomorphic and subidiomorfic titanite segregations were presented in the matrix consisting mostly of plagioclase crystals and of the subordinate amphibole and epidote segregations. The total REE content in these titanites varied in the range from 1500 to 2400 ppm (Table 16). On REE patterns of some of these titanites there are observed negative Eu anomalies of low intensity (Fig. 9). It is known that along with REE and some other isomorphic impurities the titanite can accumulate different amounts of Zr in its structure. In particular, it was found that titanite from lamprophyres commonly presented in East Germany contains 9.5 wt % of ZrO_2 [119]. As demonstrated by studying the REE distribution in titanites and trachyandesite pumices of El Chichon volcano (Mexico) containing them, D (titanite / trachyandesite melt) are characterized by very high values: La (46), Ce (87), Nd (152), Sm (204) , Eu (181), Tb (248), Yb (104), Lu (92) [83, 59]. The graph of D is arched upwards line with a maximum for Tb. T. Green [120] summarized the data on the estimates of distribution coefficients for La, Sm, Ho and Lu between titanite and melts of different composition - basalt-andesite, andesite and rhyolite obtained in experiments at different *PT*-conditions (Fig. 10). For example, by using products of crystallization of basalt-andesitic melt at $T = 1000°C$ and $P =$ 0.75 GPa the following values of D (titanite / melt) were obtained: La (~2), Sm (~9), Ho (~8.5), Lu (~5). Generally, the values of D (titanite / silicate melt) increase with increasing SiO_2 content in melts, as well as with increasing pressure and decreasing crystallization temperature. According to the results of tests on REE from coexisting titanites, apatites and perovskites of different alkaline rocks (jacupirangites, ijolites, nepheline syenites) forming xenoliths in tuffs of Oldoinyo Lengai volcano (Tanzania), it was found that in the case of perovskite absence in these rocks the La and Nd mainly accumulated in apatites and Ce - in titanite. In addition, it was determined that for Zr the values of D (titanite / perovskite) in these rocks were about 15 [111]. Perkins & Pearce [121] while considering the optimization techniques for the REE analysis in bulk samples of titanite-bearing rocks using the ICP-MS method, drew attention to the fact that the presence in these rocks of more or less significant amounts of accessory titanite should be taken into account when interpreting the results of the analysis. Their opinion is based on the grounds that titanites along with zircons, monazites and other accessory minerals containing significant REE amounts are quite resistant to reagents used in the decomposition of the samples. Because of this, some amounts of their microparticles are often not fully decomposed, respectively, the REE they contain are not turning into the analyzed solutions and this leads to underdetermination of these elements in the analyzed rocks.

T. Sahama was the first to propose a model of isomorphous occurrence of REE into titanite structure and according to it, during the crystallization the REE ions and, possibly, the ions of Na, Mn, Sr and Ba substituted Ca ions in them, while Ti ions could be substituted by ions of Al, Fe^{3+}, Fe^{2+}, Mg, Nb, Ta, V and Cr [122, 123]. Later on, this model has been upgraded and got the following form: $[Ca^{2+} + Ti^{4+}] \leftrightarrow [LREE, Y]^{3+} + [Al^{3+}, Fe^{3+}]$ [117]. At present there are two more alleged models of the isomorphous occurrence of REE in the titanite structure [119]: 1) $Ca^{2+} + Ti^{4+} \rightarrow REE^{3+} + (Al, Fe)^{3+}$; 2) $2Ca^{2+} + Ti^{4+} \rightarrow 2REE^{3+} + Fe^{2+}$.

8. Perovskites

Perovskites are among the relatively rare types of accessory minerals of magmatic rocks enriched with REE. Most often they are found in kimberlites, lamproites, melilitic and leucite basalts, carbonatites, jacupirangites, ijolites, nepheline syenites, olivine nephelinites, and rarely found in rocks of titanomagnetite and chromites deposits, and also in the picrites, some contact-metasomatic formations, chlorite schist, limestone and meteorites. Below we con-

Table 16. Average REE compositions of titanites from some metamorphic rocks and granodiorite (ppm)

	San-Antonio province (Newfoundland, Canada) [94], LA ICP-MS						Peninsular Ranges, (South California, USA) [35], IDMS	
Element	46 (3)		48 (3)		49 (2)		06 (3)		Grom-1
	Aver.	St. dev.	Aver.	St. deviation	Aver.	Standard deviation	Aver.	St. dev.	*Granodiorite*
	Metamorphic rocks								
La	134	55,35	177	47,30	68,95	44,13	207	70,56	N.d
Ce	423	129	588	76,3	268	154	785	195	3305
Pr	63,9	21,3	100	6,96	48,2	24,0	137	45,8	N.d
Nd	342	101	548	18,8	299	142,9	760	342	2680
Sm	113	27,9	172	3,89	116	52,6	251	183	655
Eu	39,7	10,4	61,5	0,71	34,8	17,6	73,8	39,6	165
Gd	152	27,6	213	8,15	160	76,6	247	222	564
Tb	26,1	4,38	34,0	1,40	26,3	12,5	34,3	30,1	N.d
Dy	183	25,2	242	9,27	196	98,0	182	171	470
Ho	37,4	4,39	47,1	1,19	38,95	19,4	23,4	19,6	N.d
Er	111	12,9	136	1,14	114	55,1	45,4	30,7	237
Tm	15,5	1,99	19,0	0,57	16,5	9,23	4,57	3,43	N.d
Yb	106	13,4	129	9,23	111	48,9	21,7	12.7	207
Lu	14,5	2.20	16,7	1,85	14,8	6,30	1.94	1,28	N.d
Total	1761	N.d	2484	N.d	1512	N.d	2773	N.d	»
$(La/Yb)_n$	0,85	»	0,92	»	0,42	»	6,42	»	»

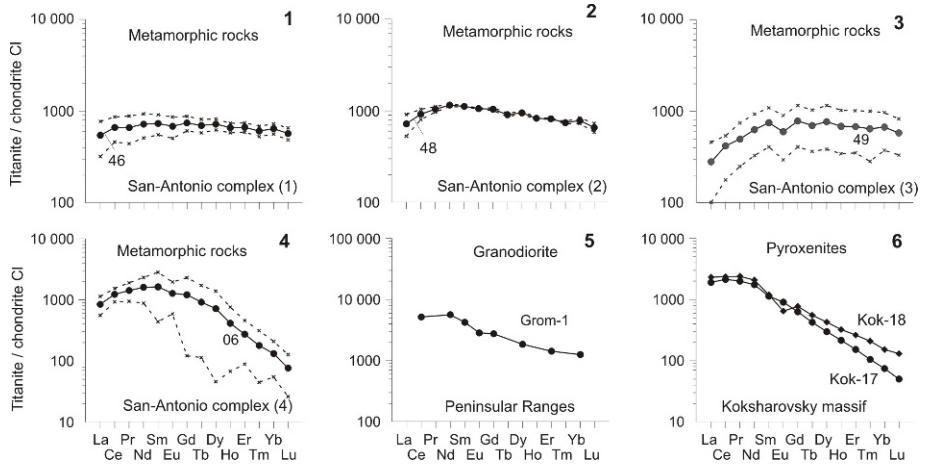

Figure 9. Chondrite-normalized REE patterns for titanites from pyroxenites, granodiorites, and some metamorphic rocks. Dotted lines show the patterns for maximum and minimum REE-compositions of individual grains of titanites.

sider some regularities of REE distribution in perovskites by the example of kimberlite samples of several provinces (Table 17). Studies on perovskites from some kimberlite occurrences of Southern Africa showed that the perovskite presented in them is characterized by generally higher REE concentration in comparison with the mineral from kimberlites of South India [107]. It was also ascertained that in perovskites from Benfontein sill and Wesselton province the values of parameter $(La/Ce)n < 1$. In mineral samples from kimberlites of Premier pipe and Dharwar craton the values of parameter $(La/Sm)n > 1$. In all of these perovskites of the occurrences mentioned an intense REE fractionation is observed, their REE patterns tend to have a steep negative slope (Fig. 11). The patterns of perovskites of Benfontein sill and Wesselton province have minor Ce anomalies (Fig. 12). The same peaks are present in the patterns of perovskite from kimberlites of Monastery pipe, as well as Bellsbank, De Beers, Liqhobong and Green Mountain provinces [107]. Having considered the general regularities of REE distribution in perovskites, the stated researchers paid attention to the fact that the configuration of REE patterns of this mineral in many respects is similar to the configuration of patterns of kimberlites, in which they reside. In kimberlites and

Table 17. REE compositions of perovskites from kimberlites, olivine nephelinites, kamafugites, and carbonatites from some manifestations (ppm).

	South Africa				South India									Meimecha-Kotuy prov. (Russia)	
	Benfontein sill		Wesselton province	Premier pipe										[data Yu.Vasiliev]	
	[57], WDS				[17], WDS										
Element	Bnf-1	Bnf-2	WM-3	PM-5	P3	P4	P4a	CH10	P11/2C	KK10	NP	PD/2	PD/2a	Vas-1	Vas-2
	Kimberlites													*Olivine nephelinites*	
La	8842	8024	7478	2729	9590	7360	7040	4590	5210	2600	3800	2620	3060	6100	6100
Ce	26066	25169	24162	6805	22800	17490	19380	9170	12380	6680	7570	4050	5670	14200	14200
Pr	2914	2803	2862	530	2820	2440	1520	2440	2850	660	440	210	620	2400	2400
Nd	10811	10537	11077	2589	9590	6690	7110	4620	4770	2980	3090	2520	2130	6400	6400
Sm	1207	1362	1267	345	1040	850	700	480	420	190	220	100	170	6100	6100
Gd	650	755	729	165	60	140	650	740	60	280	530	370	260	1140	1240
Total	49840	47895	46846	12998	45840	34830	35750	21300	25630	13110	15120	9500	11650	36340	36440
$(La/Sm)_n$	4,98	5,81	5,45	6,33	6,02	7,81	8,62	10,9	16,5	11,3	4,98	5,81	5,45	0,63	0,63
$(La/Ce)_n$	0,83	0,81	1,05	1,10	1,10	0,95	1,31	1,10	1,02	1,31	1,69	1,41	1,12	1,12	0,88

	Alto Paranaiba province (Brazil)										Koksharovsky, (Russia)
	[91], LA ICP-MS										[107], ICP-MS
Element	Ind-r	Ind-c	Lim-c1	Lim-c2	Pan-c	Pan-r	SR-c1*	Sr-c2*	Mal-c1*	Mal-c2*	Kok-16
	Kimberlites and kamafugites										*Carbonatite*
La	6990	6990	13011	14555	10423	1771	5134	7837	3762	3030	6652
Ce	22985	20392	36067	35637	25792	2092	9017	21081	9742	6322	14022
Pr	2051	1869	4265	3279	2517	196	1009	1916	802	528	1561
Nd	7505	7204	11366	10643	8707	654	4157	6782	2723	1850	4624
Sm	922	943	1307	954	1107	121	526	903	446	307	669
Eu	209	199	236	161	202	35	125	204	114	87	188
Gd	410	408	450	314	427	101	345	400	229	186	520
Tb	32,1	34,2	31,8	22,9	32,8	11,4	40,6	38	22	19,2	62,1
Dy	114	124	93,9	85,4	116	53,2	190	155	86,5	84	282
Ho	12,2	13,9	11	9,5	14,3	8,4	29,3	18,6	10,5	11,2	39,8
Er	17,4	21,2	15	16,2	22,3	14,5	54	31,7	17	19,2	73,8
Tm	1,51	1,64	1,15	1,17	1,74	1,38	3,78	2,69	1,4	1,82	7,16
Yb	6,17	6,42	4,44	7,74	6,83	6,02	19,8	12,5	5,92	8,48	31,5
Lu	0,53	0,55	0,32	0,51	0,58	0,5	2,92	1,04	0,45	0,69	3,6
Total	41256	38207	66860	65686	49370	5065	20653	39383	17962	12455	28736
$(La/Yb)_n$	765	735	1978	1269	1030	199	175	423	429	241	143

	Africa								Somerset Island (Canada)	
	[167], LA ICP-MS									
Element	W3-680	W2-680a	W2-680b	ND#WX	BF-18b	OND1-2	TF-7	Kao-1b	JP1-102	JP1-103
	Kimberlites									
La	7150	7084	6754	5732	8264	2004	2619	3437	5170	4841
Ce	18764	19455	16860	13443	22421	4583	5740	7997	13242	11548
Pr	2227	2315	2002	1586	2721	548	652	983	1804	1565
Nd	8978	8979	8158	6472	10869	2295	2613	3750	6639	5875
Sm	1179	1165	1067	884	1333	372	386	481	805	711
Eu	268	266	233	204	278	97,9	96,6	108	165	157
Gd	602	622	510	446	614	233	214	278	352	331
Tb	50,2	50,5	47,6	42,1	48,9	24,4	21,8	21,2	32	31
Dy	179	177	181	159	168	98,5	89,3	84,4	122	120
Ho	20,4	20,9	20,9	18,7	18,4	12,9	11,4	9,84	15	15
Er	30,3	37,2	33,5	29,8	27,1	21,2	19,7	16,2	23	24
Tm	2,34	2,66	2,66	2,29	2,00	1,77	1,67	1,29	1,96	2,11
Yb	9,73	11,3	11,3	10,1	8,24	7,57	7,60	5,53	8,18	8,57
Lu	0,75	0,82	0,94	0,82	0,66	0,64	0,67	0,47	0,76	0,81
Total	39461	40179	35882	29030	46773	10300	12473	17173	28381	25229
$(La/Yb)_n$	496	460	403	383	677	179	233	420	427	381

kamafugites of Alto Paranaiba province (Brazil) the REE and other impurities were identified both in perovskites and in coexisting olivines, clinopyroxenes, phlogopites and ilmenites. Total REE content in perovskites of these rocks varies in the range from 12 455 to 66 860 ppm, and the values for $(La/Yb)_n$ range from 175 to 1030. According to data obtained by the microprobe fluorescent technique, the contents of La, Ce, Nb, Na and Sr in the perovskites of Indaia manifestation of the mentioned province decreased from the inner zones to the periphery of their grains. At the same time, the analyses by LA ICP-MS method that were carried out on a single grain of perovskite of the same kimberlite manifestation, have shown that in its inner zone the total REE content is slightly lower than in

Element	JP1-104	C8	PC-03	PC-04	BND2-2	Tunraq	EL-6	Ham	Amayersuk	BSD5-1
					Kimberlites					
La	4591	6977	7042	6970	5209	5662	6138	6734	7527	7292
Ce	10909	15810	16083	16754	11191	12499	14148	15546	17603	17320
Pr	1467	1683	2096	2184	1225	1645	1854	2005	2237	2189
Nd	5454	6352	7574	7813	4636	5999	6682	7165	8050	8111
Sm	663	695	822	844	579	726	729	809	886	933
Eu	147	149	170	171	135	158	154	172	179	191
Gd	317	301	342	339	290	338	306	347	358	397
Tb	29,1	25,8	29,5	28,8	27,0	30,6	25,5	30,1	30,5	34,1
Dy	115	94,3	110	105	103	119	95	111	112	128
Ho	14,3	10,8	13,0	12,5	12,5	14,3	11,1	13,0	12,9	15,1
Er	22,4	17,5	20,4	19,4	20,5	23,1	17,5	19,7	20,1	23,7
Tm	1,94	1,38	1,64	1,56	1,71	1,94	1,37	1,68	1,57	1,91
Yb	8,50	6,17	6,72	6,68	7,75	7,81	5,61	6,66	6,45	7,98
Lu	0,78	0,52	0,60	0,60	0,70	0,79	0,51	0,56	0,58	0,77
Total	23740	31923	34311	35250	23438	27225	30168	32961	37004	36645
$(La/Yb)_n$	365	763	707	704	454	489	739	682	788	617

Somerset Island (Canada)
[167], LA ICP-MS

Note. WDS long wave dispersion spectroscopic method; c core of grain, r rim of grain; (*) - samples from kamafugites.

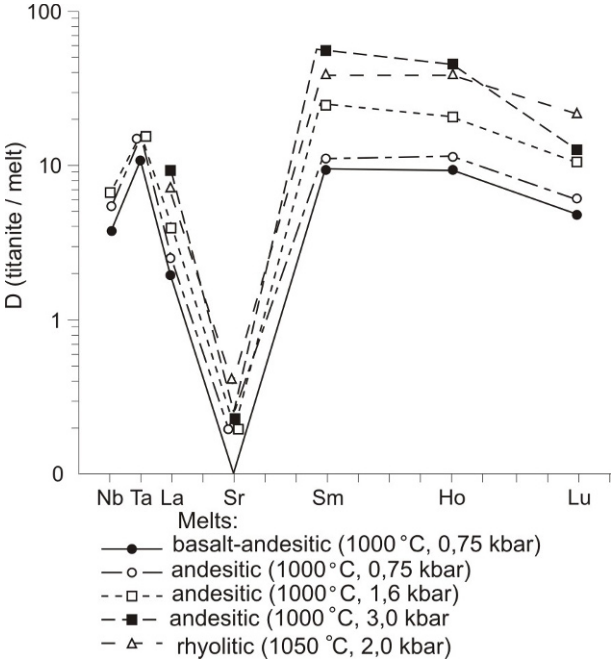

Figure 10. The graphs of coefficients of Nb, La, Sr, Sm, Ho and Lu distribution (D) between titanites and basalt-andesitic, andesitic, and rhyolitic melts under different PT-conditions (experimental data [Green, 1994]).

the outer zone. In addition, the total REE content in the outer zone of the perovskite grain from kimberlites of Pantano manifestation of the same province also turned out to be significantly lower than in its inner zone.

Studies on regularities of distribution of REE and other impurities in perovskites from some kimberlite occurrences of South Africa and Somerset Province (Canada), which were conducted by [124], showed that the total REE compositions in the mineral samples from the occurrences of Southern Africa vary from 10 300 to 46 773 ppm, and the values for $(La/Yb)_n$ - from 179 to 677. In perovskites of Somerset Province the total REE compositions ranged from 23 438 to 37 004 ppm, values for $(La/Yb)_n$ – from 381 to 788. The patterns of distribution of chondrite-normalized REE compositions in perovskites from kimberlites of South Africa and Somerset province are the lines with a very steep negative slope that are almost identical in configuration and location. By the nature of their REE patterns, the perovskites studied by [124], in many respects are similar to the patterns of mineral samples from Alto Paranaiba Province, Benfontein sill and Wesselton province (Fig. 12). A large concentration of REE and their slightly less intense fractionation were ascertained in perovskite from carbonatites of Koksharovsky alkaline ultramafic massif (Primorie, Russia), as well as in the samples of mineral from olivine nephelinites of Meimecha-Kotuy province (Siberian platform, Russia). The high modal contents of perovskite in kimberlites can greatly affect the overall level of REE accumulation, as well as the configuration of the patterns of their distribution in these rocks. This conclusion follows from the identified positive correlation between REE compositions of kimberlites, on the one hand, and the contents of TiO_2 in them, on the other hand [68].

Estimates of the values of D (perovskite / silicate melt), which were obtained based on the results of experimental studies, have shown that for La, Sm, Eu and Tb the values of these coefficients are slightly greater than 1, which means that during the crystallization of perovskites the REE possessed properties of compatible elements. Con-

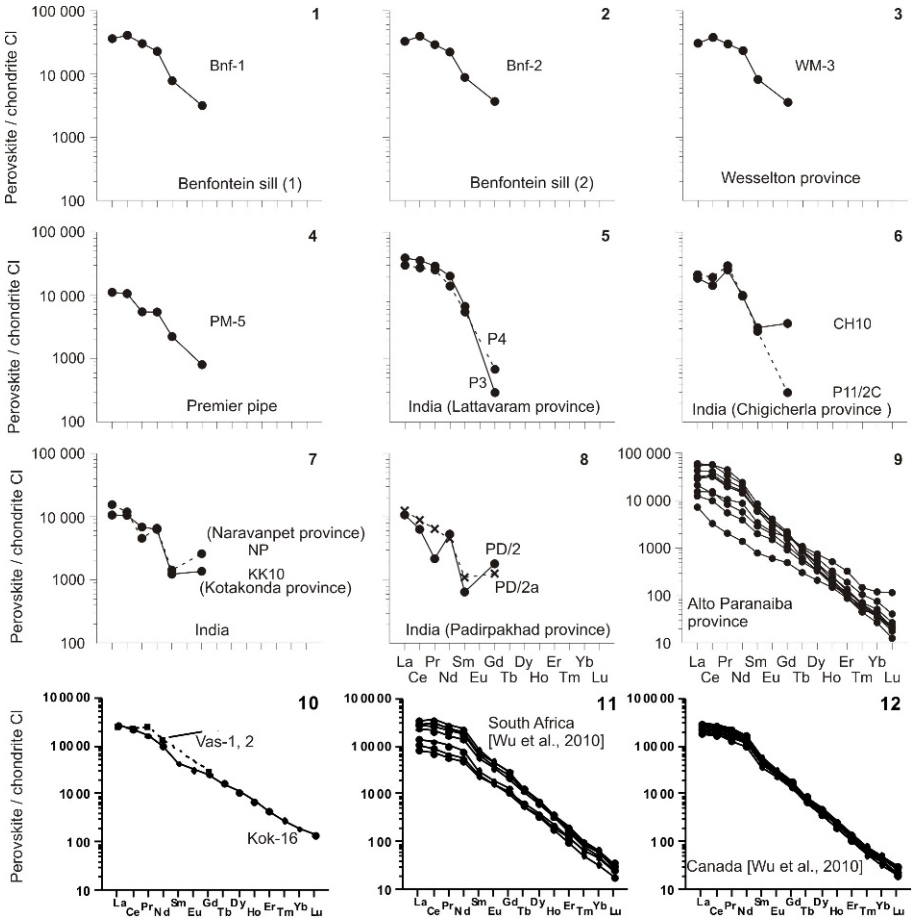

Figure 11. Chondrite-normalized REE patterns for perovskites from kimberlites from Indian provinces (1-8); from kimberlites and kamafugites from Alto Paranaiba province, Brazil (9); olivine nephelinites from Meimecha-Kotuy province and carbonatites from Koksharovsky massif, Russia (10); kimberlites from South Africa (11) and from Canada (12).

trasting to them, the values of D for Yb and Lu do not exceed 1, therefore these REE possessed properties of incompatible elements during their isomorphous incoming into the structure of perovskites (Table 18). Some of the data on D (perovskite / melt) values estimates for REE were obtained by [107] during their studies on natural and experimental systems. For natural systems the D (REE) values were determined between kimberlites and melilite-nepheline basalts, on the one hand, and the perovskites they contain, on the other hand. The following diagram shows that for the perovskite/kimberlite system the D values for La, Ce, Pr, Nd, Sm, Gd and Ho > 1. A similar trend is ascertained for D (La, Nd, Sm) in the perovskite / melilite-nepheline basalt system. For both of these systems the curves of changes in the values of D have a common negative slope. The curves shown in the same picture reflect the changes in the values of D (perovskite / kimberlite) for the natural system and for some systems studied during the experiment and also have a common negative slope, but the D values for the experimental systems were lower than for the natural system. In addition, in some kimberlites the accessory apatite plays the role of a concentrator of significant LREE amounts, along with the perovskite, but the modal contents of them are usually much smaller than those of perovskite.

The study of REE distribution between minerals from jacupirangites, ijolites and nepheline syenites represented as xenoliths in tuffs of Oldoinyo Lengai volcano (Tanzania) showed that in the cases when there was absence of titanites in these rocks the values of D (perovskite / apatite) were: La - 9, Ce -16, Nd - 9,5. However, when samples of the same rocks contained titanites, the values of D (perovskite / apatite) for these elements were much lower [111]. An opportunity in the rocks examined one of the minerals are not in equilibrium.

Table 18. The coefficients of REE distribution (D) between perovskites and silicate melts (experimental data [97]).

Element	Nag-1	Nag-2	Nag-3	Nag-4	Nag-5
La	2,4	2,96	2,15	2,44	3,04
Ce	N.d.	N.d.	N.d.	N.d.	N.d.
Pr	»	»	»	»	»
Nd	»	»	»	»	»
Sm	2,76	3,12	2,16	2,47	3,01
Eu	2,28	2,67	2,07	1,87	2,04
Gd	N.d.	N.d.	N.d.	N.d.	N.d.
Tb	1,45	1,83	1,37	1,49	1,77
Dy	N.d.	N.d.	N.d.	N.d.	N.d.
Ho	»	»	»	»	»
Er	»	»	»	»	»
Tm	»	»	»	»	»
Yb	0,482	0,517	0,445	0,443	0,553
Lu	0,408	0,412	0,389	0,413	0,432

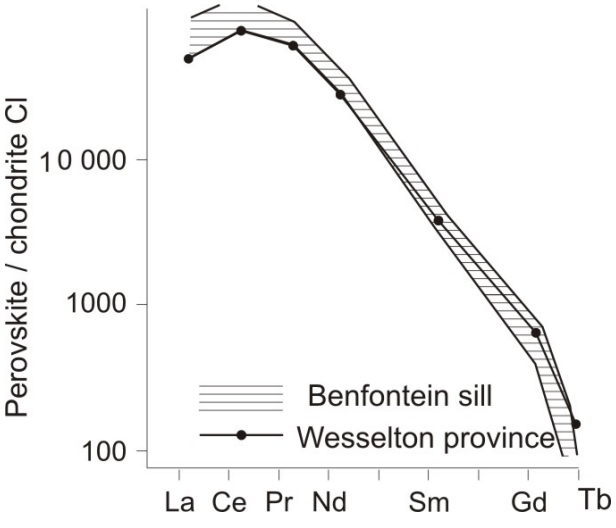

Figure 12. Chondrite-normalized average composition REE patterns for perovskites from kimberlites of Benfontein sill ($n = 2$) and Wesselton province ($n = 6$) (data [57]).

Having considered very scarce data on the contents of REE in perovskites, we emphasize again that this mineral, presented as an accessory phase in some varieties of magmatic rocks, can accumulate in its structure very substantial LREE amounts and much smaller quantities of medium and heavy elements. Therefore, if there is a significant modal content of perovskite in the rocks it might have a noticeable effect on the REE distribution in these rocks, which is well illustrated by the kimberlites. The high values of LREE distribution coefficients between perovskite and its parent melts indicate that during the isomorphic incoming into its structure the LREE usually possessed properties of compatible elements.

9. Micas

Micas are primarily presented in magmatic rocks with high content of silica, alkaline and volatile components, as well as in metamorphic and some metasomatic rocks. Less frequently micas occur as a secondary phase in some rocks of mafic and ultramafic composition and what is more, most often they are represented by phlogopite.

Analytical data on the REE composition of micas from high-magnesium rocks is now available in fairly limited amounts and characterizes the composition of this mineral not from all the varieties of these rocks but mainly from kimberlites, peridotites, wehrlites, websterites and clinopyroxenites (Table 19). Total REE contents in phlogopites from wehrlites and pyroxenites composing xenoliths from minettes of Bearpav province (Montana, USA) vary from 29 to 112 ppm, while the chondrite-normalized La contents are higher (10.2–54.2 t.ch.) than Yb contents (3.6–7.2 t.ch.) [125]. The REE patterns of these phlogopites have the shape of lines with a gentle negative slope and are described by the values of (La/Yb)n parameter in the range of 2.3–7.5 (Fig. 13). Phlogopites from ultramafic rocks that form xenoliths in alkaline basalts from Vitim province are characterized by total REE contents that are lower (1.4–20 ppm) than the previous ones [Litasov, 1998]. The REE composition, which is very close to phlogopites from Vitim province, was identified in the phlogopites from concentrate that have been isolated from kimberlite sample from Yubileynaya pipe (Yakutia), the total REE content of which is 10.8 ppm [126]. Phlogopites from ultramafic xenoliths of Vitim province, as well as from the kimberlites of Yubileynaya pipe, are characterized by a more intensive REE fractionation in comparison with the mineral from Bearpav province. Thus, in phlogopites from Vitim province the values of (La/Yb)n parameter vary

Table 19. REE compositions of phlogopites, and biotites from some magmatic rocks (ppm).

	Bearpav province (USA)			Vitim province (Russia)				Yubileynaya pipe (Yakutia, Russia)	Germany, Austria		Twin Peaks (USA)
	[23], ICP-MS			[82], SIMS				[2], ICP-MS	[51]		[101]
Element	201	237	188	V878	LF-4	V244	V439	Asch-3	RRa	32M	N-4
	Wehrlite	*Pyroxenites*		*Peridotites*				*Kimberlite*	*Nephelinite*		*Rhyolite*
La	2,50	4,05	13,3	0,420	0,980	4,04	0,970	2,12	0,970	0,990	81,1
Ce	8,25	14,3	43,1	0,020	0,270	0,040	0,060	5,70	1,60	1,60	168
Pr	1,50	2,46	6,45	N.d	N.d	N.d	N.d	0,520	0,200	N.d	N.d
Nd	7,79	10,9	27,4	0,690	1,24	11.7	1,71	1.65	0,850	»	61,0
Sm	2,36	3,61	6,30	0,080	0,180	1,26	0,150	0,260	0,051	0,097	7,88
Eu	0,69	1,14	1,45	0,030	0,060	0,430	0,060	0,113	0,051	0,097	0,400
Gd	2,13	3,17	5,25	N.d.	N.d.	N.d.	N.d.	0,202	0,086	N.d.	N.d.
Tb	0,29	0,470	0,750	»	»	»	»	0,020	0,012	»	0,710
Dy	1,64	2,70	3,89	0,110	0,200	1,65	0,250	0,135	0,080	»	4,23
Ho	0,290	0,480	0,700	N.d.	N.d.	N.d.	N.d.	0,015	N.d.	»	N.d.
Er	0,680	1,28	1,75	0,050	0,070	0,740	0,100	0,022	»	»	»
Tm	N.d.	N.d.	N.d.	N.d.	N.d.	N.d.	N.d.	0,006	0,004	»	»
Yb	0,600	1,17	1,20	0,020	0,040	0,140	0,030	0,026	0,029	»	2,49
Lu	0,090	0,160	0,160	N.d.	N.d.	N.d.	N.d.	0,007	0,004	»	0,370
Total	28,8	45,9	112	»	»	»	»	10,8	3,94	»	N.d.
(La/Yb)$_n$	2,8	2,3	7,5	14,2	16,5	19,5	21,8	55,0	22,6	»	22,0

	Twin Peaks (USA)		Koksharov-sky massif (Russia)	Alto Paranaiba province (Brazil)							
	[101], INAA		[107]	[91], LA ICP-MS							
Element	N-8	N-20	Kok-20	Ind-c	Ind-r	Lim-c	Lim-r	Pan-c	Pan-r	Po-c	Ver-c	Mal-c
	Rhyolites		*Nepheline syenite*	*Kimberlites*								
La	459	41,5	0,77	0,028	0,038	0,897	2,14	0,171	10,97	0,411	5,03	0,99
Ce	770	100	0,73	N.d.	0,051	0,662	2,22	0,292	7,12	0,108	9,6	0,44
Pr	N.d.	N.d.	0,11	0,004	0,008	0,055	0,162	0,037	0,572	0,016	1,22	0,044
Nd	187	39,0	0,38	N.d.	0,053	0,201	0,571	0,078	2,3	N.d.	5,84	0,12
Sm	23,1	6,45	0,11	0,02	N.d.	0,017	0,162	N.d.	0,581	»	1,01	0,049
Eu	1,67	0,220	0,013	0,017	0,028	0,019	0,057	0,005	0,247	0,042	0,352	0,05
Gd	N.d.	N.d.	0,05	0,022	N.d.	0,027	0,12	0,002	0,739	0,025	0,04	0,046
Tb	2,71	0,700	0,01	0,002	»	0,003	0,01	N.d.	0,108	N.d.	0,133	0,01
Dy	16,4	4,49	0,06	0,005	0,003	0,035	0,062	»	0,509	»	0,58	0,046
Ho	N.d.	N.d.	0,01	N.d.	0,001	0,005	0,008	»	0,078	»	0,116	0,005
Er	»	»	0,02	»	N.d.	0,012	0,043	0,015	0,208	0,032	0,282	N.d.
Tm	»	»	N.d.	»	0,003	0,004	0,007	N.d.	0,024	0,011	0,033	0,003
Yb	12,7	2,84	0,05	0,015	N.d.	0,017	0,012	0,052	0,216	N.d.	0,193	N.d.
Lu	2,00	0,42	0,01	N.d.	0,005	0,01	N.d.	N.d.	0,024	»	0,035	0,003
Total	N.d.	N.d.	2,32	0,11	0,19	1,96	5,57	0,65	23,7	0,65	24,5	1,81
(La/Yb)$_n$	24,4	9,9	10,4	1,26	N.d.	35,6	120	2,22	34,3	N.d.	17,6	N.d.

in the range from 14.2 to 21.8, while in the mineral from kimberlites of Yubileynaya pipe ~55. On REE patterns of phlogopites from ultramafic xenoliths of Vitim province there are negative Ce anomalies, which are absent on the pattern of the mineral from kimberlites, while the latter show a weak positive Eu anomaly. Mica that is presented in the olivine nephelinite from Germany and Austria is characterized by relatively low overall REE accumulation in comparison with the mineral from the occurrences mentioned above.

The total REE contents of phlogopites from kimberlites of Alto Paranaiba province range from 0.11 to 24.5 ppm, and these minerals from various occurrences are markedly different in the configuration of REE patterns. On REE patterns of the central and outer zones of phlogopite grains from Indaia manifestation of this province there are intense positive Eu anomalies. Furthermore, the inner and outer zones of grains of phlogopite from kimberlites of Limeira manifestation are characterized by significant enrichment with LREE, while positive Eu anomalies on their patterns are of lower intensity. The REE content in the outer zone of phlogopite grain is slightly higher than in its inner zone. A similar trend, but in the absence of clearly defined Eu anomalies, was observed in phlogopite from kimberlites of Pantano manifestation, but the content of almost all the REE in it was significantly higher in the outer zone than in the inner zone. We should also note the increased concentration of REE in the inner zone of grain of phlogopite

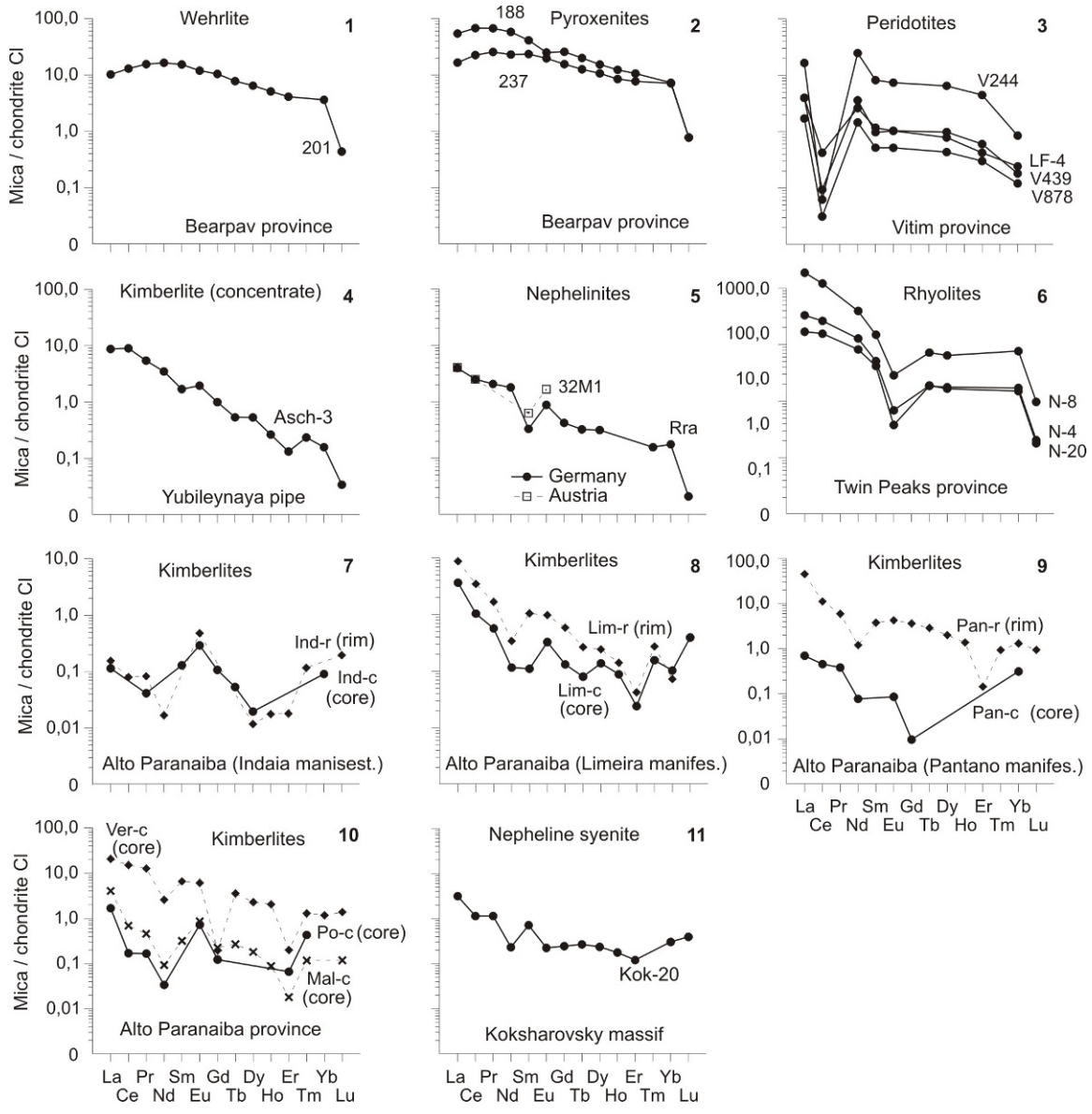

Figure 13. Chondrite-normalized REE patterns for biotites and phlogopites from wehrlite (1), pyroxenite (2), peridotite (3), kimberlites (4, 7-10), nephelinite (5), and nepheline syenite (11) of some provinces and manifestations.

from kimberlites of Veridiana manifestation, as well as the presence of positive Eu anomalies in the patterns of the central zones of grains of phlogopite from other kimberlite occurrences of Alto Paranaiba province.

A study of biotites from nepheline syenites forming Koksharovsky alkaline ultramafic massif (Primorie province, Russia) showed that the overall level of REE accumulation, as well as the intensity of REE fractionation, are lower than most of the above-described phlogopites from kimberlites. The biotites from rhyolites of volcanic complex in Twin Peaks province (USA) have relatively high total REE contents. Their chondrite-normalized REE patterns show a predominance of LREE over HREE and a significant Eu deficit.

Studies on REE composition of individual mica samples and basanites and basalts containing them provided approximate estimates of the values of D (mica / melt) that appeared to be generally very low (Table 20). The D graphs have a complex configuration, which may be due to insufficiently correct determination of the contents of some elements. T. Green [120] published data on the values of D (phlogopite / melt) for some impurities including

Table 20. The coefficients of REE distribution between micas and basanitic, and basaltic melts.

	Basanitic melt		Basaltic melt
	K_d (mica/matrix) (experimental data)		K_d (mica/melt) kombinated
	[Irving, Frey, 1984]		[Litasov, 1998
Element	IrF-1(min.)	IrF-2(max.)	Lit-1
La	0,006	0,036	0,031
Ce	0,005	0,027	0,007
Pr	N.d.	N.d.	0,011
Nd	0,017	»	0,012
Sm	0,004	0,028	0,012
Eu	0,022	0,036	0,031
Gd	0,014	N.d.	0,026
Tb	0,015	»	N.d.
Dy	0,019	»	0,026
Ho	N.d.	»	0,03
Er	»	»	0,03
Tm	»	»	N.d.
Yb	0,02	0,041	0,03
Lu	0,018	0,031	0,04

REE, which were obtained based on the results of physical experiments (Fig. 14). The data imply that the D values for La, Sm, Ho and Lu do not exceed 1 and also that the coefficient variation curves in the segment from La to Ho has a positive slope, while in the section from Ho to Lu it acquires a negative slope. We should emphasize that according to the limited analytical data, there are somewhat significant differences ascertained between micas of magmatic and metamorphic rocks, which are in the general level of REE accumulation and in the configuration of the patterns of their chondrite-normalized contents. Chondrite-normalized LREE contents in most of the samples of mica are slightly higher than the contents of MREE and HREE, and, accordingly, their patterns have a common negative slope. It should also be emphasized that phlogopites from kimberlites, wehrlites, peridotites and pyroxenites are able to concentrate in its structure much smaller amounts of REE compared to biotites from rhyolites and metamorphic rocks.

10. Conclusions

Through the development of modern microprobe methods to determine REE concentrations, and by technological advances lowering of the limits of REE detection, during the recent years the study of the regularities or patterns of distribution of these trace elements has expanded not only on rock-forming, but also on minor and accessory minerals of the ultramafic and mafic rocks, including garnets, chrome-spinels, ilmenites, zircons, apatites, titanites, perovskites and micas. These minerals are significantly different from each other in the general chemical composition, crystal-chemical properties and formation conditions. These minerals have different ability to accumulate REE and other impurities. An appropriate use of data on the REE distribution in these minerals can help to gain geochemical insight into their diagnosis, discrimination, systematization and genetic interpretation.

Geochemical studies suggest that the same types of accessory minerals that are presented in ultramafic and mafic rocks of different composition and origin, and in magmatic complexes composed of these lithologies, differ in the level of REE accumulation, the degree of fractionation and in several other features. These differences are due to various factors, such as an initial concentration of REE in parental melts, as well as differences in temperature, pressure and redox conditions of melts generation and minerals crystallization. Along with the general level of accumulation and other parameters of REE distribution in minor and accessory minerals, we have calculated distribution coefficients of REE between minerals and their parent melts, as well as between coexisting mineral phases based on data from natural and experimental samples. Given the ability to concentrate in its structure one or another amount of isomorphous REE impurity, the accessory and minor minerals from the ultramafic, mafic and related rocks can be divided into the following five groups: 1) garnets and zircons that accumulate significant amounts of REE with substantial prevalence of chondrite-normalized contents of HREE; 2) apatites and perovskites that can accumulate significant amounts of REE with substantial predominance of LREE; 3) titanites that accumulate medium amounts of light and heavy REE at near their chondrite-normalized concentrations, 4) micas that accumulate medium amounts of REE with a slight predominance of chondrite-normalized LREE contents over HREE contents; 5) ilmenites and chrome-spinels that accumulate

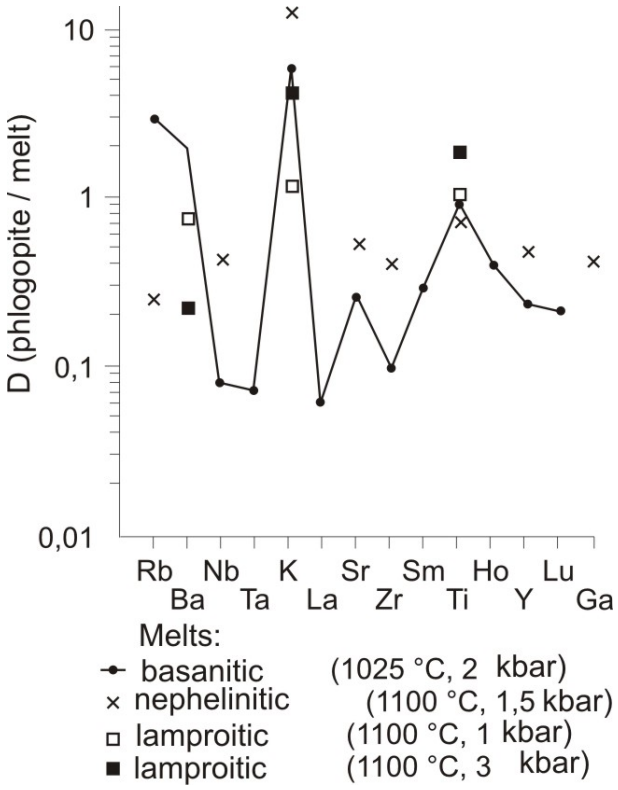

Figure 14. The graphs of coefficients of REE distribution between phlogopites and basanitic, nephelenitic, and lamproitic melts under different PT-conditions (experimental data [32]).

a limited amount of REE often with HREE predominance. It is important to note that along with isomorphous REE impurity that reside directly in their structure, in some cases the crystals of minor and accessory minerals may contain one or another amount of non-structural impurity of these elements, which was accumulated in microcracks and different microinclusions as a result of infiltration of the epigenetic fluids.

References

[1] Sobolev N. V., Paragenetic types of garnets. Publishing House Nauka, Moscow, 1964 (in Russian)

[2] Haskin L. A., Frey F. A., Dispersed and not-so-rare earths. *Science,* 1966, 152, 299

[3] Masuda A., Lanthanide concentration rations between pyroxene and garnet. *Earth Planet. Sci. Lett.,* 1967, 3, 25–28

[4] Stachel T., Viljoen K. S., Brey G., Harris J. W., Metasomatic processes in lherzolitic and harzburgitic domains of diamondiferous lithospheric mantle: REE in garnets from xenoliths and inclusions in diamonds. *Earth Planet. Sci. Lett.,* 1998, 159, 1–12

[5] Nixon P. H., van Calstern P. W., Boyd F. R., Hawkestworth C. J., Harzburgites with garnets of diamond facies from Southern African kimberlites. In: Nixon P.H., Mantle xenoliths, J. Wiley & Sons, 1987, 523–533

[6] Pokhilenko N. P., Sobolev N. V., Boyd F. R., Pearson D. G., Shi-muzu N. T., The megacrystalline pyrope peridotites in the lithosphere of the Siberian platform: mineralogy, geochemistry and problem of origin. *Russian Geology and Geophysics*, 1993, 34, 71-84 (in Russian)

[7] Shimizu N., Pokhilenko N. P., Boyd F. R., Pearson D. G., Geochemical characteristics of mantle xenoliths from kimberlite pipe Udachnaya. *Geologia i Geofisika*, 1997, 38, 194-205 (in Russian)

[8] Stachel T., Aulbach S., Brey G. P., Harris J. W., Leost I., Tappert R., Viljoen K. S.,The trace element composition of silicate inclusions in diamonds: review. *Lithos,* 2004, 77, 1–19

[9] Shatskii V. S., High-pressure mineral assemblages of eclogites-bearing complexes of the Urals-Mongolian folded belt. PhD thesis, Geology and mineralogy science, Novosibirsk, Institute of Geology and Geophysics of Siberian branch of Academy of Sciences of USSR, 1990 (in Russian)

[10] Bakirov A. B., Some questions of a metamorphism of the Atbashinsky ridge. Questions Precambrian stratigraphy and the lower Palaeozoic of Kyrgyzia. Academy of Sciences of the Kyrgyz Soviet Socialist Republic, 1964 (in Russian)

[11] Lesnov F. P., Volkova N. I., Bakirov A. B., Sakiev K.S., Novgorodtsev O.S., New data on the composition of minerals and the conditions of formation of eclogites from Atbashi ridge (Southern Tien Shan). Petrology of igneous and metamorphic complexes. Tomsk State University, 2004, 255-263 (in Russian)

[12] Lesnov F. P., Kuchkin A. M., Palessky S. V., Volkova N. I., Rare earth elements in garnets from eclogites of Atbashi metamorphic complex (Southern Tien Shan, Kyrgyzstan). Metallogeny of ancient and modern ocean-2005. Formation and development of deposits in island arc systems. Institute of Mineralogy of Ural branch of the Russian Academy of Sciences, 2005, 63-67 (in Russian)

[13] Mazzucchelli M., Rivalenti G., Vannucci R., Bottazzi P., Ottolini L., Hofmann A. W., Sinigoi S., Demarchi G., Trace element distribution between clinopyroxene and garnet in gabbroic rocks of the deep crust: An ion microprobe study. *Geochim. Cos-*

mochim. Acta., 1992, 56, 2371–2385

[14] Nicolescu S., Cornell D. H., Sodervall U., Odelius H., Secondary ion mass spectrometry analysis of rare earth elements in grandite garnets and other skarn related silicates. *Eur. J. Mineral.,* 1998, 10, 251–259

[15] Schwandt C. S., Papike J. J., Sheare C. K., Brearle A. J., A SIMS investigation of REE chemistry of garnet in garnetite associated with Broken Hill Pb-Zn-Ag orebodies, Australia. *Canadian Mineralogist,* 1993, 31, 371–379

[16] Gaspar M., Knaak C., Meinert L. D., Moretti R., REE in skarn systems: A LA-ICP-MS study of garnets from the Crown Jewel gold deposit. *Geochim. Cosmochim. Acta,* 2008, 72, 185–205

[17] Shimizu N., Richardson S. H., Trace element abundance patterns of garnet inclusions in peridotite-suite diamonds. *Geochim. Cosmochim. Acta,* 1987, 51, 755–758

[18] Hoal K. E. O., Hoal B. G., Erlank A. J., Simizu N., Metasomatism of the mantle lithosphere recorded by rare earth elements in garnets. *Earh Planet. Sci. Lett.,* 1994, 126, 303–313

[19] Shimizu N., Boyd F. R., Sobolev N. V., Pokhilenko N. P., Chemical zoning of garnets in peridotites and diamonds. V.M. Goldschmidt conference, Edinburg, *Pabl. Miner. Mag.*, 1994, 831–832

[20] Pearson D. G., Milledge H. J., Diamond growth conditions and preservation: inferences from trace elements in a large garnet inclusion in Siberian diamond. Proc.7th Intern. Kimberlite Conf., Cape Town, 1998, 667–669

[21] Shimizu N., Sobolev N. V., Young peridotite diamonds from the Mir kimberlite pipe. *Nature,* 1995, 375, 394–397

[22] Demaiffe D., El Fadili S., Andre L., Geochemical and isotopic (Sr, Nd) study of eclogite nodules from Mbuji Mayi kimbrlite, Kasai, Congo. Proc. 7th International Kimberlite Conference, 1998, Cape Town, 190-192

[23] Shimizu N., Sobolev N. V., Efimova E. S., Chemical heterogeneity of garnet inclusions and juvenile in peridotitic diamonds from Siberia. *Geologia i Geofisika*, 1997, 38, 337-352 (in Russian)

[24] Jacob D. E., Kjarsgaard B., Horn I., Trace element concentrations laser ablation ICP-MS in subcalcic garnets from Saskatchewan and Somerset island, Canada. Proc. 7th International Kimberlite Conference, Cape Town, 1998, 361–363

[25] Pokhilenko N. P., McDonald J. A., Melnyk W., Hall A.F., Shimizu N., Vavilov M.A., Reimers L.F., Irvin J., Pokhilenko L.N., Vasilenko V.B., Kuligin S.S., Sobolev N.V., Kimberlites of Camsell Lake field and some features of constuction, and composition of lithosphere roots sourth-eastern part of Slave Craton, Canada. *Proc. 7th Intern. Kimberlite Conf. Extended Abstracts*, Cape Town, 1998, 699–701

[26] Spetsius Z. V., Griffin W.L.,Trace element composition of garnet kelyphites in xenoliths from Udachnaya as evidence of their origin. *Proc. 7th International Kimberlite Conference,* Cape Town, 1998, 853–856

[27] Lesnov F. P., On the trend of the distribution coefficients of rare earth elements between garnet and melt. Petrology of igneous and metamorphic complexes. Tomsk State University, 2001, 65–70 (in Russian)

[28] Spetsius Z. V., Taylor W. R., Griffin W. L., Major and trace element partitioning between mineral phases in diamondiferous and non-diamondiferous eclogites from the Udachnaya kimberlite pipe, Yakutia. *Proc.7th International Kimberlite Conference*, Cape Town, 1998, 856–858.

[29] Schnetzler C. C., Philpotts J. A., Partition coefficients of rare earth elements between igneous matrix and rockforming mineral phenocrysts–II. *Geochim. Cosmochim. Acta,* 1970, 34, 331–340

[30] Shimizu N., Kushiro L., The partitioning of rare earth elements between garnet and liquid at high pressure: preliminary experiments. *Geophys. Res. Lett.,* 1975, 3, 413–416

[31] Irving A. J., Frey F. A., Distribution of trace elements between garnet megacrysts and host volcanic liquids of kimberlitic to rhyolitic compositon. *Geochim. Cosmochim. Acta,* 1978, 42, 771–787

[32] Beattie P., On the occurence of apparent non-Henry's law in experimental partitioning studies. *Geochim. Cosmochim. Acta,* 1993, 57, 47–55

[33] Mysen O. B., Experimental determination of rare earth element partitioning between hydrous silicate melt, melt, amphibole and garnet peridotite minerals at upper mantle pressure and temperatures. *Geochim. Cosmochim. Acta,* 1978, 42, 1253–1263

[34] van Westrenen W., Blundy J., Wood B., Crystal-chemical controls on trace element partitioning between garnets and anhydrous silicate melt. *American Mineralogist,* 1999, 84, 838–847

[35] Salters V. J. M., Longhi J., Trace element partitioning during the initial stages of melting beneath mid-ocean ridges. *Earth Planet. Sci. Lett.,* 1999, 166, 15–30

[36] Inoue T., Rapp R., Zhang J. Gasparik T., Weidner D. J., Irifune T., Garnet fractionation in a hydrous magma ocean and the origin of Al-depleted komatiites: melting experiments of hydrous pyrolite with

REEs at high pressure. *Earth Planet. Sci. Lett.,* 2000, 177, 81–87

[37] Nicholls I. A., Harris K. L., Experimental rare earth partition coefficients for garnet, clinopyroxene and amphibole coexisting with andesitic and basaltic liquids. *Geochim. Cosmochim. Acta,* 1980, 44, 287–308

[38] Caporuscio F. A., Smith J. R., Trace element crystal chemistry of mantle eclogites. *Contrib. Miner. Petrol.,* 1990, 105, 550–561

[39] Pride C., Muecke G. K., Rare earth element distributions among coexisting granulite facies minerals, Scourian complex, NW Scotland. *Contrib. Mineral. Petrol.*, 1981, 76, 463–471

[40] Bocchio R., De Capitani L., Ottolini L., Cella F., Trace element distribution in eclogi and their clinopyroxene/garnet pair: a case study from Soazza (Switzerland). *Europ. J. Miner.* 2000, 12, 147–161

[41] Piatenko Yu. A., Ugriumova N. G., Mineralogical Crystal Chemistry of rare earth elements. *Izvestia Academy of Sciences USSR. Geology Series*, 1988, 11, 75-86 (in Russian)

[42] Hickmott D. D., Shimizu N., Trace element zoning in garnet from the Kwoiek Area, British Columbia: disequilibrium partitioning during garnet growth? *Contrib. Mineral. Petrol.,* 1990, 104, 619–930

[43] Cherniak D. J., Rare earth element and galium diffusion in yttrium garnet. *Phis. Chem. Miner.*, 1998, 26, 156–163

[44] Quartieri S., Chaboy J., Antonioli G., Geiger C. A., XAFS characterization on the structural site of Yb in synthetic pirope and grossular garnets. *Phis. Chem. Miner.,* 1999, 27, 88–94

[45] Vakhrusheva N. V., Ivanov K. S., Erokhin Yu. V., Ronkin Yu. L., Distribution of REE in ultramafic rocks and ore-forming chromic soinels of Voykar-Syn'insky massif. *Ophiolite: geology, petrology, metallogeny and geodynamics*. Ekaterinburg: Publishing House of Institute of geology and geochemistry. Ural branch of Russian Academy of Sciences, 2006, 92–95 (in Russian)

[46] Stosch H. G., Seck H. A., Geochemistry and mineralogy of two spinel peridotite suites from Dreiser Weiher, West Germany. *Geochim. Cosmochim. Acta,*1980, 44, 457–470

[47] Stosch H. G., Rare earth partitioning between minerals from anhydrous peridotite xenoliths. *Geochim. Cosmochim. Acta,* 1982, 46, 793–811

[48] Krivenko A. P., Podlipskii M. Yu., Agafonov L. V., Petrology and mineralogy of the ultramafic rocks from Ergak massif. The status and exploration of natural resources of Tuva and adjacent regions of Central Asia. Geoecology of the environment and society. Tuvinian Institute of for Exploration of Natural Resources of Siberian branch of the Russian Academy of Sciences, 2004, 61-77 (in Russian)

[49] Mongush A. A., Lesnov F. P., Oydup Ch. K., Popov V. A., On mineralogy of olivines, serpentines and chromites from rocks of the southern part of Ergaksky ultramafic massif (Kurtushibinsky ophiolite belt). State and development of natural resources of Tuva and adjacent regions of Central Asia. Geoecology of the environment and society. Tuvinian Institute of for Exploration of Natural Resources of Siberian branch of the Russian Academy of Sciences, 2004, 78-82 (in Russian)

[50] Lesnov F. P., Podlipsky M. Yu., Palessky S. V., The first data on rare earth elements composition of the accessory chrome-spinels from rock of Ergaksky ultramafic massif (Western Sayan), The Structure and diversity of the mineral world. Institute of Geology of Komi Scientific Center of Ural branch of the Russian Academy of Sciences, 2008, 79-81 (in Russian)

[51] Lesnov F. P., Podlipsky M. Yu., Poliakov G. V., Palessky S. V., Geochemistry of accessory chrome-spinels from ultramafic rocks of Ergaksky chromites-bearing massif and the conditions of its formation (West Sayan). *Doklady of the Russian Academy of Sciences*, 2008, 422, 660-664 (in Russian)

[52] McDonough W. F., Stosch H.-G., Ware N. G., Distribution of titanium and rare earth elements between peridotite minerals. *Contrib. Mineral. Petrol.,* 1992, 110, 321–328

[53] Shannon R. D., Reversed effective ionic radii and systematic studies of interatomic distances in halides and chalcogenides. *Acta Crystallographica,* 1976, A32, 751–767

[54] Paster T. P., Schauwecker D. S., Haskin L. A., The behavior of some trace elements during solidifi cation of the Skaergaard layered series. *Geochim. Cosmochim. Acta,* 1974, 38, 1549–1579

[55] Borisenko L. F., Liapunov S. M., About distribution La, Ce, Sm, Eu, Tb, Yb and Lu in an ilmenite of various magmatic formations. *Doklady of Academy of Sciences of USSR*, 1980, 253, 454–457 (in Russian)

[56] Nash W. P., Crecraft H. R., Partition coefficients for trace elements in silica magmas. *Geochim. Cosmochim. Acta,* 1985, 49, 2309–2322

[57] McKay G., Wagstaff J., Yang S. R., Zr, Hf, and REE partition coefficients for ilmenite and other minerals in nigh Ti lunar mare basalts: An experimental study. *Proc.16th Lunar Plan. Sci. Conference,* 1986, 229–237

[58] Zack T., Brumm R., Ilmenite/liquid partition coefficients of 26 trace elements determined through il-

menite/clinopyroxene partitioning in garnet pyroxenites. *Proc. 7th International Kimberlite Conference*, Cape Town, 1998, 986–987

[59] Nowell G. M., Pearson D. G., Kempton P. D., Noble S. R, Smith C. B, Origins of kimberlites: A Hf isotope perspective. *Proc. 7th Intern. Kimberlite Conference,* Cape Town, 1999, 616–624

[60] Lesnov F. P., Role of rare earth elements in studying the genesis of kimberlite. *New Ideas in Earth Sciences: Proceedings of the 6-th International Conference,* Moscow, MGGRU, 2003, 32 (in Russian)

[61] Jang Y. D., Naslund H. R., Major and trace element variation in ilmenite in the Skaergaard intrusion: petrologic implication. *Chem. Geol.,* 2002, 193, 109–125

[62] Lesnov F. P., Bobrov V. A., Palessky S. V., On the rare-earth composition of the ilmenites from rocks of Tigrovy mafic-ultramafic massif (Sikhote-Alin' ridge). Petrology of igneous and metamorphic complexes, Tomsk State University, 2004, 51-58 (in Russian)

[63] Golubeva I. I., Afon'kin M. M., Makhlaev L. V., Metamorfogenic ilmenite in parashists of Harbeysky complex (Polar Ural Mountains). Mineralogy of Ural - 2007. Institute Mineralogy of Ural branch of the Russian Academy of Sciences, 2007, 156–160 (in Russian)

[64] Scheka S. A., Oktiabr'skii R. A., Vrzhosek A. A., Starkov G. N., Main regularity of evolution of mafic-ultramafic magmatism in the Primorie. Igneous rocks of the Far East. Far East Science Centre of Academy of Sciences of USSR, 1973, 9-61 (in Russian)

[65] Scheka S. A., Vrzhosek A. A., Vysotskii S. V., Jurassic meymechite-picrite complexes of Primorie, Russia: comparative study with komatiite and Japanese picrites suites. Plume and problems of deep sources of alkaline magmatism. *Proc. Int. Conf.* Khabarovsk, 2003, 184–200

[66] Ashcepkov I. V., Vladykin N. V., Pokhilenko N. P., Logvinova A. M., Afanasiev V. P., Kostrovitskii S. I., Alymova N. V., Stegnitsky Yu. B., Khmel'nikova O. S., Rotman A. Y., Variations of ilmenite compositions from Yakutian Kimberlites and problems of their origin. Institute of Geography of Siberian branch of Russian Academy of Sciences, Napoly-Irkutsk, 2007

[67] Lesnov F. P., State and problems of research in the field of geochemistry of rare earth elements in kimberlites. Petrology of igneous and metamorphic complexes. Tomsk State University, 2002, 126-133 (in Russian)

[68] Vasilenko V. B., Lesnov F. P., Zinchuk N. N., About an associativity of distributions of rare-earth elements and rock-forming oxides in the rocks of kimberlite formations. Problems of forecasting, searches and studying of mineral deposits on a XXI-st century threshold. ALROSA Company, TSNIGRI. Voronezh State University, 2003, 33–38 (in Russian)

[69] Pearce N. J. G., Zirconium and niobium-bearing ilmenites from the Igalico dyke swarm, South Greenland. *Mineralogical Magazine,* 1990, 54, 585–588

[70] Bea F., Montero P., Ortega M. A., LA-ICP-MS evaluation of Zr reservoirs in common crustal rocks: implications for Zr and Hf geochemistry, and zircon-forming processes. *Canadian Mineralogist,* 2006, 44, 693–714

[71] Morisset C. E., Scoates J. S., Origin of zircon rims around ilmenite in mafic plutonic rocks of Proterozoic anorthosite suites. *Canadian Mineralogist,* 2008, 46, 289–304

[72] Asavin A. M., Distribution Zr, Hf, Nb, Ta, Th, U in equilibriums of mineral – melt (revive). *Gekhimiya.* 1994, 10, 1398-1417

[73] Zheng J., Griffin W. L., O'Reilly S. Y., Yang J. S., Zhang R. Y., Zircons in mantle xenoliths the Triassic Yangtze-North China continental collision. *Earth Planet. Sci. Lett.*, 2006, 247, 130–142

[74] Saltykova A. K., Nikitina L. P., Matukov D. I., U-Pb age of zircons from the mantle peridotite xenoliths in Cenozoic alkali basalts from Vitim plateau (Transbaikalia). Reports of Russian Mineralogy Society, 2008, 3, 1-22 (in Russian)

[75] Grieco G., Ferrario A., Von Quadt A., Koeppel W., Mathez E. A., Zircon-bearing chromitites of the phlogopite peridotite of Finero (Ivrea zone, Southern Alps): Evidence and geochronology of metasomatized mantle slab. *J. Petrol.*, 2001, 42, 89–101

[76] Lesnov F. P., Oydup Ch. K., Palessky S. V. et al. The first data on the geochemistry of zircons from gabbro in Hayalygsky mafic-ultramafic massif (South-Western Tuva). *State and development of natural resources of Tuva and adjacent regions of Central Asia. Geoecology of the environment and society. Issue 9.* Tuvinian Institute for Exploration of Natural Resources of Siberian branch of the Russian Academy of Sciences, 2007, 83-90 (in Russian)

[77] Savel'eva G. N., Suslov P. V., Larionov A. N., Vendian tectono-magmatic events in mantle ophiolite complexes of the Polar Urals: the data U-Pb dating of zircon from chromitites. Geotektonika, 2007, 2, 23-33 (in Russian)

[78] Malich K. N., Efimov A. A., Ronkin Yu. L., Archean U-Pb zircon age of from dunites of Lower-Tagilsky massif (Platinum-bearing belt of the Urals). *Doklady of the Russian Academy of Sciences,* 2009, 427, 101-

105 (in Russian)
[79] Fedotova A., Bibikova E. V., Simakin S. G., Geochemistry of zircons (microprobe data) as indicators of mineral genesis at geochronological researches. *Geokhimya*, 2008, 9, 980-997 (in Russian)
[80] Lesnov F. P., The isomorphism of rare earth elements in zircons and conditions of their crystallization. *Mineralogical perspectives-2011*. Institute of Geology of Komi Science center of Russian Academy of Sciences, 2011, 92-94
[81] Belousova E. A., Griffin W. L., O'Reill S. Y., Trace element composition and catodluminiscence properties of kimberlite zircons. *Proc. 7th International Kimberlite Conference,* Cape Town, 1998, 67–69
[82] Berryman A. K., Stiefenhofer J., Shee S. R. et al. The discovery and geology of the Timber Creek kimberlites, northern territory, Australia. *Proc. 7th Intern. Kimberlite Conf.,* Cope Town, 1999, 30–39
[83] Hamilton M. A., Pearson D. G., Stern R. A., Boyd F. R., Constraints on MARID petrogenesis: SHRIMP II U-Pb zircon evidence for pre-eruption metasomatism at Kampfersdam. *Proc. 7 th International Kimberlite Conference*. Cape Town, 1998, 296–298
[84] Root D.B., Hacker B.R., Mattinson J.M., Wooden J.L., Zircon geochronology and ca. 400 Ma exhumations of Norwegian ultrahigh-pressure rocks: an ion microprobe and chemical abrasion study. *Earth Planet. Sci. Lett.,* 2004, 228, 325–341
[85] Liati A., Froitzheim N., Assessing the Valais ocean, Western Alps: U-Pb SHRIMP zircon geochronology of eclogites in the Balma unit, on top of the Monte Rosa nappe. *Eur. J. Mineral.*, 2006, 18, 299–308
[86] Kaulina T. V., Formation and transformation of zircon in polymetamorphic complexes. Geological Institute of Kola Science Centre of the Russian Academy of Sciences. 2010
[87] Yatsenko G. M., Panov B. S., Belousova E. A., Lesnov F. P. et al., Distribution of rare earth elements in zircons from minettes in Kirovograd block (Ukraine). *Doklady of Russian Academy of Sciences*, 2000, 370, 524-528 (in Russian)
[88] Song S. G., Zhang L. F., Niu Y. N. et al., Geochronology of diamond-bearing zircons from garnet peridotite in the North Quidam UHPM belt, Northern Tibetan Plateau: a record of complex histories from oceanic lithosphere subduction to continental collision. *Earth Planet. Sci. Lett.,* 2005, 234, 99–118
[89] Zhang R. Y., Yang J. S., Wooden J. L. et al., U-Pb SHRIMP geochronology of zircon in garnet peridotite from the Sulu UHP terrane, China: implications for mantle metasomatism and subduction-zone UHP metamorphism. *Earth Planet. Sci. Lett.*, 2005, 237, 729–743
[90] Krasnobaev A. A., Bea F., Fershtater G. B., Age, morphology and geochemical characteristics of zircons from mafic rocks of the Urals (ophiolites and Platinum-bearing belt) and the associated acid rocks. *Geology and metallogeny of ultramafic-mafic and granitoid intrusive associations of folded regions*. Institute Geological and Geochemistry of Ural branch of the Russian Academy of Sciences, 2004, 211-216 (in Russian)
[91] Ronkin Yu. L., Nesbitt R. W., REE geochemistry of single crystals of zircon from Berdyaushsky massif, Southern Urals. *The structure and evolution of the mineral world: Proceedings of the International Seminar*. Syktyvkar: Publishing House Geoprint, 1997, 131-132 (in Russian)
[92] Zinger T. F., Bortnikov N. S., Sharkov E. V., Borisovsky S. E., Antonov A. V., Effect of plastic deformation in zircon on its chemical composition (for example, the gabbro from zone of the spreading of the Mid-Atlantic Ridge, depression Markov, 6° N). *Doklady of the Russian Academy of Sciences*, 2010, 433, 785-791 (in Russian)
[93] Lesnov F. P., Gora M. P., Bobrov V. A., Kovaliova V. A., Distribution of REE and questions of genesis of Beriozovsky mafic-ultramafic massif (Sakhalin Islands). *Tikh. Geol.* 1998, 17, 42-58 (in Russian)
[94] Hoskin P. W. O., Ireland T.R., Rare element chemistry of zircon and its use as provenance indicator. *Geology*, 2000, 28, 627–630
[95] Murali A. V., Parthasarthy R., Mahadevan T. M., Das M. S., Trace element characteristics, REE patterns and partition coefficients of zircons from different geological environments: A case study on Indian zircons. *Geochim. Cosmochim. Acta,* 1983, 47, 2047–2052
[96] Thomas J. B., Bodnar R. J., Shimizu N., Sinha A. K., Determination of zircon/melt trace element partition coefficient from SIMS analysis of melt inclusions in zircon. *Geochim. Cosmochim. Acta,* 2002, 66, 2887–2901
[97] Hinton R. W., Upton G. J., The chemistry of zircon: variation within and between large crystals from syenite and alkali basalt xenoliths. *Geochim. Cosmochim. Acta,* 1991, 55, 3287–3302
[98] Trail et al 2011
[99] Trail et al 2012
[100] Voytkevich G. V., Miroshnikov F. E., Povarenikh A. S., Prokhorov V. G., Short reference book on geochemistry. Publishing House Nedra, Moscow,1970 (in Rus.)
[101] Osipenko A. B., Sidorov E. G., Shevchenko S. S. et

al., Geochemistry and U-Pb geochronology of zircons from the garnet amphibolite peninsula of Kamchatka Cape (Eastern Kamchatka). Geochemiya, 2007, 3, 259-268 (in Russian)

[102] Poitrasson F., Hancher J. M., Scheltegger U., The current state and future of accessory mineral research. *Chem. Geol.,* 2002, 200, 3–24

[103] Hoskin P. W. O., Kinny P. D., Wyborn D., Chappell B. W., Identifying accessory mineral saturation during differentiation in granitoid magmas: an integrated approach. *J. Petrol.,* 2000, 41, 1365–1396

[104] Hanchar J. M., Finch R. J., Hoskin P. W. O. et al., Rare earth elements in synthetic zircon. Part 1: Synthesis and rare earth element and phosphorus doping. *American Mineralogist,* 2001, 86, 667–680

[105] Cherniak D. J., Hanchar J. M., Watson E. B., Rare-earth diffusion in zircon. *Chemical Geology,* 1997, 134, 289-301

[106] Irving A. J., Frey F. A., Trace element abundances in megacrysts and their host basalts: Constrains on partition coefficients and megacrysts genesis. *Geochim. Cosmochim. Acta,* 1984, 48, 1202–1221

[107] Jones A. P., Wyllie P. J., Minor elements in perovskite from kimberlites and distribution of the rare elements: an electron probe study. *Earth Planet. Sci. Lett.,* 1984, 69, 128–140

[108] Belousova E. A., Griffin W. L., O'Reilly S. Y., Fisher N. I., Apatite as indicator mineral for mineral exploration: trace element compositions and their relationship to host rock type. J. *Geochemical Exploration*, 2002, 76, 45–69

[109] Ozawa K., Shimizu N., Open-system melting in the upper mantle: Constraints from the Hayachine-Miyamori ophiolite, northeastern Japan. *J. Geophys. Res.,* 1995, 100, 22315–22335

[110] Watson E. B., Green T. H., Apatite/liquid partition coefficients for the rare earth elements and strontium. *Earth Planet. Sci. Lett.*, 1981, 56, 405–421

[111] Dawson J. B., Smith J. V., Steel I. M., Trace-element distribution between coexisting perovskite, apatite and titanites from Oldoinyo Lengai, Tanzania. *Chem. Geol.* 1994, 117, 285–290

[112] Liakhovich V. V., Features of the distribution of rare earth elements in accessory minerals of granites. *Geokhimiya*, 1967, 7, 828-832 (in Russian)

[113] Gromet L. P., Silver L. T., Rare earth element distributions among minerals in a granodiorite and their petrogenetic implications. *Geochim. Cosmochim. Acta,* 1983, 47, 925–939

[114] Fershtater G. B., Anatectic granites and the composition of the crust of the Ural Paleozoic orogen. *Petrography at XXI Century frontier: Results and Prospects.* Geoprint, 2000, 345-348 (in Russian)

[115] Shagalov E. S., Gabbroids from Syrostansky massif as a possible representative of sub-alkaline interplate magmatism in the Urals. *Geochemistry of igneous rocks: Proceedings of the 21-th All-Russia. Seminar and schools "Alkaline magmatism of the Earth.* Kola Science Centre of of Russian Academy of Sciences, 2003, 169-170 (in Russian)

[116] Egorova V. V., Basic melt crystallization in deep magma chambers as an example gabbroid xenoliths and intrusions of the West Sangilen. *PhD Thesis,* Institute Geology and mineralogy Siberian branch of Russuan Academy of Sciences, 2005 (in Russian)

[118] Lesnov F. P., On the distribution of rare earth elements in titanites (short review). *Metallogeny of ancient and modern ocean-2006. Formation and development of deposits in uneven ocean margins.* Institute of Mineralogy of Ural branch of Russian Academy of Sciences, 2006, 291-295 (in Russian)

[117] Russell J. K., Groat L. A., Halleran A. A. D., LREE-rich niobian titanite from mount Bisson, British Columbia: chemistry and exchange mechanisms. *Canadian Mineralogist,* 1994, 32, 575–587

[118] Nakada S., Magmatic processes in titanites-bearing dacites, central Andes of Chile and Bolivia. *American Mineralogist,* 1991, 76, 548–560

[119] Seifert W., Kramer W., Accessory titanites: an important carrier of zirconium in lamprophyres. *Lithos,* 2003, 71, 81–98

[120] Green T. H., Experimental studies of trace-element partitioning applicable to igneous petrogenesis – Sedona 16 years later. *Chem. Geol.,* 1994, 117, 1–36

[121] Perkins W. T., Pearce N. J. G., Problems and progress in the determination of trace and ultra trace elements by ICP-MS and application to petrogenetic studies of igneous rocks. *J. Conf. Abstract,* 1996, 1, 459

[122] Sahama Th. G., On the chemistry of the mineral titanites. *Bull. Geol. Comm. Finlande,* 1946, 24, 88

[123] Sahama Th. G., Vahatalo V., X-rey spectrographic study of the rare earths in some Finnish eruptive rocks and minerals. *Bull. Geol. Comm. Finlande,* 1941, 126, 50

[124] Wu F. Y., Yang Y. H., Mitchel R. H., Li Q. L., Yang J. H., Zhang Y. B., In situ U-Pb age determination and Nd isotopic analysis of perovskites from kimberlites in southern Africa and Somerset Island, Canada. *Lithos,* 2010, 115, 205-222

[125] Downes H., McDonald R., Upton B. G. J. et al., Ultramafic xenoliths the Bearpaw Mountains, Montana, USA: Evidence for multiple metasomatic events in lithospheric mantle beneath the Wayoming cra-

ton. *J. Petrol.* 2004, 45, 1631–1662

[126] Aschepkov I. V., Vladykin N. V., Nikolaeva I. V. et al., About mineralogy and geochemistry of mantle inclusions and structure of mantle columns kimberlite pipe Yubileynaya, the Alakitsky field, Yakutia. *Doklady of the Russian Academy of Sciences*, 2004, 395, 1–7 (in Russian)